NASA/CP-2008-215469

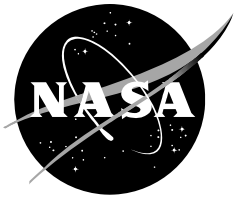

Abstracts of the Annual Meeting of Planetary Geologic Mappers, Flagstaff, AZ, 2008

Edited by:

Leslie F. Bleamaster III
Planetary Science Institute, Tucson, AZ

Kenneth L. Tanaka
U.S. Geological Survey, Flagstaff, AZ

Michael S. Kelley
NASA Headquarters, Washington, DC

June 2008

NASA STI Program ... in Profile

Since its founding, NASA has been dedicated to the advancement of aeronautics and space science. The NASA scientific and technical information (STI) program plays a key part in helping NASA maintain this important role.

The NASA STI program operates under the auspices of the Agency Chief Information Officer. It collects, organizes, provides for archiving, and disseminates NASA's STI. The NASA STI program provides access to the NASA Aeronautics and Space Database and its public interface, the NASA Technical Report Server, thus providing one of the largest collections of aeronautical and space science STI in the world. Results are published in both non-NASA channels and by NASA in the NASA STI Report Series, which includes the following report types:

- TECHNICAL PUBLICATION. Reports of completed research or a major significant phase of research that present the results of NASA Programs and include extensive data or theoretical analysis. Includes compilations of significant scientific and technical data and information deemed to be of continuing reference value. NASA counterpart of peer-reviewed formal professional papers but has less stringent limitations on manuscript length and extent of graphic presentations.

- TECHNICAL MEMORANDUM. Scientific and technical findings that are preliminary or of specialized interest, e.g., quick release reports, working papers, and bibliographies that contain minimal annotation. Does not contain extensive analysis.

- CONTRACTOR REPORT. Scientific and technical findings by NASA-sponsored contractors and grantees.

- CONFERENCE PUBLICATION. Collected papers from scientific and technical conferences, symposia, seminars, or other meetings sponsored or co-sponsored by NASA.

- SPECIAL PUBLICATION. Scientific, technical, or historical information from NASA programs, projects, and missions, often concerned with subjects having substantial public interest.

- TECHNICAL TRANSLATION. English-language translations of foreign scientific and technical material pertinent to NASA's mission.

Specialized services also include creating custom thesauri, building customized databases, and organizing and publishing research results.

For more information about the NASA STI program, see the following:

- Access the NASA STI program home page at *http://www.sti.nasa.gov*

- E-mail your question via the Internet to help@sti.nasa.gov

- Fax your question to the NASA STI Help Desk at (301) 621-0134

- Phone the NASA STI Help Desk at (301) 621-0390

- Write to:
  NASA STI Help Desk
  NASA Center for AeroSpace Information
  7115 Standard Drive
  Hanover, MD 21076-1320

NASA/CP-2008-215469

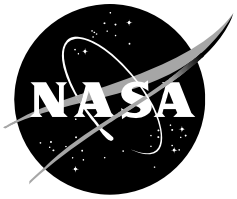

Abstracts of the Annual Meeting of Planetary Geologic Mappers, Flagstaff, AZ, 2008

Edited by:

Leslie F. Bleamaster III
Planetary Science Institute, Tucson, AZ

Kenneth L. Tanaka
U.S. Geological Survey, Flagstaff, AZ

Michael S. Kelley
NASA Headquarters, Washington, DC

National Aeronautics and
Space Administration

NASA Headquarters
Washington, DC 20546

June 2008

Acknowledgments

This publication is supported by a grant from the NASA Planetary Geology and Geophysics Program.

Available from:

NASA Center for AeroSpace Information
7115 Standard Drive
Hanover, MD 21076-1320
(301) 621-0390

This report is also available in electronic form at

http://astrogeology.usgs.gov/Projects/PlanetaryMapping/

Report of the Annual Mappers Meeting
U.S. Geological Survey
Flagstaff, Arizona
June 23-26, 2008

The annual Planetary Geologic Mappers Meeting is the primary venue for mappers to present the results of their work funded through the Planetary Geology and Geophysics (PG&G) program. It also provides the opportunity for researchers and students to exchange ideas, share experiences, and discuss mapping methodologies and technological advances. Approximately 40 people attended all or parts of this year's mappers meeting and associated workshop and field trip; several others submitted abstracts and maps *in absentia*. The 2008 meeting was convened by Les Bleamaster (Planetary Science Institute - PSI), Ken Tanaka (U.S. Geological Survey), and Michael Kelley (NASA Headquarters), and was hosted by the U.S. Geological Survey (USGS) in Flagstaff, Arizona. Trent Hare, Jim Skinner, and Corey Fortezzo (all USGS) provided administrative, logistical, and technical support.

The meeting kicked off on Monday, June 23rd with a hands-on Geographic Information Systems (GIS) workshop for planetary mappers. The workshop, organized and run by Hare, Skinner, and Fortezzo, provided instruction on how to: 1) organize mapping projects (using a geodatabase approach), 2) produce and edit shapefiles (map drafting), 3) incorporate shapefile annotation, and 4) import and modify geologic map symbology. It is anticipated that this type of workshop will accompany the mappers meeting at least every other year whenever meetings are convened in Flagstaff.

Oral presentations and poster discussions took place on Tuesday, June 24th and Wednesday, June 25th. Geologic Mapping Subcommittee (GEMS) Chairperson, Les Bleamaster, commenced the meeting, and Ken Tanaka (Map Coordinator) followed with a brief introduction and Planetary Geologic Mapping Program update, which included a particularly important new requirement for mappers — from now on, maps submitted for USGS map editing and production (post technical review) would be accepted in Illustrator (graphics) and Word (text) formats only (details are given in an author checklist available through the Planetary Geologic Mapping web page, http://astrogeology.usgs.gov/Projects/PlanetaryMapping/). Michael Kelley (new PG&G Discipline Scientist) discussed his initial months at headquarters and provided a PG&G program status report. Science presentations marched their way from the inner to the outer Solar System, kicking off with Alessandro Frigeri (Universita degli Studi di Perugia) discussing his use of GRASS (an open-source GIS software program) to compile a single digital mosaic of the existing 1:5M Atlas of Mercury series. Debra Hurwitz (Brown University) gave two presentations: one for her own mapping of the V-1 quadrangle on Venus, and a second to report on the activities of her colleagues at Brown University. Les Bleamaster (PSI) followed with a progress report on mapping of V-50 and 1:10M Helen Planitia quadrangles, Venus and introduced a new project to map Mawrth Vallis and Nili Fossae on Mars. Continuing with the hybrid Venus/Mars presentations, David Crown (PSI) outlined a plan for completing the V-30 quadrangle of Venus and discussed new mapping on the northwest side of Hellas Planitia, Mars. The remainder of Tuesday's presentations focused on Mars. Jim Zimbelman (Smithsonian Institution) presented new findings about the Medusae Fossae Formation, Joe Boyce

(University of Hawaii) discussed his and Peter Mouginis-Mark's 1:200K mapping of Tooting crater, and Tracy Gregg (University of Buffalo) reported on her continued mapping in Hesperia Planum. After a second break out session, James Dohm (University of Arizona) introduced a new project to map the Argyre region of Mars. Jim Skinner (USGS) discussed year two results from his mapping in the southern Utopia Planitia region and emphasized the utility of mapping in GIS. Ken Tanaka concluded the day one presentations with results of 1:2M-scale polar mapping of Mars. Tuesday concluded with a picnic dinner hosted by Ron Greeley (ASU) at his Flagstaff residence - many thanks to Ron and his wife, Cindy, for being such gracious hosts.

Wednesday morning began with brief presentations by Jen Blue (USGS) discussing planetary nomenclature issues, and David Portree (USGS) introducing himself as the new Regional Planetary Image Facility (RPIF) data manager of the USGS Flagstaff location. Science presentations continued where we left off, with Mars. Ross Irwin (Smithsonian Institution) presented work prepared with John Grant on Holden crater and requested greater participation from the mapping and surface processes community in the Mars Science Laboratory landing-site selection process. Corey Fortezzo (USGS) discussed the geologic evolution of highlands near Margaritifer, Arabia, and Noachis Terrae and emphasized the use of geographic names to divide and identify site-specific locations for both unit descriptions and abbreviations. Laszlo Keszthelyi (USGS) presented mapping of Athabasca Valles that sparked discussion about map units and the extent to which interpretation should be included in map unit names (i.e., Athabasca "lava" flows vs. Athabasca "lobate" flows). Ken Tanaka rounded out the Mars presentations discussing the year two results of his five-year project to produce a new 1:20M-scale global map of Mars. After the final breakout session, the Galilean satellites were front and center and well represented by Arizona State University's David Williams, Melissa Bunte, and Thomas Doggett reporting on the progress of the global map of Io, high-resolution regional maps of Io, and the global map of Europa, respectively. Following the mapping presentations, Paul Umhoefer of Northern Arizona University, gave an overview of the geology of the Colorado Plateau and a brief introduction of the field trip sites to be visited. Jim Skinner distributed field guides and GIS data products for the two field trip areas.

Mappers saw an early start to Thursday morning, meeting at 6:30 am for the field trip to Lees Ferry and SP crater. Paul Umhoefer pointed out the various Quaternary volcanics as we left Flagstaff and began the ~100 mile journey northward toward the confluence of the Paria and Colorado Rivers. Once on site, Paul highlighted several features of the region and emphasized several aspects of the geology that perhaps would not be immediately clear using remote data alone, such as different appearances of the same material on flat and sloping surfaces, the role of mass wasting vs. river down-cutting for scarp retreat along the Colorado River, and the similar appearance of eroded lag gravels vs. river deposits. Lunch on the shore of the Colorado River provided a much needed break from the 100°F+ heat. The second stop, SP crater, allowed a quick hike to the lava flow - cinder cone contact and a chance to assess the scale of the flow's marginal levees and blocky surface texture. Both areas provided excellent ground-based observations that were put into context with remote data sets.

In closing, many themes were introduced and revisited throughout this year's meeting. Two main issues were discussed. First, what is in a unit name? It was clear that there are

several opinions concerning this issue, but mappers should be clear in their representation of units and description should remain the primary focus. However, interpretations can be managed and prove useful if scale- and site-specific, and clearly stated as such. Second, how should mappers deal with surface mantling deposits and modified, dissected, or eroded units? It seems that all present were in favor of preserving the ability to display these types of units through a variety of stipple patterns, inset figures, and/or manipulatable layers within a digital map product. This final option emphasizes the need for the mapping community to move toward digital products, and thus leads to the final remarks in this report.

As a result of several conversations during GEMS lunches and with USGS personnel, it is the recommendation of GEMS that beginning next year all mapping bases and ancillary data products be supplied by the USGS in GIS compatible formats. These data will include the projected mapping base or mosaic, other useful spatially registered data sets (e.g., digital terrain models and thematic maps derived from spectral, radar, or other data) as per the mapper's successful proposal, and released image footprints with web links if available. There will be no "standard product" as individual mapping areas are scale and resolution dependent. These data will be distributed as a personal geodatabase in GIS project form. Language to this effect will be included in the ROSES 2009 announcement.

It naturally follows that planetary maps will now be expected to be produced and submitted in digital format compatible with GIS software packages. To fully implement this "upgrade," it has been decided that GIS format (in addition to the currently accepted Illustrator format) will be required for maps submitted for USGS review, editing, and publishing beginning January 2011. Proposers can request support for GIS training courses, hardware, and software by fully demonstrating such needs.

The next mappers meeting will convene between June 20th and June 26th at a location yet to be determined.

CONTENTS

Formation and Evolution of Lakshmi Planum (V-7), Venus: Assessment of Models using Observations from Geological Mapping.
M.A. Ivanov and J.W. Head

Geologic Map of the Meskhent Tessera Quadrangle (V-3), Venus: Evidence for Early Formation and Preservation of Regional Topography.
M.A. Ivanov and J.W. Head

Geological Mapping of the Lada Terra (V-56) Quadrangle, Venus: A Progress Report.
P. S. Kumar and J.W. Head

Geology of the Lachesis Tessera Quadrangle (V-18), Venus.
G.E. McGill

Geologic Mapping of the Juno Chasma Quadrangle, Venus: Establishing the Relation Between Rifting and Volcanism.
D.A. Senske

Geologic Mapping of V-19, V-28, and V-53.
E.R. Stofan, P. Martin, and J.E. Guest

Moon

Lunar Geologic Mapping Program: 2008 Update.
L. Gaddis, K. Tanaka, J. Skinner, and B.R. Hawke

Geologic Mapping of the Marius Quadrangle, the Moon.
T. K.P. Gregg and A. Yingst

Mars

Geologic Mapping along the Arabia Terra Dichotomy Boundary: Mawrth Vallis and Nili Fossae, Mars: Introductory Report.
L.F. Bleamaster III and D.A. Crown

New Geologic Map of the Argyre Region of Mars.
J.M. Dohm, K.L. Tanaka, and T.M. Hare

Geologic Evolution of the Martian Highlands: MTMs -20002, -20007, -25002, and -25007.
C.M. Fortezzo and K.K. Williams

Mapping Hesperia Planum, Mars.
T.K.P. Gregg and David A. Crown

Geologic Mapping of the Meridiani Region, Mars.
B.M. Hynek

Geology of Holden Crater and the Holden and Ladon Multi-Ring Impact Basins, Margaritifer Terra, Mars.
R.P. Irwin III and J.A. Grant

Geologic Mapping of Athabasca Valles.
L.P. Keszthelyi, W.L. Jaeger, K. Tanaka, and T. Hare

Geologic Mapping of MTM -30247, -35247 and -40247 Quadrangles, Reull Vallis Region of Mars.
S.C. Mest and D.A. Crown

Geologic Mapping of the Martian Impact Crater Tooting.
P. Mouginis-Mark and J.M. Boyce

Geology of the Southern Utopia Planitia Highland-Lowland Boundary Plain: First Year Results and Second Year Plan.
J.A. Skinner, Jr., K.L. Tanaka, and T.M. Hare

Mars Global Geologic Mapping: Amazonian Results.
K.L. Tanaka, J.M. Dohm, R. Irwin, E.J. Kolb, J.A. Skinner, Jr., and T.M. Hare

Recent Geologic Mapping Results for the Polar Regions of Mars.
K.L. Tanaka and E.J. Kolb

Geologic Mapping of the Medusae Fossae Formation on Mars (MC-8 SE and MC-23 NW) and the Northern Lowlands of Venus (V-16 and V-15).
J.R. Zimbelman

Galilean Satellites

Geologic Mapping of the Zal, Hi'iaka, and Shamshu Regions of Io.
M.K. Bunte, D.A. Williams, and R. Greeley

Global Geologic Map of Europa.
T. Doggett, P. Figueredo, R. Greeley, T. Hare, E. Kolb, K. Mullins, D. Senske, K. Tanaka, and S. Weiser

Material Units, Structures/Landforms, and Stratigraphy for the Global Geologic Map of Ganymede (1:15M).
G.W. Patterson, J.W. Head, G.C. Collins, R.T. Pappalardo, L.M. Prockter, and B.K. Lucchitta

Global Geologic Mapping of Io: Preliminary Results.

D.A. Williams, L.P. Keszthelyi, D.A. Crown, P.E. Geissler, P.M. Schenk, J. Yff, W.L. Jaeger, and J.A. Rathbun

MERGING OF THE USGS ATLAS OF MERCURY 1:5,000,000 GEOLOGIC SERIES. A. Frigeri[1], C. Federico[1], C. Pauselli[1], A. Coradini[2], [1]Geologia Strutturale e Geofisica, Dipartimento di Scienze della Terra, Universita degli Studi di Perugia, I-06126, Perugia, Italy (afrigeri@unipg.it), [2]Istituto di Fisica dello Spazio Interplanetario - INAF, Roma, Italy.

Introduction: After 30 years, the planet Mercury is going to give us new information. The NASA MESSENGER [1] already made its first successful flyby on December 2007 while the European Space Agency and the Japanese Space Agency ISAS/JAXA are preparing the upcoming mission BepiColombo [2].

In order to contribute to current and future analyses on the geology of Mercury, we have started to work on the production of a single digital geologic map of Mercury derived from the merging process of the geologic maps of the Atlas of Mercury, produced by the United States Geological Survey, based on Mariner 10 data.

The aim of this work is to merge the nine maps so that the final product reflects as much as possible the original work. Herein we describe the data we used, the working environment and the steps made for producing the final map.

Original data: The USGS Atlas of Mercury 1:5,000,000 Geologic Series is a group of nine maps produced by various authors between 1980 and 1990 (see Table 1). In 2000 these maps were converted by USGS to a digital vector interchange format suitable to be used with Geographic Information Systems (GIS). The data as well as metadata are available for download from the USGS PIGWAD server (http://webgis.wr.usgs.gov/).

I. no	Quad.	Authors	Year
I-1660	H-1	Grolier, Boyce	1984
I-1409	H-2	McGill, King	1983
I-1408	H-3	Guest, Greeley	1983
I-1233	H-6	De Hon, Scott, Underwood	1981
I-2048	H-7	King, Scott	1990
I-1199	H-8	Schaber, McCauley	1980
I-1659	H-12	Spudis, Prosser	1984
I-1658	H-11	Trask, Dzurisin	1984
I-2015	H-15	Strom, Malin, Leake	1990

Table 1: 1:5,000,000 Geologic Maps of Mercury published by USGS up to 1990.

The working environment: The working environment was set up on a GNU/Linux based workstation with ISIS and GRASS GIS software installed on it. The Geographic Resources Analysis Support System (GRASS), originally developed by the U.S. Army Construction Engineering Research Laboratories between the 1980s and the 1990s, is a complete suite for the processing of spatially referenced data and now is released as a Free Open Source Software and maintained by an international team of developers [3]. Since 2007 GRASS GIS supports reading PDS and ISIS data using the Geographic Data Abstraction Library (GDAL). Besides this feature, GDAL also offers import/export to almost every digital raster map format. In the first years of development GRASS was known mainly for its raster processing capabilities. Since version 5.0, it now offers a new vector engine which allows the user to process vector data more efficiently. As with GDAL, a specialized library called OGR Simple Features Library guarantees importing and exporting vector data in a wide range of formats.

The merging process: The nine digital geologic maps have been imported into the GRASS GIS database, in Cylindrical projection, using a planetary radius of 2439 km.

The three distinct information layers available are: 1) the geologic units, 2) the structures and 3) a miscellaneous layer which consists of albedo features, mostly associated with craters. To support the editing process we also imported the scan of the USGS I-1149 shaded relief map to provide an overview of the morphology where required.

We first started to work on the geologic units, which require particular care as topological integrity has to be maintained throughout the merging process. First of all we verified that tabular information linked to the geometrical objects was coherent, so that the same geologic unit was going to be identified by the same code in all the maps. Then, after trimming the extension of every single map, we started the merging process by editing boundaries shared by pairs of maps. The overall consistency of the geometry of the geologic contacts on the boundaries of the maps is good apart from a subtle shift due to the interpretation process.

In the editing process, however, we have found two main families of mismatches along the maps' boundaries. There are areas that show geologic units on one side that are not present on the other side. In other zones, the units are detected on both maps and contacts coincide on the boundaries, but the areas are assigned to different geologic units. At this stage of the work we decided to maintain intact the coherence of the original data, without applying any kind of interpretation. All the editing operations have been done just to solve the topological problems of the map that arose in the subsequent merging phases.

The colors of the geologic units were sampled

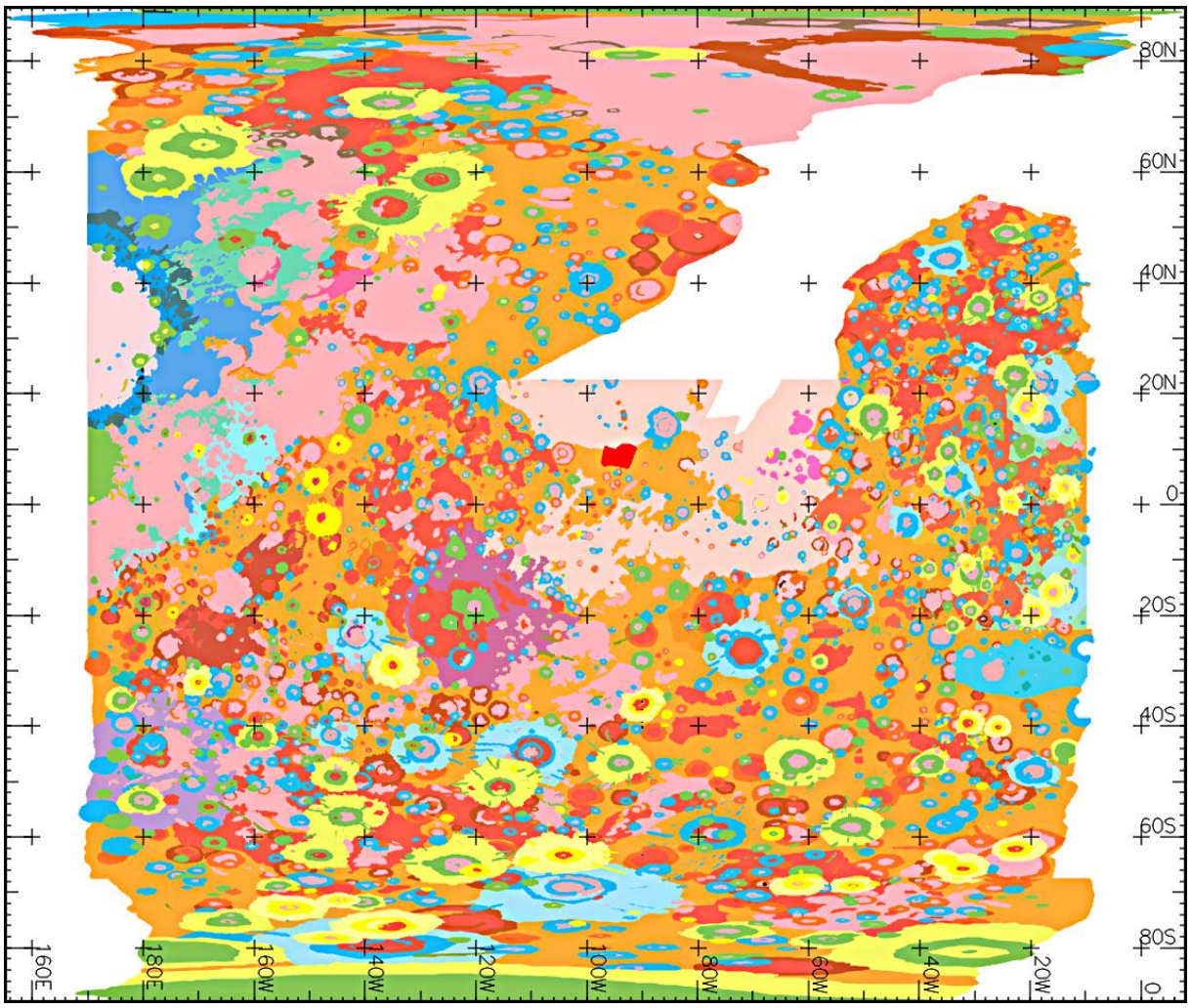

Figure 1: The geologic information of the nine maps of the 1:5,000,000 Atlas of Mercury series, merged in a single map and displayed in GRASS GIS in Simple Cylindrical projection; the color scheme follows the original authors' work (Table 1).

Results and Discussion: Figure 1 shows the complete geologic map in its full extent.

A single digital geologic map of Mercury has several advantages. The analyses of zones that before were falling among two, three or four quadrangles is much simplified and a cleaner overview of the geologic setting is now possible. The features of the complete map can be quickly queried in a single step. Single map ingestion on web based mapping services is much simpler.

As MESSENGER and BepiColombo will send more detailed and accurate data than Mariner 10, it will be possible to perform a renewal process of the geologic map both by filling unmapped areas and by improving the accuracy and resolution of mapped units, as done for example by Skinner et al. [4] who have updated the geologic map of Mars, originally based on Viking data, with a newer and more accurate one delivered by recent missions.

With the upcoming release of the first MESSENGER data on the Planetary Data System (planned on July 15th, 2008), newer imagery of both mapped and unmapped areas of Mercury [5] can be overlaid on the geologic map to detect common features, differences and to observe new details.

References: [1] Solomon S. C. et al. (2007), *Space Sci. Rev., 131*, 3-39. [2] Benkhoff J. and Schulz R. (2006), *Adv. Geosci.*, *3,* 51-62. [3] Neteler M. and Mitasova E. (2008), *Open Source GIS: A GRASS GIS Approach. Third Edition.* [4] Skinner J. A. et al. (2006), *LPSC XXXVII*, abstract #2331. [5] Prockter L. M. et al. (2008), *LPSC XXXIX,* abstract #1211.

GEOLOGIC MAPPING OF THE V-36 THETIS REGIO QUADRANGLE: 2008 PROGRESS REPORT. A. T. Basilevsky[1,2] and J. W. Head[2], [1]Vernadsky Institute of Geochemistry and Analytical Chemistry, RAS, Moscow, Russia, atbas@geokhi.ru, [2]Department of Geological Sciences, Brown University, Providence, RI 02912 USA.

Introduction: This work is a continuation to the photogeologic mapping of the V-36 quadrangle, that is part of the USGS 1:5M planetary mapping project [1]. Here we report on progress in mapping of this quadrangle. Comparing with the last year results, when the western half of the quadrangle had been mapped, we have now also partly mapped the eastern half (Figures 1, 2, 3).

Mapping Results: As a result of mapping, eleven material stratigraphic units and three structural units have been identified and mapped. The material units include (from older to younger): tessera terrain material (tt), material of densely fractured plains (pdf), material of fractured and ridged plains (pfr), material of shield plains (psh), material of plains with wrinkle ridges (pwr), material of smooth plains of intermediate brightness (psi), material of radar-dark smooth plains (psd), material of lineated plains (pli) material of lobate plains (plo), material of craters having no radar-dark haloes (c1), and material of craters having clear dark haloes (c2).

The morphologies and probably the nature of the material units in the study area are generally similar to those observed in other regions of Venus [2]. The youngest units are lobate plains (plo) which here typically look less lobate than in other areas of the planet. Close to them in age are smooth plains which are indeed smooth and represented by two varieties mentioned above. Lineated plains (pli) are densely fractured in a geometrically regular way. Plains with wrinkle ridges, being morphologically similar to those observed in other regions, here occupy unusually small areas. Shield (psh) plains here are also not abundant. Locally they show wrinkle ridging. Fractured and ridged plains (pfr), which form in other regions, the so called ridge belts, are observed as isolated areas of clusters of ridged plains surrounded by other units. Densely fractured plains (pdf) are present in relatively small areas in association with coronae and corona-like features. Tessera terrain (tt) is dissected by structures oriented in two or more directions. Structures are so densely packed that the morphology (and thus nature) of the precursor terrain is not known.

Structural units include tessera transitional terrain (ttt), fracture belts (fb) and rifted terrain (rt). Tessera transitional terrain was first identified and mapped by [4] as areas of fractured and ridged plains (pfr) and densely fractured plains (pdf) deformed by transverse faults that made it formally resemble tessera terrain (tt). The obvious difference between units tt and ttt is the recognizable morphology of precursor terrain of unit ttt. Fracture belts are probably ancient rift zones [3]. Rifted terrain (rt), as in other regions of Venus, is so saturated with faults that according to the recommendation of [1, 5] it should be mapped as a structural unit.

Conclusions: Our mapping analysis and results show that although the mapped units are generally similar to those observed in other regions of the planet, some of them have unusual areal abundances that imply unique aspects of the geologic history of this region. In particular, the unusually high abundance of rifted terrain (rt) and tessera transitional terrain (ttt) have interesting implications and demand additional studies.

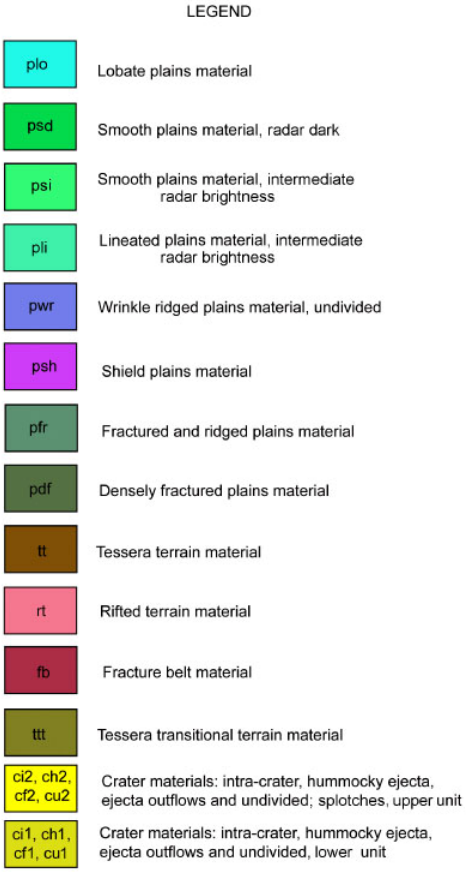

Figure 1. Legend for V-36 Thetis Regio.

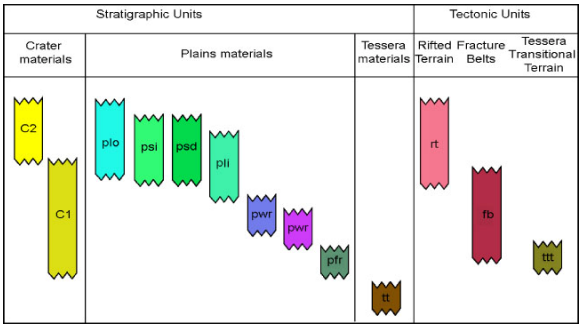

Figure 2. Correlation chart for V-36 Thetis Regio.

References: [1] Tanaka, K. L. (1994) USGS Open File Report 94-438. [2] Basilevsky, A. T. & Head, J. W. (2000) Planet. Space Sci., 48, 75-111. [3] Banerdt et al. (1997) in Venus II, U. Arizona Press, 901-930. [4] Ivanov, M. A. & Head, J. W. (2001) JGR, 106, 17,515-17,556. [50] Wilhelms, D. (1990) in Planetary Mapping, NY, 208-260.

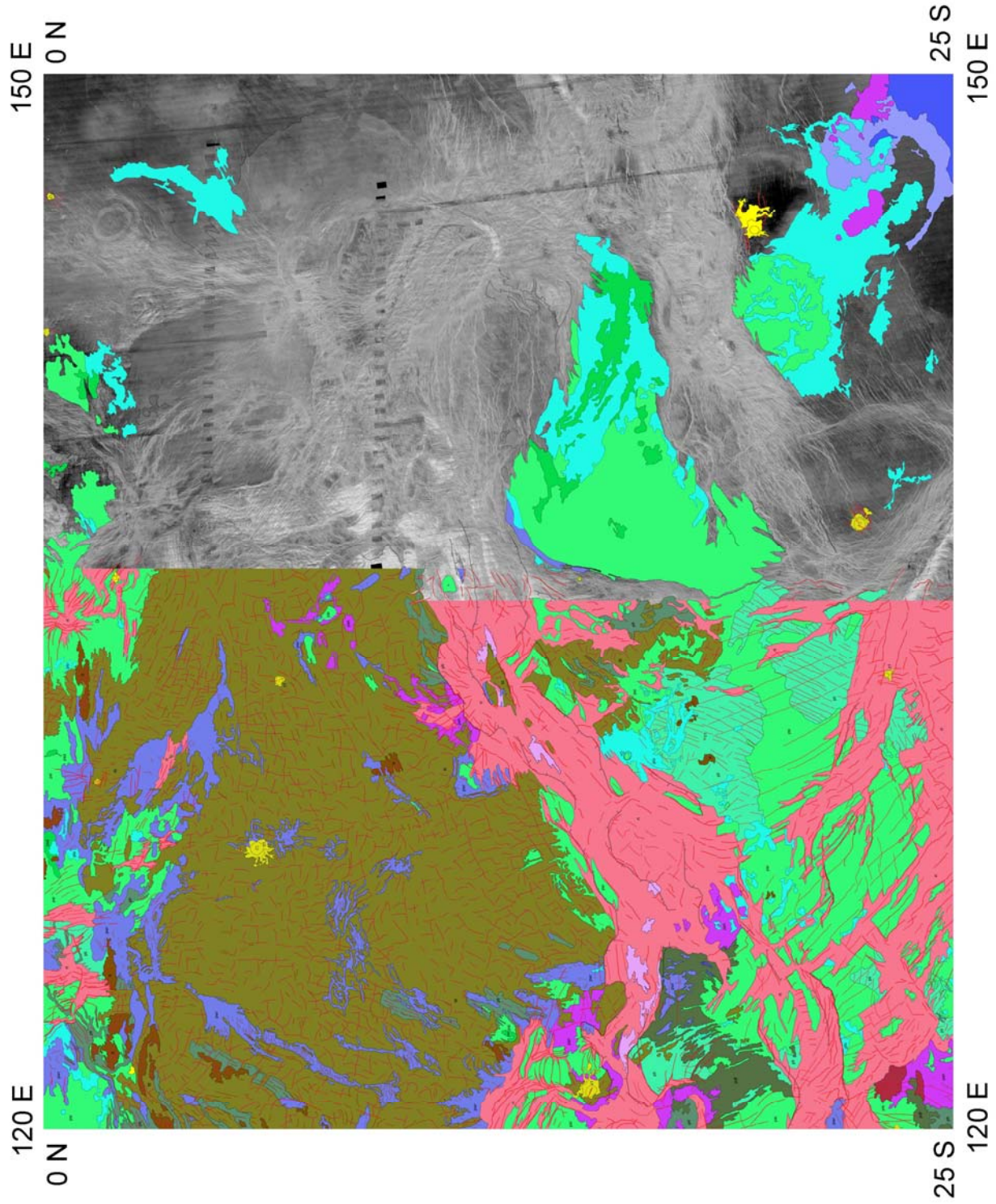

Figure 3. Geologic map of the V-36 Thetis Regio quadrangle. Status on May 29, 2008.

STRUCTURAL MAPS OF THE V-17 BETA REGIO QUADRANGLE, VENUS. A. T. Basilevsky[1,2] and J. W. Head[2], [1]Vernadsky Institute of Geochemistry and Analytical Chemistry, RAS, Moscow, Russia, atbas@geokhi.ru, [2]Department of Geological Sciences, Brown University, Providence, RI 02912 USA.

Introduction: This work resulted from the photogeologic mapping of the V-17 quadrangle, which is dominated by the Beta Regio structural uplift. This mapping is part of the USGS 1:5M planetary mapping project [1]. The V-17 map has been accepted for publication and now is in the final editing and production process [2]. The results of the photogeologic analysis, mapping and interpretations have been recently published by [3]. Here we report on the structural maps which are part of the products of the V-17 project. We find them to be useful for structural analysis and interpretations and suggest that other mappers use this tool.

Structural maps: These represent slices of the geologic map into 7 time-stratigraphic levels whose descriptions are found in [3-6]. From older to younger they are: 1) Tessera material unit (t), 2) Densely fractured plains material unit (pdf), 3) Fractured and ridged plains material unit (pfr), 4) Tessera transitional terrain structural unit (tt), 5) Fracture belts structural unit (fb), 6) Shield plains (psh) and plains with wrinkle ridges (pwr) material units combined, and 7) Lobate (pl) and smooth (ps) plains material units combined and, approximately contemporaneous with them, the structural unit of rifted terrain (rt). Each slice shows the generalized pattern of structures typical of these units. Figures 1-7 show the seven maps and Figure 8 shows the combined map illustrating what is shown in the seven maps. To visualize the Beta Regio uplift outlines, the major structure of this area, we show the +0.5 km and +2.5 km contour lines, corresponding respectively to the base and the mid-height of the uplift.

It is seen in Figures 1-2 and 4 the trends of t, pdf and tt occupy relatively small areas and their structures seen in these small windows appear rather variable and with almost no orientation heritage with time. Figure 3 shows that swarms of ridge belts trend mostly NW and go through the Beta structure with no alignment with it, suggesting that this structure did not yet exist at this time.

Figure 5 shows that fracture belts align along the northern base of the Beta uplift suggesting onset of the formation of this structure. Figure 6 shows that wrinkle ridges do not show alignment with the Beta uplift suggesting that this already forming structure was not high enough to exert topographic stress in its vicinity. Figure 7 shows that the Beta uplift has Devana Chasma as an axial rift zone, suggesting a genetic link between the uplift and rifting. Figure 8 shows that structural trends in this area significantly changed with time.

There are several centers of radiating fractures, all mapped earlier by [7]. The most prominent are the following four, centered at 34.5°N, 293.5°E; 39°N, 277°E; 40°N, 279.5°, and 42°N, 287.5°. The first three of these are part of the fracture belt. The fourth one, an unnamed astrum centered at Wohpe Tholus, is composed of several generations of structures. Its NE and SE sectors have abundant faults associated with unit pdf. Its SW sector is partly made of structures associated with unit fb. The young, post-regional-plains astrum structures radiate in almost all directions.

References: [1] Tanaka, K.L. (1994) *USGS Open File Report* 94-438. [2] Basilevsky, A.T. (2008) Geologic Map of the Beta Regio quadrangle (V-17), Venus, USGS Geologic Investigation Series, (in press). [3] Basilevsky, A.T., Head, J.W. (2007) Icarus 192, 167-186. [4] Basilevsky, A.T., Head, J.W. (1998) J. Geophys. Res. 103, 8531-8544. [5] Basilevsky, A.T. & Head, J.W. (2000) *Planet. Space Sci., 48,* 75-111. [6] Basilevsky and McGill (2007) in Exploring Venus as a Terrestrial Planet. AGU Geophysical Monograph Series. Wasington, D.C., 23-43. [7] Ernst et al. (2003) Icarus, 164, 282-316.

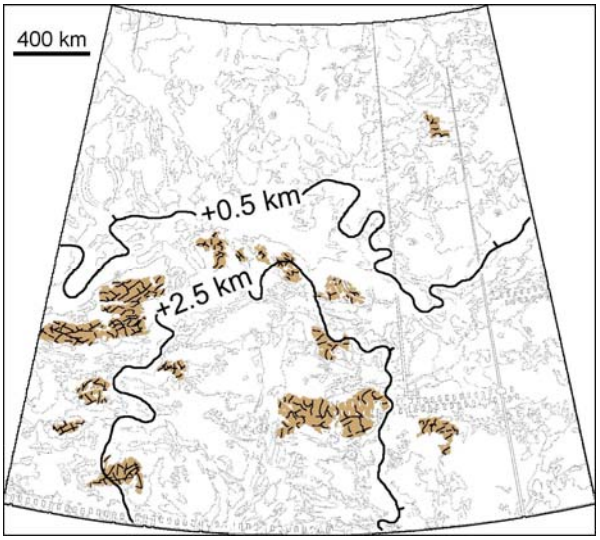

Figure 1. Tessera unit (t) and its dominant structures.

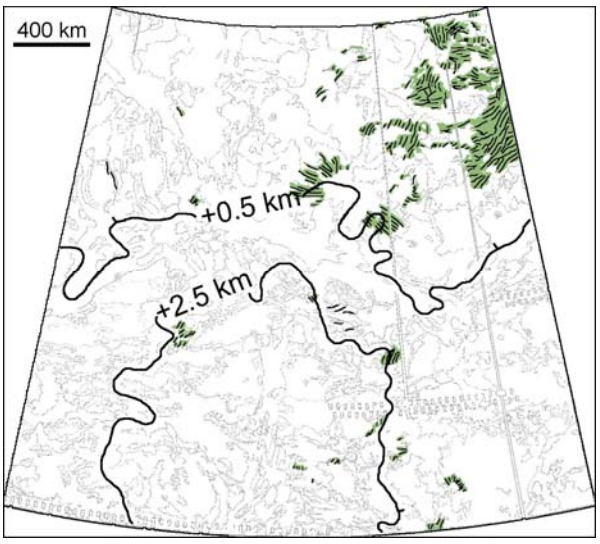

Figure 2. Densely fractured plains unit (pdf) and its structures.

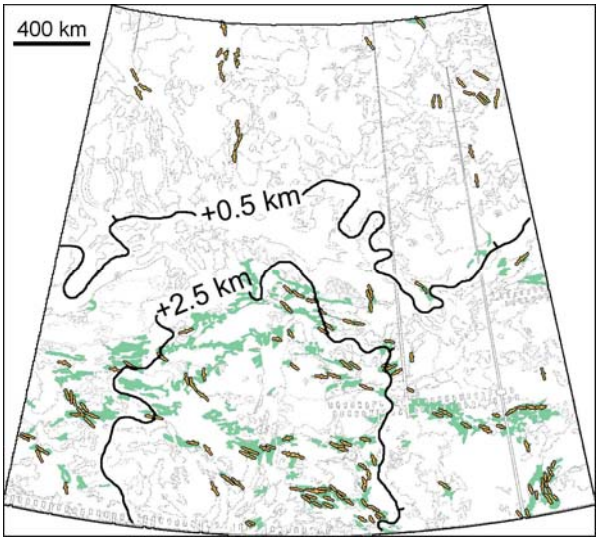

Figure 3. Material unit pfr and its typical ridge belt structures.

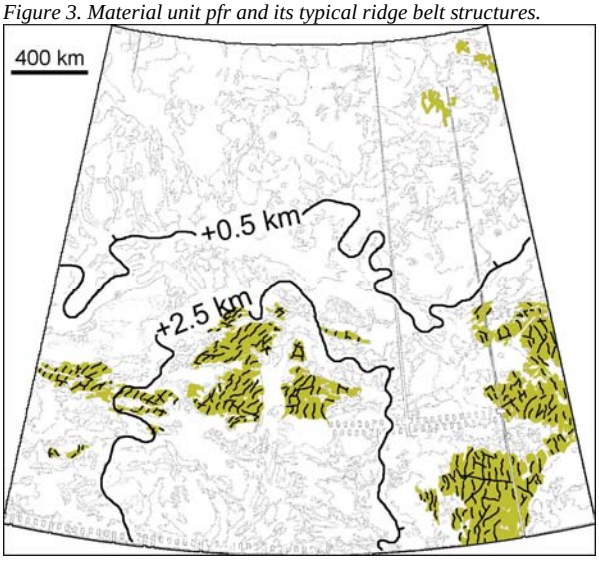

Figure 4. Tessera transitional terrain unit (tt) and its structures.

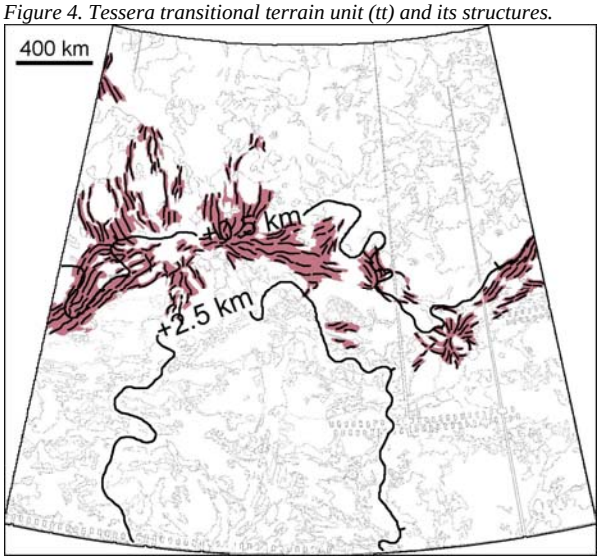

Figure 5. Fracture belts structural unit (fb) and its structures.

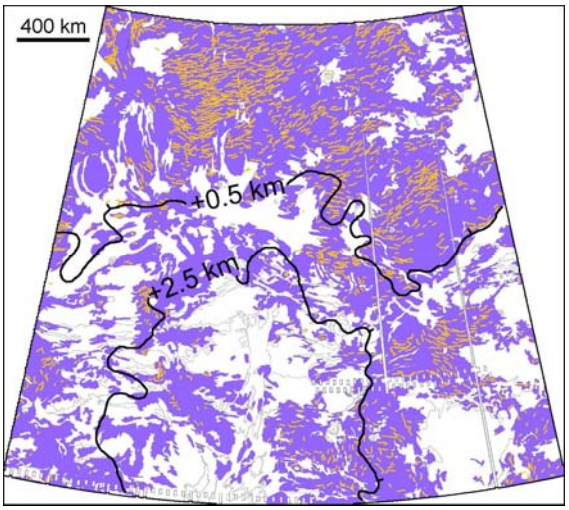

Figure 6. Shield plains (psh) and plains with wrinkle ridges (pwr) material units combined, and wrinkle ridges.

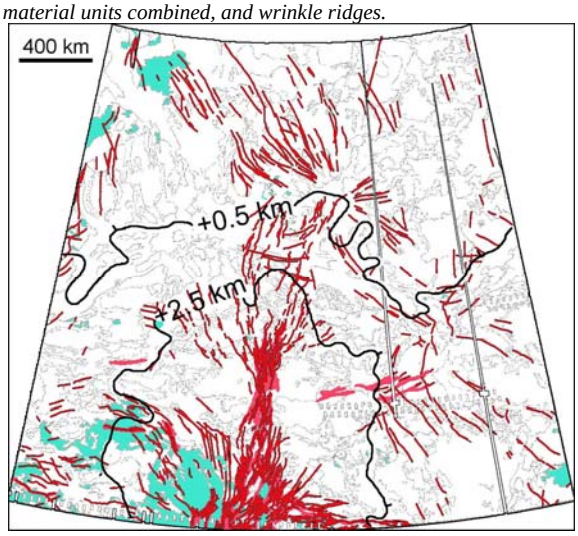

Figure 7. Lobate (pl) and smooth (ps) plains material units and structural unit of rifted terrain (rt).

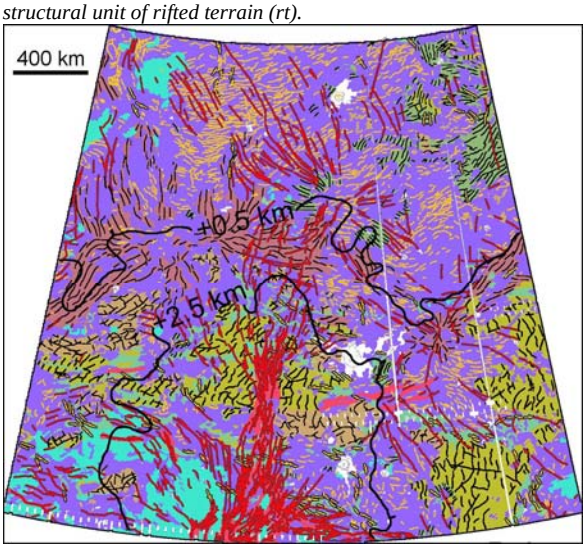

Figure 8. All units considered and their structures combined.

GEOLOGIC MAPPING OF ISABELLA QUADRANGLE (V-50) AND HELEN PLANITIA, VENUS. Leslie F. Bleamaster III, Planetary Science Institute, corporate address - 1700 E. Ft. Lowell Rd., Suite 106, Tucson, AZ 85719; mailing - 3635 Mill Meadow Dr., San Antonio, TX 78247; lbleamas@psi.edu.

Isabella Quadrangle: (25-50°S, 180-210°E) is host to numerous coronae and small volcanic centers (paterae and shield fields), focused (Aditi and Sirona Dorsa) and distributed (penetrative north-south trending wrinkle ridges) contractional deformation, and radial and linear extensional structures, all of which contribute materials to and/or deform the expansive surrounding plains (Nsomeka and Wawalag Planitiae). Regional plains, which are a northern extension of regional plains mapped in the Barrymore Quadrangle V-59 [1], dominate the V-50 quadrangle. Previous mapping divided the regional plains into two members: regional plains, members a and b [2]. A re-evaluation of these members has determined that a continuous and consistent unit contact does not exist; however, the majority of this "radar unit" or "surficial unit" will still be displayed on the final map as a stipple pattern as it is a prevalent feature of the quadrangle.

With minimal tessera or highland material, much of the quadrangle's oldest materials are plains units (the regional plains). Much of these plains are covered with small shield edifices that exhibit a variety of material contributions (or flows). In the northwest, several flows emerge and flow to the southeast from Diana-Dali Chasmata. Local corona- and mons-fed flows superpose the regional plains; however, earlier stages of volcano-tectonic centers marked by arcuate and radial structural elements, including terrain so heavily deformed that it takes on a new appearance, may have developed prior to or concurrently with the region plains. North-trending deformation belts disrupt the central portion of the map area and wrinkle ridges parallel these larger belts.

Isabella crater, in the northeastern quadrant, is highly asymmetric and displays two prominent ejecta blanket morphologies, which generally correlate with distance from the impact structure suggesting that ejecta block size or ejecta blanket thickness may be the cause. The crater floor is very dark and shows no direct connection with the large outflow to the south, which emphasizes the asymmetry observed. Isabella crater ejecta and outflow materials clearly postdate several small craters in the vicinity.

Helen Planitia: In addition to V-50, this project consists of mapping Helen Planitia at 1:10M-scale (0-57°S/180-300°E), which covers over 70 million square kilometers (approximately $1/8^{th}$) of the surface of Venus and the southern portion of the Beta-Atla-Themis (BAT) region. The BAT province is of particular interest with respect to evaluating global paradigms regarding Venus' geologic history and thermal evolution, considering it is "ringed" by volcano-tectonic troughs (Parga, Hecate, and Devana Chasmata), has an anomalously high-density of volcanic features with concentrations 2-4 times the global average [3], and is spatially coincident with young terrain as shown by the Average Surface Model Age [4 and 5]. The BAT province is key to better understanding Venus' current volcanic and tectonic modes.

Last year's efforts were focused on mapping the distribution and orientation of structural trends and flow morphologies, and the demarcation of flow unit boundaries. Several hundred radial and circular features (both digitate and lobate flow fields and fracture, fault, and ridge suites) were mapped in this fashion and matched closely the existing coronae and/or volcanic landform databases [6 and 7].

The majority of these radial/circular features lie within a few hundred kilometers of the Parga Chasmata rift system marking a southeast trending line of relatively young volcano-tectonic activity. Although some very localized embayment and crosscutting relationships display clear relative age relations between centers of activity, the majority of Parga Chasmata volcanism and tectonism overlaps in time from Atla Regio in the west to Themis Regio in the east, extending ~10,000 linear kilometers.

Efforts by Martin et al. [8] resulted in a comprehensive categorization of 131 coronae along Parga Chasmata. Their morphologic and spatial analyses concluded that there are no significant correlations between corona type (annulus characteristics or topography) and size with respect to volcanic output or chasma-related tectonics. However, recent geophysical analysis by

Dombard et al., [9] has identified seven sites within the BAT region that may represent contemporary activity. Four of these sites fall within the Helen Planitia region: Maram (600 km), Atete (600 km), Kulimina (170 km), and Shiwanokia (500 km) Coronae. Mapping relations show that each of the four coronae represents some of the youngest local activity [10]. All four coronae also share similar plan form characteristics displaying radiating flows in excess of several hundred kilometers, fractures and faults that trend parallel to Parga Chasmata, and moderately steep concentric bounding scarps. They also fall directly along the main trend of Parga Chasmata rifting, which may suggest that while using strict spatial relations concludes no relationship between coronae and Parga Chasmata [e.g., 5], temporal-spatial relations correlating high-resolution mapping with putative active geophysical centers provides evidence of active rifting and volcanism on the Venusian surface.

The degree to which coronae and chasmata are genetically related remains elusive given the inability to determine, at least with certainty, Venus' surface age. Detailed stratigraphic analyses coupled with geophysical examination may provide the means to understand contemporary processes that may be extrapolated over history – the present is the key to the past.

Mapping of these centers along Parga and within the surrounding plains continues and the generation of quality control maps has begun (see Figure 1 below).

References: [1] Bleamaster III, L.F., (2007) Open-File Report 2007-1233. [2] Johnson, J.R. et al., (1999) USGS Geo. Inv. Sers. I-2610. [3] Head et al., (1992) J. Geophys. Res., 97(E8), 13,153-13,197. [4] Phillips, R.J. and Izenberg, N.R., (1995) Geophys. Res. Lett., 22, 1517-1520. [5] Hansen, V.L. and Young, D.A., (2007) GSA Special Paper. [6] Crumpler L.S. et al., (1997) in Venus II, 697-756. [7] Stofan E.R. et al., (2001) Geophys. Res. Lett., 28, 4267-4270. [8] Martin et al., (2007) J. Geophys. Res., 112,E04S03, doi:10.1029/2006JE002758. [9] Dombard et al., (2007) J. Geophys. Res., 112, E04006, doi:10.1029/2006JE002731. [10] Bleamaster III, L.F., (2007) LPSC XXXVIII, abstract 2434.

Figure 1. Side-by-side comparison of mapping by Ivan Lopez (left) and Les Bleamaster (right), (merged product in the middle) of 10ºx10º region at the cartographic boundaries of V-52, V-53, and V-60 in HPRSA. This exercise (quality control mapping) illustrates the advantage of having multiple sets of eyes on the same "ground" and the importance of compromise for determining unit boundaries. Although unit boundaries were different, relative time relations were mostly consistent.

RENEWED MAPPING OF THE NEPTHYS MONS QUADRANGLE (V-54), VENUS. N.T. Bridges, Jet Propulsion Laboratory, California Institute of Technology (MS 183-501, 4800 Oak Grove Dr., Pasadena, CA 91109; nathan.bridges@jpl.nasa.gov).

Introduction: After a long hiatus due to competing tasks with the PI, mapping of Venus' Nepthys Mons Quadrangle (V-54, 300-330°E, 25-50°S) has been resumed, with planned submission late in 2008 or early 2009. Major goals are to determine the style of volcanism and tectonism over time, the evolution of shield volcanoes, the evolution of coronae, the characteristics of plains volcanism, and what these observations tell us about the general geologic history of Venus. This abstract largely repeats earlier progress reports, with some updates to show GEMS that the PI intends to complete this task in the near future.

Methods: Geologic units and structures have been mapped onto hardcopy FMAPs and then transferred to the 1:5 million-scale map base (Figure 1). Pseudostereo anaglyphs have proved an indispensable tool and have resulted in a virtual complete revision of previously mapped areas [1,2]. At FMAP scale, structural trends and inferred ages are broken out using different symbols and colors. These are in the process of being transferred to a 1:5 million-scale structure map separate from the geologic map. The geologic units, structures, impact craters, coronae, and volcanoes are being arranged in time-stratigraphic sequences as the mapping progresses.

General Stratigraphy and Structure: Using basic geologic mapping principles [3], 33 units are broken out, consisting of flow materials (11 units), volcanic construct materials (5 units), plains materials (12 units), tessera material (1 unit, with considerable structural variability), and impact crater materials (4 units). Tesserae, distributed as scattered inliers, appears to be the oldest unit and is truncated by tectonized plains and other plains units. Stratigraphically above these regional plains units are scattered fields of shields and associated flows. Polygonal flows are common and appear to show a range of ages. Flows associated with coronae and shield volcanoes are intermediate to young in age. In all cases, craters appear to be younger than adjacent units, consistent with other areas on Venus [4]. No craters have been found on the large shields.

Interesting Results and Observations:

Tesserae: To better understand the complex structural relationships within tesserae, I have mapped out individual structural trends and attempted to estimate the history of activation for these mapped sets, following in many respects efforts of previous workers [5].

Polygonal and Shield Plains: Polygonal plains are now mapped as a single unit of intermediate age (as opposed to three previously [1,2]) but several members with locally-distinct stratigraphic positions are apparent. Shield-rich plains are intermediate to young, consistent with observations in some quadrangles [6,7] and inconsistent with others [8,9] (i.e., small shields form throughout the geologic history of Venus). The polygonal plains are commonly associated with and, in many cases, difficult to distinguish from, shield plains (Figure 1). This suggests that the polygons are lava flow cooling structures, as opposed to the manifestation of cooling stresses from planet-wide global change [10-12]. However, the polygons are enigmatic features that are still poorly understood and we are open to other interpretations as the mapping progresses.

Large shield volcanoes and coronae: One of the original goals of this mapping effort was to find stratigraphic relationships among coronae, large shield volcanoes, and intermediate structures. Many of the relationships are quite complex, requiring detailed structural mapping such as that described for the tesserae, above. Many "shields" (e.g., Tefnut Mons) have corona-like radial structures and there is commonly no obvious distinction between “corona,” “mons,” and “patera.” The flows from these features can be mapped out and in some cases stratigraphic relationships determined; in other examples, this is more difficult. Large flows from shields/coronae commonly post-date regional plains and many local structures.

References: [1] Bridges, N.T. (2001), *Lun. Plan. Sci. XXXII*, 1376. [2] Bridges, N.T. (2001), *Planetary Mappers' Meeting*, Albuquerque, NM. [3] Wilhelms, D.E. (1972), *Geologic Mapping of the Second Planet*, Interagency Report: Astrogeology 55, U.S. Geological Survey. [4] Schaber, G.G. et al. (1992), *JGR, 97*, 13,257-13,301. [5] Hansen, V.L. (2000), *Earth Plan. Sci. Lett., 176*, 527-542. [6] Aubele, J.C. (1996), *LPSC XXVII*, 49-50. [7] Basilevsky, A.T. and J.W. Head (1998), *JGR, 103*, 8531-8544. [8] Addington, E.A. (1999), *LPSC XXX*, 1281. [9] Guest, J.E. and E.R. Stofan (1999), *Icarus, 139*, 55-66. [10] Bullock, M.A. and D.H. Grinspoon (1996), *JGR, 101*, 7521-7529. [11] Solomon, S.C. et al. (1999), *Science, 286*, 87-90. [12] Anderson, F.S. and S.E. Smrekar (1999*), JGR, 104*, 30,743-30,756.

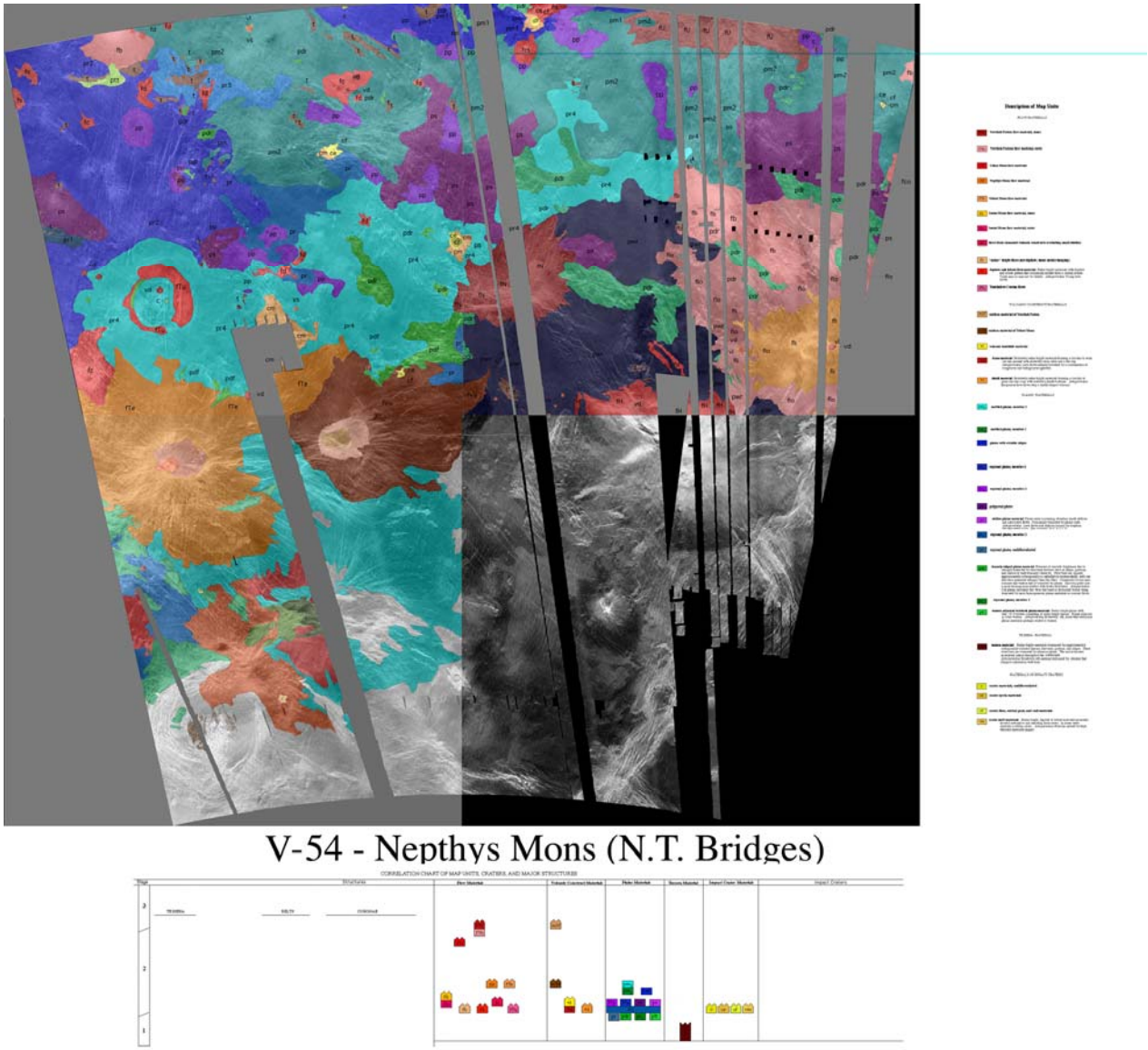

Figure 1: Preliminary geologic map of V-54. The SE corner has been mapped at FMAP scale but is not yet transferred to the basemap.

Mapping the Sedna-Lavinia Region of Venus.

Bruce A. Campbell and Ross F. Anderson, *Center for Earth and Planetary Studies, Smithsonian Institution, MRC 315, PO Box 37012, Washington, DC 20013-7012.*

Overview. Geologic mapping of Venus at 1:5 M scale has shown in great detail the flow complexes of volcanoes, coronae, and shield fields, and the varying structural patterns that differentiate tesserae from corona rims and isolated patches of densely lineated terrain. In most cases, however, the lower-elevation plains between the higher-standing landforms are discriminated only on the basis of potentially secondary features such as late-stage lava flooding or tectonic overprinting. This result, in which volcanoes and tesserae appear as "islands in the sea," places weak constraints on the relative age of large upland regions and the nature of the basement terrain. In this work, we focus on the spatial distribution and topography of densely lineated and tessera units over a large region of Venus, and their relationship to apparently later corona and shield flow complexes. The goal is to identify likely connections between patches of deformed terrain that suggest earlier features of regional extent, and to compare the topography of linked patches with other such clusters as a guide to whether they form larger tracts beneath the plains.

Mapping Approach. We are mapping the region from 57S to 57N, 300E-60E. Since the 1:5 M quadrangles emphasize detail of tessera structure and corona/edifice flows, we simply adopt the outlines of these features as they relate to the outcrops of either "densely lineated terrain" or tessera (Fig. 1). The densely lineated material is mapped in many quadrangles based on pervasive structural deformation, typically with a single major axis (in contrast to the overlapping orthogonal patterns on tesserae). This unit definition is often extended to include material of corona rims. We do not at present differentiate between plains units, since earlier efforts show that their most defining attributes may be secondary to the original emplacement (e.g., lobate or sheet-like flooding by thin flow units, tectonic patterns related to regional and localized stress regimes) [1].

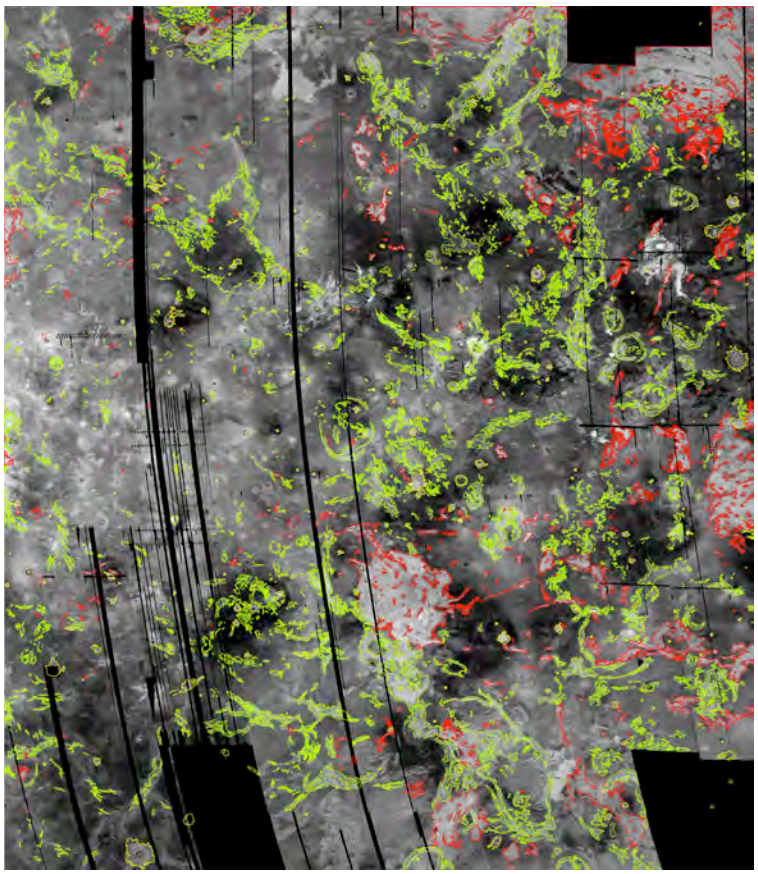

Fig. 1. Radar base map of the Sedna-Lavinia region in Cylindrical projection. Tessera terrain outlined in red, densely lineated terrain shown in green, and craters shown in yellow.

Preliminary Results. In maps for quads V-9 and V-20 [2,3], we suggested that a pattern of SW-NE trending tessera fragments might reflect an earlier, contiguous regional fabric. We are using Magellan topography data linked with the mapped unit boundaries to study the relationship of these fragments (Fig. 2).

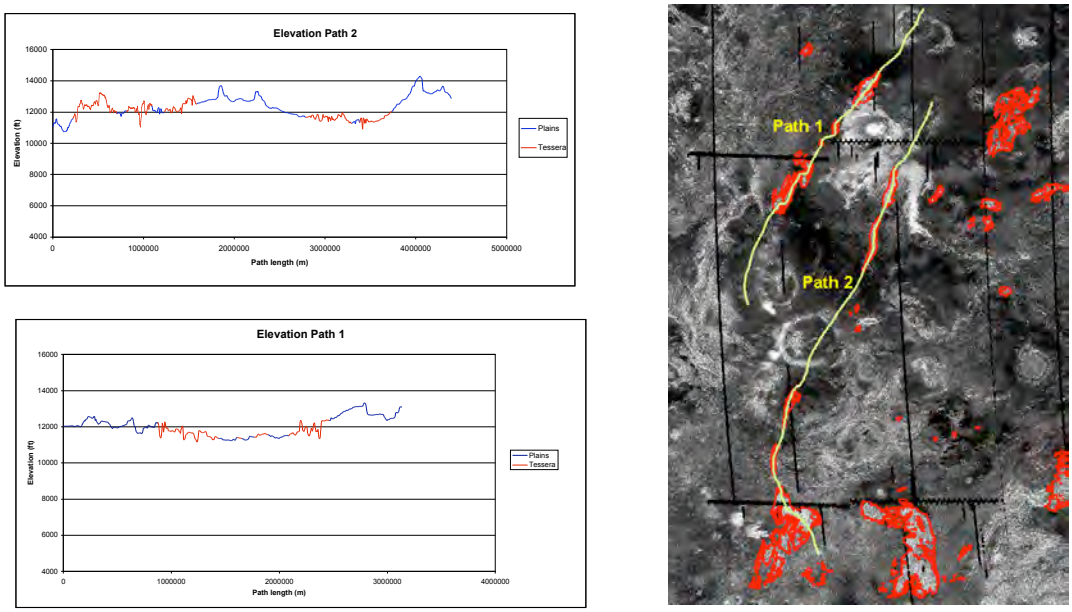

Fig. 2. Two elevation charts for profiles across Bell Regio (at north) and a cluster of coronae west of Mead crater to the south. Green traces show paths through tessera fragments outlined in red.

Tessera terrain along Path 1, west and north of Tepev Mons, has relatively similar elevation to the two linear fragments, south of Tepev, shown in Path 2. The northern outcrops on Path 2 also appear to lie in a topographic saddle between the volcanic constructs of Bell Regio and eastern Eistla Regio. The large outcrop and smaller fragments south of eastern Eistla, however, are ~1 km above those surrounding Bell Regio, and abut (or are superposed by) materials of Calakomana Corona. If there is a regional tessera background that links the two sets of outcrops, this basement must slope downwards toward the north. There are other areas, such as northeast of Alpha Regio, where fragments of tessera terrain appear to link larger outcrops. The densely lineated terrain also forms chains of apparently associated patches, sometimes in a roughly parallel distribution to outcrops or larger blocks of tessera. Further work will attempt to map these connections to develop a model for the extent of highly deformed terrain and possible age relationships among the major upland regions.

References. [1] Hansen, V.L., 2000, Geologic mapping of tectonic planets, Earth and Planetary Science Letters, v. 176, p. 527-542. [2] Campbell, B.A., and D.A. Clark, Geologic map of the Mead Quadrangle (V-21), Venus, U.S. Geological Survey Atlas of Venus, *Sci. Inv. Map 2897,* 2006. [3] Campbell, B.A., and P.G. Campbell, Geologic map of the Bell Regio (V-9) Quadrangle, Venus, *U.S. Geological Survey, I-2743*, 2002.

GEOLOGIC MAPPING OF THE GUINEVERE PLANITIA QUADRANGLE OF VENUS. David A. Crown[1], Ellen R. Stofan[2], and Leslie F. Bleamaster III[1], [1]Planetary Science Institute, 1700 E. Ft. Lowell Rd., Suite 106, Tucson, AZ 85719, [2]Proxemy Research, P.O. Box 338, Rectortown, VA 20140, crown@psi.edu.

Introduction: The Guinevere Planitia quadrangle of Venus (0-25°N, 300-330°) covers a lowland region east of Beta Regio and west of Eistla Regio, including parts of Guinevere and Undine Planitiae. The V-30 quadrangle is dominated by low-lying plains interpreted to be of volcanic origin and exhibiting numerous wrinkle ridges. Using Pioneer Venus, Goldstone, and Arecibo data, previous investigators have described radar bright, dark, and mottled plains units in the Guinevere Planitia region, as well as arcuate fracture zones and lineament belt segments that define the Beta-Eistla deformation zone [1-5].

Magellan SAR images show that volcanic landforms compose the majority of the surface units in V-30 [6-7]. The quadrangle contains parts of four major volcanoes: Atanua (9°N, 307°), Rhpisunt (3°N, 302°), Tuli (13°N, 314°), and Var (3°N, 316°) Montes, and three coronae: Hulda (12°N, 308°), Madderakka (9°N, 316°), and Pölöznitsa (1°N, 303°). Seymour crater, located at 18°N, 327°, is associated with extensive crater outflow deposits.

Scientific Objectives: Scientific objectives for mapping V-30 include analysis of: 1) the geologic evolution of venusian plains, 2) styles of volcanism within venusian plains, including the formation of shield volcanoes, lava flows and flow fields, lava channels, and small volcanic constructs, and 3) the geologic context for steep-sided dome formation. Previous research related to geologic mapping has included morphologic and radar remote sensing analyses of venusian steep-sided domes and terrestrial silicic domes as potential analogues [8-10], as well as analyses of the morphologic and radar backscatter properties of lava flows associated with volcanoes in Guinevere Planitia [11].

Data Sets: Preparation of the 1:5M-scale geologic map of the Guinevere Planitia quadrangle includes analysis of Magellan data, including synthetic aperture radar (SAR) images and altimetry, roughness (RMS slope), reflectivity, and emissivity data sets. Full-resolution Magellan image mosaics (FMAPs) and synthetic parallax stereo images produced by the U.S. Geological Survey are key mapping products for unit characterization and determination of stratigraphic relationships.

Mapping Results: Mapping completed to date [6-7, 12-13] has defined four main types of geologic units in the Guinevere Planitia quadrangle: flow materials, plains materials, upland terrain, and crater materials. Scattered throughout the map area are embayed remnants of intensely deformed materials; some of these show two or more tectonic fabrics (*tessera*) and others show one dominant orientation of lineaments (*lineated upland material*). Tesserae are locally high-standing and always embayed by the surrounding units. Within lineated uplands, patches of plains units are observed.

The extensive volcanic plains evident across the V-30 quadrangle have been divided into two units. *Mottled, lineated plains* are generally large expanses of rolling topography that contain a variety of small volcanic domes, cones, shields, and flows. Zones of tectonic disruption are common. Mottled, lineated plains are typically embayed by the regional plains but flows apparently sourced within mottled, lineated plains also locally superpose regional plains. *Guinevere regional plains* form low-lying regions that exhibit uniform radar brightness over large distances and are generally radar dark. Flow margins can be identified, but small volcanic edifices are not abundant. Fractures and ridges are common, and several canali are evident. Guinevere regional plains frequently embay exposures of upland terrain and mottled, lineated plains. Typically, volcanic flows are superposed on the regional plains. Locally plains embay the flanks of the major volcanoes in the map area.

Volcanic flow materials in V-30 have been divided into two major morphologic types. *Plains-forming flow materials* are extensive, radar bright or dark, relatively flat-lying sheets and can extend for hundreds of kilometers from their apparent source vents; some plains-forming flows are associated with coronae. *Lobate flow materials* are narrow, sinuous, overlapping radar bright and dark deposits with lobate margins that form radial patterns around their source vents; lobate flow materials have accumulated to form the surfaces of the major volcanoes in the map area. Numerous small domes, cones, and shields are observed in association with lobate flow materials on these large volcanoes. Flow materials superpose exposures of upland terrain and the plains. Flows associated with the major volcanoes are locally the youngest geologic features across the quadrangle.

Brian et al. [14] recently defined a new topographic rise, Laufey Regio, that includes Var and Atanua Montes and a series of coronae and their associated flow materials. Laufey Regio, 0.5 km high and 1000 x 2000 km across, is considered to be a volcano-dominated rise in a late-stage of evolution; a complex, nondirectional geologic history was

described, with protracted and overlapping episodes of volcanic and tectonic activity.

Crater materials mapped in V-30 include the ejecta, rim, and floor deposits of nine recognized impact craters, several of which exhibit prominent crater outflow deposits. Both bright and dark splotches are found in association with impact craters. Crater materials are observed to superpose plains and the four major volcanoes in the quadrangle.

Structural features observed in Guinevere Planitia include wrinkle ridges, fractures, and lineaments found primarily in plains units, coronae and corona-like structures, and tesserae and other highly tectonized units. In the plains, structures exhibit a diversity of orientations and occur in sets of features with similar trends. Prominent E-W and SE-NW trends are observed in the regional plains at the eastern margin of V-30.

References: [1] Campbell, D.B. et al. (1989) *Science, 246*, 373-377. [2] Arvidson, R.E. et al. (1990) in *Proc. Lunar Planet. Sci. Conf., 20th*, 557-572. [3] Senske, D.A. (1990) *Earth, Mons, and Planets, 50/51*, 305-327. [4] Senske, D.A. et al. (1991) *Earth, Moon, and Planets, 55*, 163-214. [5] Stofan, E.R. et al. (1990) *Lunar Planet. Sci. Conf., XXI*, 1208-1209. [6] Crown, D.A. et al. (1993) *Lunar Planet. Sci. Conf., XXIV*, 355-356. [7] Crown, D.A. et al. (1994) *Lunar Planet. Sci. Conf., XXV*, 301-302. [8] Anderson, S.W. et al. (1998) *Geol. Soc. Am. Bull., 110*, 1258-1267. [9] Stofan, E.R. et al. (2000) *J. Geophys. Res., 105*, 26,757-26,771. [10] Plaut, J.J. et al. (2004) *J. Geophys. Res., 109* E03001, doi:10.1029/2002JE002017. [11] Byrnes, J.M. and D.A. Crown (2002) *J. Geophys. Res., 107* (E10), 5079, doi:10.1029/2001JE001828. [12] Crown, D.A. and E.R. Stofan (2006) *USGS OFR 2006-1263*. [13] Crown, D.A. et al. (2008) *Lunar Planet. Sci. Conf., XXXIX*, abstract 1725. [14] Brian, A.W. et al. (2004) *J. Geophys. Res., 109*, E07002, doi:10.1029/2002JE002010.

Figure 1. Simplified version of geologic map of V-30 quadrangle over Magellan SAR image base. Tessera = dark purple, lineated upland material = light purple, mottled, lineated plains = blue, Guinevere regional plains = green, plains-forming flow material = tan, lobate flow material = dark tan, flow materials of 4 large volcanoes = reds and oranges, impact crater material = yellow.

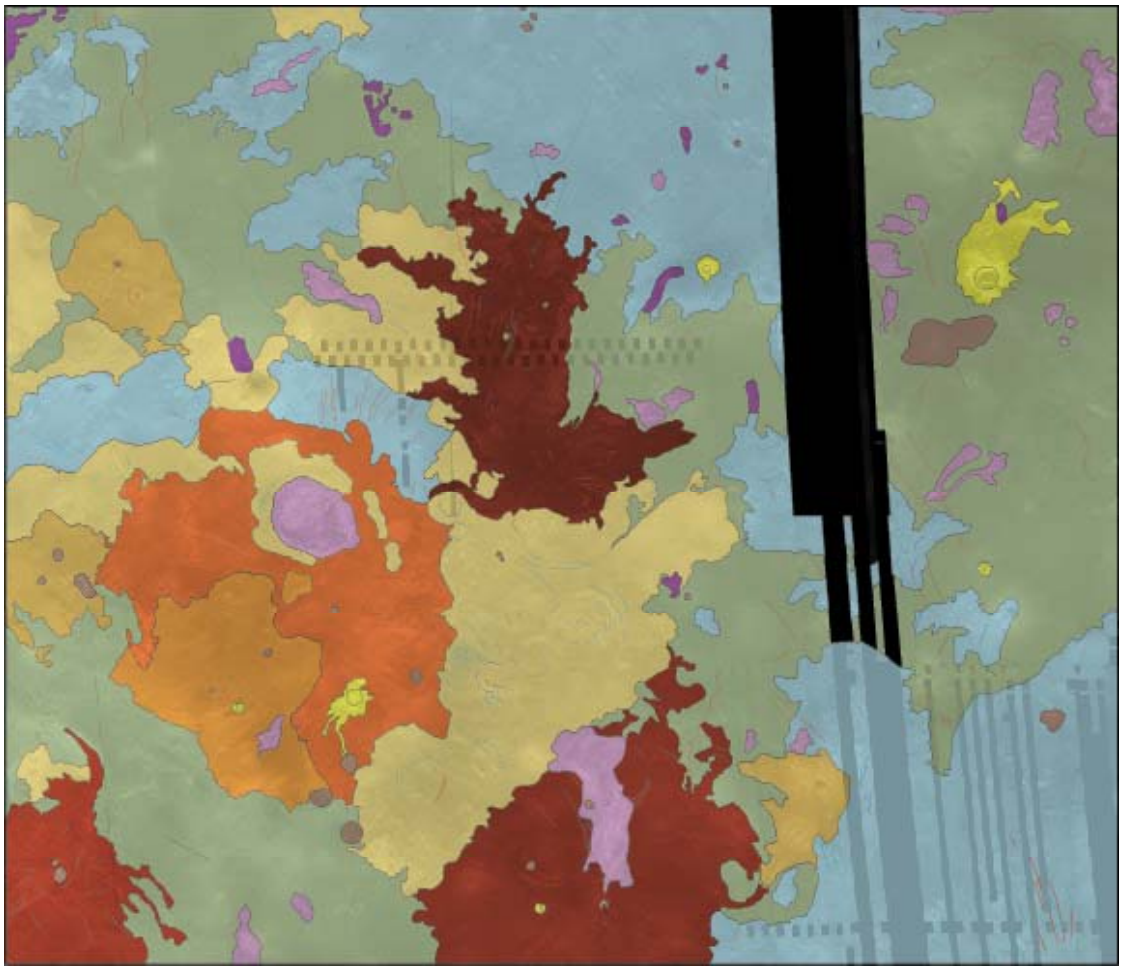

GEOLOGICAL MAPPING OF FORTUNA TESSERA (V-2): VENUS AND EARTH'S ARCHEAN PROCESS COMPARISONS. J. W. Head[1], D. M. Hurwitz[1], M. A. Ivanov[1,2], A. T. Basilevsky[1,2], and P. Senthil Kumar[1,3], [1]Dept. of Geological Sciences, Brown University, Providence, RI 02912 (james_head@brown.edu), [2]Vernadsky Institute of Geochemistry and Analytical Chemistry, RAS, Moscow, Russia, [3]National Geophysical Research Institute, Hyderabad 500007, India (senthilngri@yahoo.com).

Introduction: The geological features, structures, thermal conditions, interpreted processes, and outstanding questions related to both the Earth's Archean and Venus share many similarities [1-3] and we are using a problem-oriented approach to Venus mapping, guided by insight from the Archean record of the Earth, to gain new insight into the evolution of Venus and Earth's Archean. The Earth's preserved and well-documented Archean record [4] provides important insight into high heat-flux tectonic and magmatic environments and structures [5] and the surface of Venus reveals the current configuration and recent geological record of analogous high-temperature environments unmodified by subsequent several billion years of segmentation and overprinting, as on Earth. Elsewhere we have addressed the nature of the Earth's Archean, the similarities to and differences from Venus, and the specific Venus and Earth-Archean problems on which progress might be made through comparison [6]. Here we present the major goals of the Venus-Archean comparison and show how preliminary mapping of the geology of the V-2 Fortuna Tessera quadrangle is providing insight on these problems. We have identified five key themes and questions common to both the Archean and Venus, the assessment of which could provide important new insights into the history and processes of both planets.

Geological Mapping of the Fortuna Tessera Quadrangle (V-2): The Fortuna Tessera Quadrangle (V-2) (Fig. 1-2) lies just south of the Snegurochka Planitia Quadrangle (V-1) and between two quadrangles that we have previously mapped, Lakshmi Planum (V-7) to the west and Meskhent Tessera (V-3) to the east [7-8]. To the south it is bordered by Bereghinya Planitia (V-8 [9]) and Bell Regio (V-9 [10]). The most prominent topography in the region is the broad Ishtar Terra highland and its associated distinctive mountain belt, Maxwell Montes, representing the highest topography on Venus (Fig. 3). The vast expanse of Fortuna Tessera wraps broadly around the eastern part of Maxwell Montes and is largely separated from Laima Tessera to the southeast by two parallel deformation belts, Sigrun-Manto Fossae and Aušrā Dorsa (Fig. 2, 4), each characterized by different tectonic styles. The broad terrains of the quadrangle extend to the west into the volcanically resurfaced upland Lakshmi Planum, surrounded by the tessera and folded mountain belts of western Ishtar Terra and to the east into Meskhent Tessera [7-8, 11-15].

One of the most distinctive elements of V-2 is the presence of the folded mountain belt Maxwell Montes and the extensive Fortuna Tessera highland, clearly representing large domains of thickened crust [16-19]. Maxwell rises to about 11 km elevation and drops off to the east to about 5-6 km (Fig. 2-3), suggesting a fundamental change in crustal thickening processes. The parallel ridges and troughs of Maxwell are mirrored in the structure of western Fortuna as the tessera fabric wraps broadly around the base of Maxwell (Fig. 2). Maxwell Montes is flanked to the north and south by two basin-like features (Fig. 5) that contain unusual arcuate, overlapping corona-like structures; these regions bear some resemblance to areas of thickened crust that have delaminated and readjusted isostatically and thermally. Further to the east, a broad depression separates western and eastern Fortuna (Fig. 12), suggesting that the eastern domain may be more related to Laima and Meskhent Tesserae than to the Maxwell-dominated western Fortuna (Fig. 5). Laima Tessera is characterized by linear texture not unlike that observed on the Earth's seafloor [20] (although seafloor spreading does not currently occur), and this terrain is undergoing detailed analysis to assess its origin and relation to tessera in Fortuna. Establishing the detailed character of each of these tessera terrains [21], understanding the nature and sequence of deformation [15, 18], and assessing the relationships to crustal thickening processes are among the main goals of the mapping.

Among the most prominent features in the plains in V-2 are two parallel deformation belts, Sigrun-Manto Fossae and Aušrā Dorsa, that trend SW-NE across the central portion (Fig. 2, 4). The presence of these two parallel features provides the opportunity not only to characterize them in detail, but also to assess their temporal relationships and their relationships to crustal extension and shortening processes. For example, Sigrun Fossae (Fig. 4) shows evidence for extension (graben), associated intrusion (radial graben) and volcanism, while Aušrā Dorsa is characterized by folds and some evidence for shear, and partly intersects Sigrun. Is this deformation contemporaneous, or sequential, and how does it relate to the crustal thickening processes associated with the tessera? Could the extension be a response to crustal thickening? Could the shortening be related to the waning stages of tessera formation? These same types of questions are clearly important in Archean terrains [5].

Summary: Geological mapping and processes studies in the V-2 Fortuna Tessera Quadrangle offer key features and relationships (Fig. 2) that will permit us to address many of our important Venus-Archean thematic questions [6] including: 1) crustal thickening environments and processes, 2) the nature of diapirism and possible delamination, and 3) the nature and origin of deformation belts and their relation to crustal thickening processes.

References: 1) E. Nisbet, *The Young Earth*, Allen & Unwin, 1987; 2) K. Condie, *Archean Crustal Evolution*, Elsevier, 1994a; 3) S. Solomon & J. Head, *Science*, 252, 252, 1991; 4) W. Bleeker, *Lithos*, 71, 99, 2003; 5) K. Condie & K. Benn, *AGU Mon.*, 47, 2006; 6) J. Head et al., Venus-Archean, *EPSC* (abs), 2008; 7) M. Ivanov & J. Head, Lakshmi Planum, USGS V-7, in review, 2008; 8) M. Ivanov & J. Head, *USGS I-3018*, 2008; 9) G. McGill, *USGS I-2794*, 2004; 10) B. Campbell & P. Campbell, *USGS I-2743,* 2002; 11) V. Barsukov et al., *JGR*, 91, D399, 1986; 12) J. Head et al., *GRL*, 17, 1337, 1990; 13) A. Pronin, *Venus Geology*, U of A, 68, 1992; 14) W. Kaula et al., *JGR*, 97, 16085, 1992; 15) V. Hansen et al., *JGR*, 105, 4135, 2000; 16) J. Head, *Geology*, 18, 99; *EMP*, 50/51, 391, *EMP*, 50/51, 25, 1990; 17) M. Keep & V. Hansen, *JGR*, 99, 26015, 1994; 18) V. Hansen & J. Willis, *Icarus*, 123, 296, 1996; 19) M. Pritchard et al., *GRL*, 24, 2339, 1997; 20) J. Head, *JGR*, 95, 7119, 1990; 21) M. Ivanov & J. Head, *JGR*, 101, 14861, 1996.

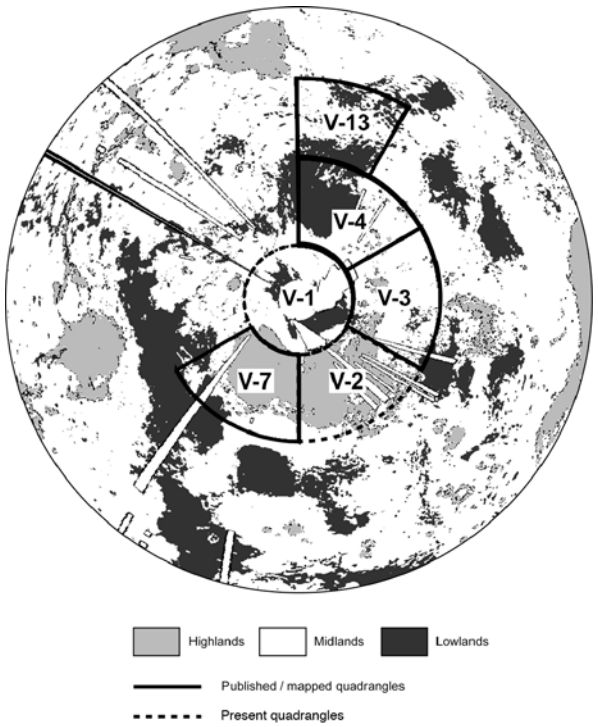

Fig. 1. Northern hemisphere of Venus. Solid lines indicate maps completed (V-4, V-13 published, V-3 in proof, V-7 in review).

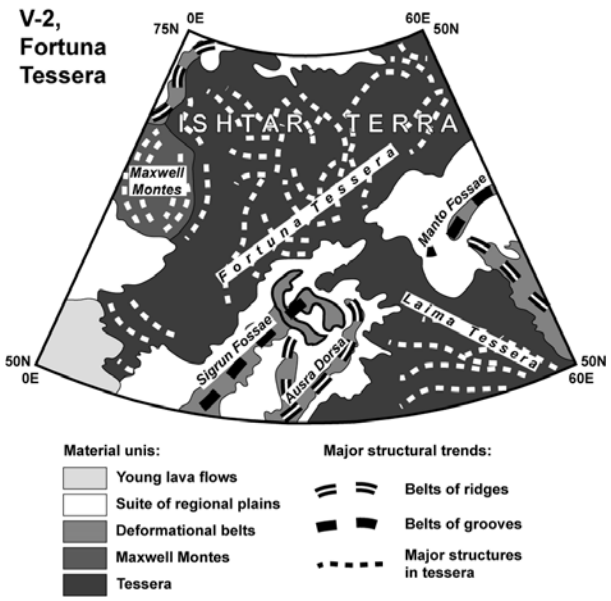

Fig. 2. Geologic sketch map of the Fortuna Tessera (V-2) quadrangle.

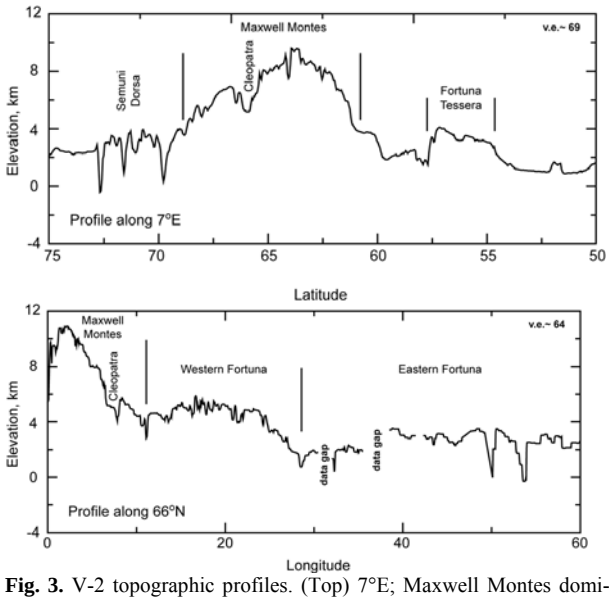

Fig. 3. V-2 topographic profiles. (Top) 7°E; Maxwell Montes dominates central portion, bordered to south by large depression (Fig. 5). (Bottom) 66°N; Maxwell Montes, elevated W., lower E. Fortuna Tessera.

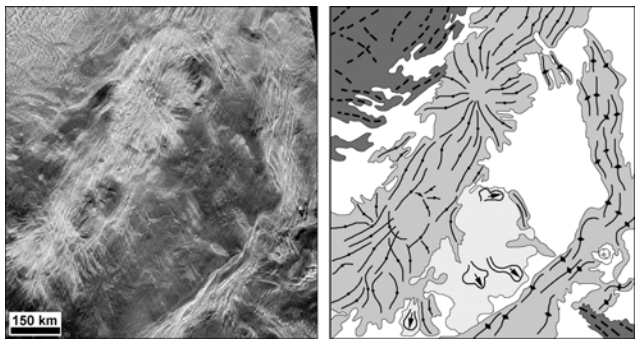

Fig. 4. Image and sketch map of two deformational belts (V-2). Sigrun Fossae (middle portion of image) consists of densely packed graben and Aušrā Dorsa (lower right) is a belt of broad curvilinear ridges. Center ~52°N, 20°E.

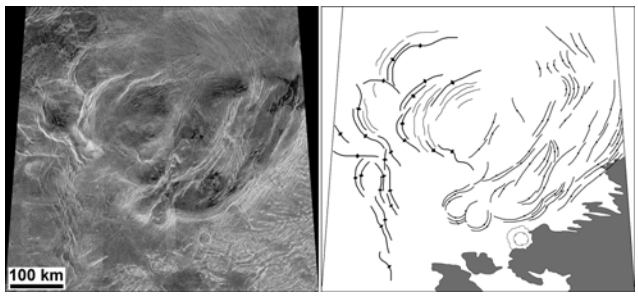

Fig. 5. Image and sketch map of a depression in the plains S. of Maxwell Montes (V-2). The depression is within regional plains and outlined by arcuate ridges in the west and arcuate graben in the east. Center ~59°N, 5°E.

GEOLOGICAL MAPPING OF THE NORTH POLAR REGION OF VENUS (V-1 SNEGUROCHKA PLANITIA): SIGNIFICANT PROBLEMS AND COMPARISONS TO THE EARTH'S ARCHEAN. J. W. Head[1], D. M. Hurwitz[1], M. A. Ivanov[1,2], A. T. Basilevsky[1,2], and P. Senthil Kumar[1,3], [1]Dept. of Geological Sciences, Brown University, Providence, RI 02912 (james_head@brown.edu), [2]Vernadsky Institute of Geochemistry and Analytical Chemistry, RAS, Moscow, Russia, [3]National Geophysical Research Institute, Hyderabad 500007, India (senthilngri@yahoo.com).

Introduction: The geological features, structures, thermal conditions, interpreted processes, and outstanding questions related to both the Earth's Archean and Venus share many similarities [1-3] and we are using a problem-oriented approach to Venus mapping, guided by perspectives from the Archean record of the Earth, to gain new insight into both. The Earth's preserved and well-documented Archean record [4] provides important insight into high heat-flux tectonic and magmatic environments and structures [5] and Venus reveals the current configuration and recent geological record of analogous high-temperature environments unmodified by subsequent several billion years of segmentation and overprinting, as on Earth. We have problems on which progress might be made through comparison [6]. Here we present the major goals of the geological mapping of the V-1 Snegurochka Planitia Quadrangle, and themes that could provide important insights into both planets:

Goals in the Geological Mapping of the Snegurochka Planitia Quadrangle (V-1): V-1 (Fig. 1-2) is centered on the N. Pole and contains two major plains areas, Snegurochka and Louhi Planitiae, forming a broad circular to angular depression about 2500 km across (Fig. 3). This depression is surrounded to the south (Fig. 1-2) by Ishtar Terra, a complex tessera/coronae region (Tethus Regio), a circular lowland (Atalanta Planitia), a fan-shaped zone of deformation belts (Lukelong to Okipeta Dorsa) converging into Dennitsa Dorsa toward the pole, and a region of multiple coronae and volcanoes (Metis Regio) adjoining the western edge of Ishtar Terra.

Contained within central V-1 are abundant *volcanic plains* (Fig. 4-5) deformed by wrinkle ridges, similar to those widely distributed on Venus [7-10] and containing extensive sinuous rilles, suggestive of high effusion rates and high-temperature lavas [11]. Key questions are: What is the evidence for their mode of emplacement in this area? How are they related in time, space, and mode of origin to the lobate plains seen at the margins of the tessera (Fig. 5-6)?

Deforming the central part of the plains, and converging toward the pole, is a series of belts representing both extensional and contractional deformation. Belts of extensional origin emerge from Metis Regio to the south, intersect with Anahit and Pomona Coronae, and then turn north at the edge of Ishtar Terra, toward the pole (Fig. 2). A series of belts of contractional origin (Dennitsa Dorsa) enter the quadrangle from the fan-shaped belt opening to the south and contain a distinctive corona-like structure (Fig. 2, 4); this belt merges with a low-elevation tessera region near the pole and then extends south in the form of Sel-Anya Dorsa into Tethus Regio, merging with Semuni Dorsa (Fig. 5), marking the margin of Fortuna Tessera. Thus, a critical goal is to establish relationships between: 1) deformation belts and the regional plains, 2) deformation belts and wrinkle ridges that deform the plains, and 3) two different types of deformation belts themselves. For example, do the geological relationships support a pre-plains, syn-plains, or post-plains age for the deformation belts? Did the two types of deformation belts form at different times, perhaps representing sequential styles of tectonism, or did they form simultaneously as part of a regional stress field?

Three major *corona* structures occur within the quadrangle and represent an opportunity to assess their comparative structure, as well as their age and geological relationships to more regional units and structures. Anahit and Pomona Coronae (Fig. 2) lie at the edge of Metis Regio and contain the classic highly deformed annulus surrounding an area of central domal uplift. Each shows evidence for a late stage volcanic center that might represent post-diapiric-rise intrusion and associated magmatism and volcanism. Some classification schemes suggest that *volcanic edifices* might represent initial or late stage phases of corona formation, or proto-coronae that did not form annuli due to contrasting thermal structure [12]. The presence of an adjacent classic *shield volcano*, Renpet Mons (Fig. 2), offers the opportunity to assess these relationships and address these questions. A third corona, Maslenitsa, lies along the southern part of Dennitsa Dorsa (Fig. 2), and shows very close and distinctive relationships with this deformation belt (Fig. 4). Do coronae represent buoyant diapiric upwelling processes and how are such processes related to regional tectonic trends and sense of deformation [13-14]?

Tessera terrain occurs in two settings (Fig. 2). A patch of low-standing tessera lies near the N. pole with several converging deformation belts; this offers the opportunity to assess the relationships of deformation belts and tessera formation. For example, tessera is defined in part as superposition of two generally orthogonal tectonic deformation patterns; we are assessing whether this tessera region results from the contemporaneous confluence of two different types of deformation belts, or are there clear superposition relationships that would help to assess the regional ages of the different deformation belts. The most significant development of tessera lies along the S. margin of V-1 in the form of the northern margin of Ishtar Terra (Itzpapalotl and Fortuna Tesserae; Fig. 5-6); these are part of one of the most distinctive and contiguous tessera terrains on Venus, second only to Aphrodite Terra. Our mapping in V-7 to the south of Itzpapalotl [15] provides an excellent setting in which to examine this important area. Furthermore, the mapping of V-2 [16] is providing an important framework for the interpretation of the northern margin of Fortuna Tessera in the Semuni Dorsa region (Fig. 5). These two occurrences permit us to assess important questions about the nature of crustal thickening processes. Itzpapalotl Tessera lies at the N. edge of a crustal plateau containing folded mountain belts (Freyja Montes) lying ~7 km above Snegurochka Planitia (Fig. 3, 6); the edge of the plateau drops 3-4 km to a distinctive lobate lava-flow-containing moat and adjacent outboard rise (Fig. 6) that bears very strong similarity to a flexural margin [17]. The deformation within Itzpapalotl shows signs of intense shortening, folding and shear [18-19]. What is the detailed relationship between the range of structures observed and topography? What are the detailed relationships between Itzpapalotl and the adjacent less-deformed volcanic plains? What deformational processes are responsible for the extreme crustal thickening implied by the topography (Fig. 3) in the absence of current plate tectonics? Additional clues to these questions can be obtained from the assessment of the Semuni Dorsa deformation

belt lying along the northern margin of Fortuna Tessera. Here the topographic rise is much less extreme (Fig. 5) and the deformation leading from the plains to the tessera is more transitional than at Itzpapalotl. Thus, these provide two examples of crustal thickening processes that are actually contiguous; initially, the differences are being documented at these two sites and the intervening margin is being traced out (Fig. 1) to complete a full comparison of this important transition.

Summary: Geological mapping and process studies in V-1 provide key features and relationships that permit us to address many important Venus-Archean thematic questions [6] including: 1) crustal thickening environments and processes, 2) the nature of diapirism, 3) the nature and origin of deformation belts, and 4) the origin and context of regional plains-forming volcanism.

References: 1) E. Nisbet, *The Young Earth*, Allen & Unwin, 1987; 2) K. Condie, *Archean Crustal Evolution*, Elsevier, 1994a; 3) S. Solomon & J. Head, *Science*, 252, 252,1991; 4) W. Bleeker, *Lithos*, 71, 99, 2003; 5) K. Condie & K. Benn, *AGU Mon*., 47, 2006; 6) J. Head et al., Venus-Archean, *EPSC* (abs), 2008; 7) J. Johnson et al., *USGS I-2610*, 1999; 8) E. Rosenberg & G. McGill, *USGS I-2721*, 2001; 9) N. Bridges & G. McGill, *USGS I-2747*, 2002; 10) A. Brian et al., *USGS I-2813*, 2005; 11) J. Kargel et al., *Icarus*, 112, 219, 1994; 12) E. Stofan et al., *Venus II*, U of A, 931, 1992; 13) K. Jha et al., *EPSL*, 125, 221, 1994; 14) L. Bleamaster & V. Hansen, USGS I-2808, 2005; 15) M. Ivanov & J. Head, Lakshmi Planum (V-7), USGS, in review, 2008; 16) J. Head et al., Fortuna Tessera (V-2), this volume, 2008; 17) S. Solomon & J. Head, *GRL*, 17, 1393, 1990; 18) J. Suppe & C. Connors, *JGR*, 97, 13545, 1992; 19) V. Hansen & J. Willis, *Icarus*, 123, 296, 1996.

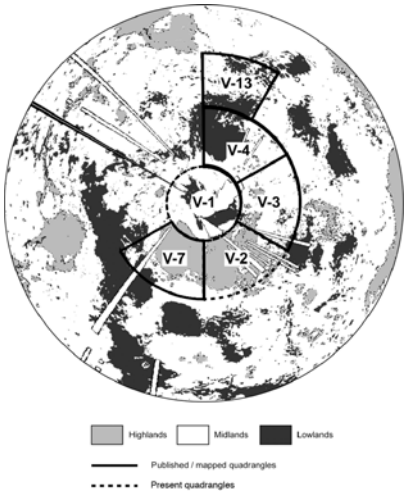

Fig. 1. Northern hemisphere of Venus. Solid lines indicate maps completed (V-4, V-13 published, V-3 in proof, V-7 in review).

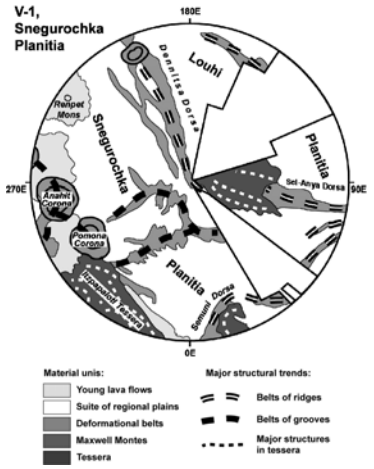

Fig. 2. Geologic sketch map of Snegurochka Planitia (V-1) quad.

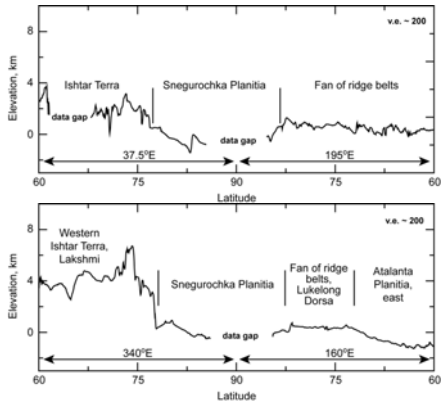

Fig. 3. Topographic profiles across V-1. (Top) Left (37.5°E; 60°N to pole); right (195°E; pole to 60°N. (Bottom) Western Ishtar Terra (Lakshmi Planum) across entire polar region along 340-160°E.

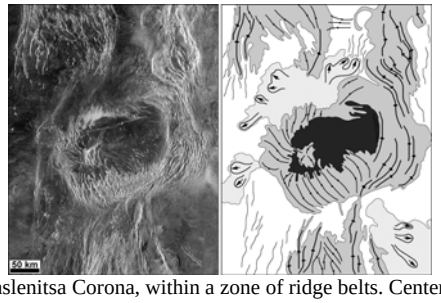

Fig. 4. Maslenitsa Corona, within a zone of ridge belts. Center ~76.5°N, 208°E. Key: black, intracorona plains; dark gray, tessera; medium gray, deformation belts; light gray, lobate plains (arrows show lobes); white, regional plains; lines, diamonds-ridges, circles-troughs, sinuous light-wrinkle ridges, dashed-tessera structural trends.

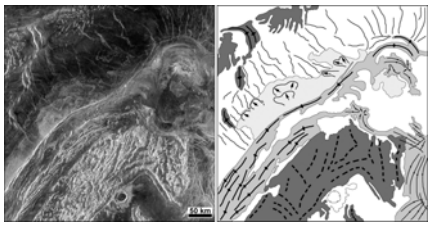

Fig. 5. NW Fortuna Tessera (V-1). Tessera (bottom) is outlined by a broad belt of ridges (Semuni Dorsa), in contact with Snegurochka Planitia regional plains. Plains surface near contact forms an elongated depression, partly filled by young flows. Center ~77°N, 12.5°E.

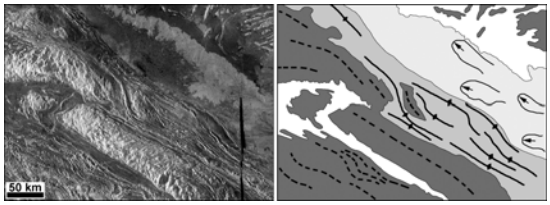

Fig. 6. A portion of Itzpapalotl Tessera, between Freyja Montes (lower left) and Snegurochka Planitia (upper right), separated by a belt of ridges; some ridges have an S shape. Elongated depression at scarp base partly filled by young flows. Center ~75.5°N, 345°E.

VENUS QUADRANGLE GEOLOGICAL MAPPING: USE OF GEOSCIENCE DATA VISUALIZATION SYSTEMS IN MAPPING AND TRAINING. J. W. Head[1], J. N. Huffman[2], A. S. Forsberg[3], D. M. Hurwitz[1], A. T. Basilevsky[1,4], M. A. Ivanov[1,4], J. L. Dickson[1], and P. Senthil Kumar[1,5], [1]Dept. of Geological Sciences, Brown University, Providence, RI 02912 (james_head@brown.edu), [2]Center for Computation and Visualization, Brown University, Providence, RI 02912, [3]Dept. of Computer Science, Brown University, Providence, RI 02912, [4]Vernadsky Institute of Geochemistry and Analytical Chemistry, RAS, Moscow, Russia, [5]National Geophysical Research Institute, Hyderabad 500007, India (senthilngri@yahoo.com).

Introduction and Background: Traditional methods of planetary geological mapping have relied on photographic hard copy and light-table tracing and mapping. In the last several decades this has given way to the availability and analysis of multiple digital data sets, and programs and platforms that permit the viewing and manipulation of multiple annotated layers of relevant information. This has revolutionized the ability to incorporate important new data into the planetary mapping process at all scales. Information on these developments and approaches can be obtained at http://astrogeology.usgs.gov/Technology/. The process is aided by Geographic Information Systems (GIS) (see http://astrogeology.usgs.gov/Technology/) and excellent analysis packages (such as ArcGIS) that permit co-registration, rapid viewing, and analysis of multiple data sets on desktop displays (see http://astrogeology.usgs.gov/Projects/webgis/).

We are currently investigating new technological developments in computer visualization and analysis in order to assess their importance and utility in planetary geological analysis and mapping [1,2]. Last year we reported on the range of technologies available and on our application of these to various problems in planetary mapping [3]. In this contribution we focus on the application of these techniques and tools to Venus geological mapping at the 1:5M quadrangle scale. In our current Venus mapping projects we have utilized and tested the various platforms to understand their capabilities and assess their usefulness in defining units, establishing stratigraphic relationships, mapping structures, reaching consensus on interpretations and producing map products. We are specifically assessing how computer visualization display qualities (e.g., level of immersion, stereoscopic vs. monoscopic viewing, field of view, large vs. small display size, etc.) influence performance on scientific analysis and geological mapping.

We have been exploring four different environments: 1) conventional desktops (DT), 2) semi-immersive Fishtank VR (FT) (i.e., a conventional desktop with head-tracked stereo and 6DOF input), 3) tiled wall displays (TW), and 4) fully immersive virtual reality (IVR) (e.g., "Cave Automatic Virtual Environment," or Cave system). Formal studies demonstrate that fully immersive Cave environments are superior to desktop systems for many tasks [e.g., 4]. There is still much to learn and understand, however, about how the varying degrees of immersive displays affect task performance. For example, in using a 1280x1024 desktop monitor to explore an image, the mapper wastes a lot of time in image zooming/panning to balance the analysis-driven need for both detail as well as context. Therefore, we have spent a considerable amount of time exploring higher-resolution media, such as an IBM Bertha display 3840x2400 or a tiled wall with multiple projectors. We have found through over a year of weekly meetings and assessment that they definitely improve the efficiency of analysis and mapping. Here we outline briefly the nature of the major systems and our initial assessment of these in 1:5M Scale NASA-USGS Venus Geological Mapping Program (http://astrogeology.usgs.gov/Projects/PlanetaryMapping/MapStatus/VenusStatus/Venus_Status.html).

1. Immersive Virtual Reality (Cave): ADVISER System Description: Our Cave system is an 8'x8'x8' cube with four projection surfaces (three walls and the floor). Four Linux machines (identical in performance to the desktop machine) provide data for the Cave. Users utilize a handheld 3D tracked input device to navigate. Our 3D input device has a joystick and is simple to use. To navigate, the user simply points in the direction he/she wants to fly and pushes the joystick forward or backward to move relative to that direction. The user can push the joystick to the left and right to rotate his/her position in the virtual world. A collision detection algorithm is used to prevent the user from going underneath the surface. We have developed ADVISER (ADvanced VIsualization for Solar system Exploration) [1,2] as a tool for taking planetary geologists virtually "into the field" in the IVR Cave environment in support of several scientific themes and have assessed its application to geological mapping of Venus. ADVISER aims to create a field experience by integrating multiple data sources and presenting them as a unified environment to the scientist. Additionally, we have developed a virtual field kit, tailored to supporting research tasks dictated by scientific and mapping themes. Technically, ADVISER renders high-resolution topographic and image datasets (8192x8192 samples) in stereo at interactive frame-rates (25+ frames-per-second). The system is based on a state-of-the-art terrain rendering system [5] and is highly interactive; for example, vertical exaggeration, lighting geometry, image contrast, and contour lines can be modified by the user in real time. High-resolution image data can be overlaid on the terrain and other data can be rendered in this context. A detailed description and case studies of ADVISER are available [1,2].

Assessment for Venus Geological Mapping: We found that the IVR ADVISER platform was very useful for the immersive environment and all participants reported a strong sense of excellent regional perspective on terrain distribution and geological map unit distribution and relationships. The platform was limited however, by the relatively low resolution of the Magellan radar image data and the very low resolution of the altimetry data. A desire to use topographic data to examine key stratigraphic relationships was often frustrated by the broad nature of the topography relative to fault and lava flow morphological relationships. Also, detailed features visible in the images (for example, small shield volcanoes <20 km diameter) were not visible in the altimetry data although it was clear that they must possess some topography. A benefit of IVR ADVISER was that several people could participate in

the visualization and analysis at the same time and hold excellent discussions on the broad geological relationships. We found that the range of tools developed for ADVISER was better suited for Mars applications than Venus applications because of the much higher-resolution image and altimetry data available for Mars. In summary, we found that for Venus mapping, the IVR ADVISER platform was best utilized for initial reconnaissance work in gaining familiarity with the major topographic elements, the broad distribution of features and units, and the general discussion among a small group of mappers of the major issues and approaches to resolving them.

2. Adaptation of ADVISER Functions to the Desktop Environment: The desktop system has a high-end nVidia graphics card; 2GB RAM and a Pentium 4 processor. A video game controller (Logitech dual-action gamepad) is used to provide navigational input to the program. In order to optimize the most useful functions of ADVISER for Venus mapping, we have exported many of the functions to the desktop environment and made comparisons of the utility and productivity of the two media [1,2]. ADVISER was originally designed for a Cave [1] because we believed the Cave's large-scale stereo display was most appropriate for doing "virtual fieldwork," but we are adapting its functionality to run on conventional desktop systems for two reasons: 1) to make it more generally accessible, and 2) to help us learn about the relative value of the information that can be gathered from both systems.

Assessment for Venus Geological Mapping: We found that the desktop system was very useful for the detailed geological mapping and the portrayal of key relationships needed to finalize unit contacts and map out and specifically delineate structures. A limitation of the desktop was the difficulty of involving more than two people in the discussion, and the overhead on panning in and out and changing contrast, and displaying multiple datasets in a time-efficient fashion.

3. High-Resolution Wall Displays: Exploration of the Middle Ground: We are now beginning to explore the middle ground between Desktop displays (DT) and Cave displays (IVR) in terms of both 1) availability to a wide range of users, and 2) utility for scientific analysis and geological mapping. In our preliminary assessment we have found that the most effective capabilities in the middle range include the semi-immersive "fishtank display" (FT) and high-resolution tiled-wall displays (TW). Among the intermediate systems are the Geowall (http://www.geowall.org) that utilizes a 1-wall stereo display. Such systems are less expensive than the Cave and are potentially better suited for wider deployment.

In our analysis of this middle ground, we have employed a 9-projector, active stereo, tiled-wall display with an effective resolution of 2400x1800, available next to the Cave in the Brown University Center for Computation and Visualization. Recent commercial demand for high-definition and high quality display (driven by the video game industry) has helped improve our capabilities in this area.

Assessment for Venus Geological Mapping: The exploration of this middle-ground has been shown to be very useful, particularly in terms of tiled displays for group discussion and analysis in the geological mapping on Venus. We found that the ability of the RAPIDVIEW system [6] was extremely helpful in panning in and out to view both high-resolution and context almost simultaneously. Furthermore, the ability to seamlessly move between superposed layered displays of radar image, topography, and geological map was essential to presentation of arguments and the development of a consensus among a large group of participating scientists that could readily view the data.

4. Summary and Conclusions: Caves in general provide for a better immersive experience, and desktops are brighter and crisper than our current Cave, but their display area is relatively small. Our current tiled wall is a middle ground and has bright, crisp images on a large display surface. This has proven most useful for fully integrated group analysis for Venus geological mapping discussions and the establishing of major questions and resolving major issues. We are currently exploring in more detail the Fishtank VR system that is most similar to a regular desktop system, but adds head-tracked stereo viewing, and typically 3D tracked input devices. The effect is comparable to looking into a fishtank where objects appear in stereo, but the working volume is physically small, effectively producing a diorama-like "world in miniature."

5. Use of Visualization Systems in Broader Education and Training in Geological Mapping: The ADVISER system was developed primarily to assist graduate-level geoscience research, but its basic function of interactively navigating 3D terrains also serves as an educational tool for training in the basic principles of geological mapping at all educational levels. We have tested these systems in Geological Sciences 5 (Mars, Moon and the Earth), an introductory geosciences course at Brown University. Students learn about scientific study and analysis, and how geologists make a multitude of observations in order to document the nature of geological processes and to unravel the history of the Earth and planets. These platforms are an engaging mechanism to illustrate how geologists use geological mapping in order to organize and document the host of scattered observations that are the clues to planetary history. Furthermore, the total immersive experience of IVR brings home immediately both the wealth of observations that can be made, as well as the need to organize these observations into important generalizations that are the core of geological mapping. Clearly, these capabilities need to be incorporated into classes in geological analysis and mapping at all levels in the future.

References: [1] Head, III, J.W. et al. (2005) Photogrammetric Engineering and Remote Sensing (PE&RS), Vol. 71:10. [2] Forsberg, A. et al. (2006) IEEE Computer Graphics and Applications, 26:4, pp. 46-54. [3] Head, J., Prabhat, Forsberg, A., Basilevsky, A., Ivanov, M., Dickson, J., Fassett, C., Levy, J., Morgan, G., and Kumar, P. (2007) Geoscience data visualization systems applied to planetary geological mapping, USGS Open File Report 2007-1233, 73-74, http://pubs.usgs.gov/of/2007/1233/. [4] Prabhat et al. (2007) Lunar and Planetary Science 38, #1297. [5] Hwa, L.M. et al. (2005) IEEE Transactions on Visualization and Computer Graphics, 11: 4, pp. 355-368. [6] Forsberg, A., Fassett, C., Huffman, J., Prabhat, Dickson, J. and Head, J. (2008) RAPIDVIEW: A Case Study of Highly Interactive Group Analysis of High-Resolution Images; In review; 15th ACM (Association for Computing Machinery) Symposium on Virtual Reality Software and Technology (VRST) Proceedings.

Acknowledgments: Support from the NASA Applied Information Systems Research Program and the NASA Planetary Geology and Geophysics Program are gratefully acknowledged.

GEOLOGIC MAP OF THE V-1 SNEGUROCHKA PLANITIA QUADRANGLE: PROGRESS REPORT. D. M. Hurwitz, J. W. Head, Department of Geological Sciences, Brown University, Providence RI 02912, debra_hurwitz@brown.edu.

Introduction: Geologic mapping of Snegurochka Planitia (V-1) reveals a complex stratigraphy of tectonic and volcanic features that can provide insight into the geologic history of Venus and Archean Earth [1,2] including 1) crustal thickening environments and processes, 2) the nature of diapirism, 3) the nature and origin of deformation belts, and 4) the origin and context of regional plains-forming volcanism. This abstract presents our progress in mapping the spatial and stratigraphic relationships of these features in the region surrounding the north pole of Venus.

Mapping Results: We have used full-resolution (75 m/pixel) images to produce a detailed map and stratigraphic column (Figures 1-3) in conjunction with the USGS mapping effort [3]. Eleven material units and two structural units have been identified and mapped similar to those identified in previous studies [e.g., 4-5]. The material units include (from older to younger) tessera material (t), densely lineated plains material (pld), deformed and ridged plains material, both radar dark and radar bright (pdd, pbd), shield plains material (ps), plains material with dense concentrations of wrinkle ridges (rp), smooth radar dark plains material (pds), smooth radar bright plains material (pbs), lobate plains material (lop), edifice features (ed), and craters material (c). The structural units identified are wrinkle ridges (wr) and extensional lineaments (ext) that deform the mapped units.

Material and Structural Units: The tessera terrain is consistently the oldest material in the region and is characterized by high elevation, extensively deformed radar bright material that is embayed by younger plains units. The fractures that define this unit are generally hard to trace in detail, as many different fracture orientations are evident. In contrast, densely lineated plains material, while also generally characterized by high elevation and a rough surface texture, have a single primary orientation of fractures. These deformed plains are also typically embayed by surrounding plains units.

The next suite of material units identified includes the regional plains material units. The oldest plains units include radar dark and radar bright deformed plains, material that is characterized by dense, small scale fractures and ridges. These units are commonly embayed by shield plains, material with a high concentration of small volcanic shields that range in size from 1-20 km in diameter. In turn, the shield plains are embayed by the radar dark and radar bright smooth plains units, deposits that have generally not been deformed by tectonic processes. Smooth radar bright plains are commonly spatially related to small shield clusters, though there are examples of smooth bright plains that lack evidence of nearby shield volcanism.

The youngest material units in Snegurochka Planitia are lobate plains and edifices. These deposits, mostly surrounding Renpet Mons (+76^o 235E) and near the Itzpapalotl Tessera-Snegurochka Planitia boundary near +76^o 10E are characterized by flows surrounding local edifice-like structures.

Gash-like fractures are mapped separately and are superposed on several units between +75^o and +87^o near 90-115E. While wrinkle ridges have been identified in other areas of this quadrangle, the ridged plains unit tends to have a much higher concentration of wrinkle ridges.

Future Work: The spatial and temporal relationships of units identified in Snegurochka Planitia are being further investigated in order to understand better the tectonic and volcanic history of Venus. The transition between regional volcanism and localized volcanism and the transition between tessera and planitia deposits both represent key questions in the geologic history of Venus, and mapping these units in detail can help determine the processes responsible for shaping the surface of Venus [1,2]. We have completed about 40% of the mapped area and are now checking the consistency and utility of the units and their sequence.

References: [1] J. Head et al., *EPSC* (abs.) 2008; [2] J. Head et al., this volume; [3] K. Tanaka, *USGS Open File Report 94-438*, 1994; [4] A. Basilevsky & J. Head, *Planet. Space Sci*., 48, 75, 2000; [5] M. Ivanov & Head, J. W., *JGR*, 106, 17,515, 2001.

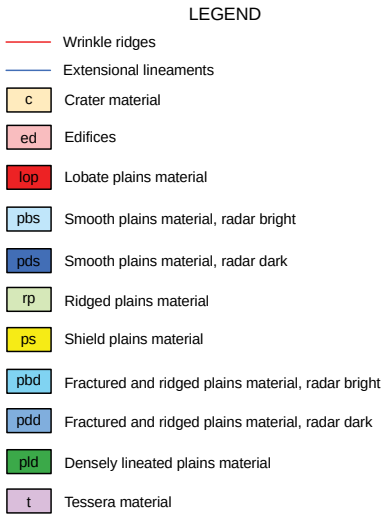

Figure 1. Legend for V-1 Snegurochka Planitia.

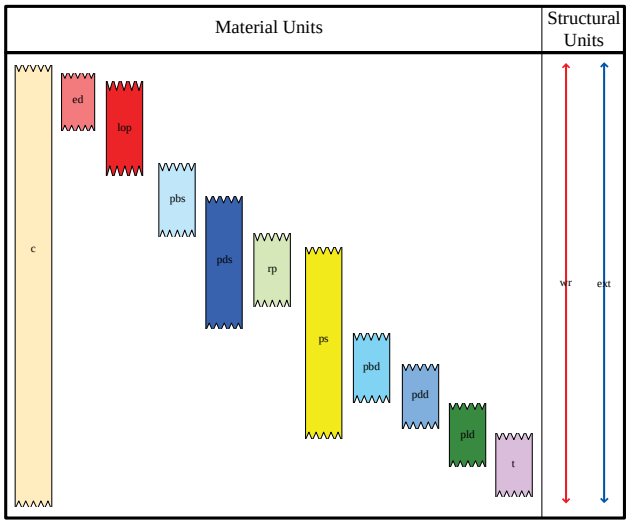

Figure 2. Stratigraphic column for V-1 Snegurochka Planitia.

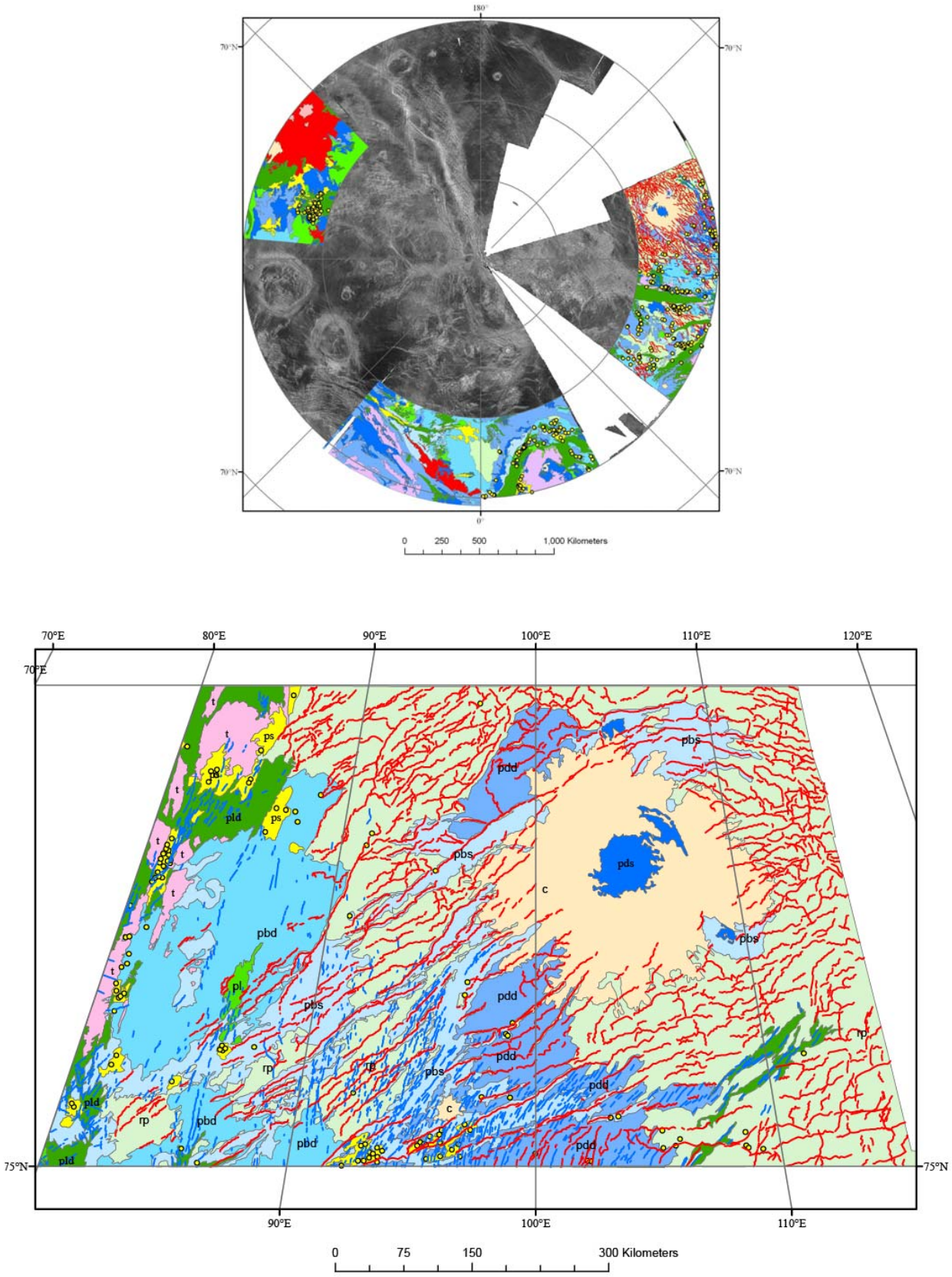

Figure 3: Geologic maps of the V-1 Snegurochka Planitia quadrangle. Status on June 9, 2008.

THE FREDEGONDE (V-57) QUADRANGLE, VENUS: CHARACTERIZATION OF THE VENUS MIDLANDS. M.A. Ivanov[1,2] and J.W. Head[2]. [1]Vernadsky Institute, RAS, Moscow, Russia, mikhail_ivanov@brown.edu; [2]Brown University, Providence, RI, USA, james_head@brown.edu.

Introduction: The Fredegonde quadrangle (V-57, 50-75°S, 60-120°E) in the southern hemisphere of Venus represents a typical region of midlands (0-2 km above MPR, [1,2]). Midlands are the most widespread topographic province on Venus (~80%) and display the richest variety of features [3-12]. Geological mapping in the V-57 quadrangle provides the possibility of defining and characterizing units that make up a region of midlands and to establish the general sequence of events there and thus address questions about the modes of formation and chronology of midlands on Venus. The map area is in contact with the uplands in the central portion of Lada Terra to the west and the lowlands of Aino Planitia to the northeast. This position also provides a transitional zone between the other two major topographic provinces, similar to that of the Meskhent Tessera (V-3) area [13]. Here we report on the results of our mapping in the V-57 quadrangle, describe the major features, units, and structural assemblages exposed there, and outline the main episodes of geologic history.

Major geologic and topographic features of the V-57 area: The Fredegonde quadrangle (Fig. 1) covers the eastern (midland) portion of Lada Terra. The most prominent features in the map area are several coronae (large and small) that occur within two chains of circular structures interconnected by belts of extensional structures, grooves and graben. The largest chain includes four coronae (Ilyana, Ambar-ona, Dunne-Musun, and Triglava) and extends in a NNE direction for several thousands of km through the central portion of the quadrangle. The second chain is in the NW corner of the map area and includes two coronae (Shyv-Amashe and Marzyana) that occur within a broad deformational zone of extensional structures. Deep canyons (Geyaguga and Xaratanga Chasmata) characterize this zone. The associations of coronae and groove belts within the Frdegonde quadrangle in many ways resembles the corona-rift/corona-groove belt complexes that occur within the marginal zones near large equidimensional basins such as Lavinia (V-55) and Atalanta (V-4) Planitiae [14,15]. Subordinate structural zones within the V-57 area are fragments of belts of contractional structures (ridges in the zone of Oshumare Dorsa) that are seen in the central portion of the quadrangle. The corona-groove chains and belts of ridges represent broad (100s of km wide) and relatively low (100s of m up to a kilometer high) topographic ridges. Extensive and shallow basin-like features (100s of km across, 100s of m deep) of Mugazo, Alma-Merghen, and Laimdota Planitiae are located between the corona-groove-chains. Mildly deformed plains units cover the surface of the basins.

Material and structural units and their relationships: The variety of material and structural units that make up the surface of the V-57 quadrangle can be combined into three groups of distinctly different relative ages (Fig. 1). (I) Group I: This group of oldest units consists of two material units, densely lineated plains (pdl) and ridged plains (pr), and one structural unit of groove belts (gb). Densely lineated plains occur as small outliers in the central map area. Ridged plains form fragments of the Oshumare Dorsa ridge belt. Groove belts consist of dense swarms of fractures and graben that interconnect coronae within the corona-groove chains. All units of this group form either local (pdl) or regional (pr and gb) elevated areas that are embayed by vast plains units. (II) Group II: This group constitutes the middle portion of the regional stratigraphic column and consists of two material units, shield plains (psh) and regional plains (rp). These units cover the majority of the quadrangle. Abundant small shield- and cone-like features (interpreted to be small volcanoes [16-18]) characterize the surface of shield plains. The volcanoes appear to be sources of the adjacent plains material. Regional plains have a morphologically smooth surface and uniform radar backscatter; sources of the plains material are not known. Wrinkle ridges deform both units of this group and sometimes cut the surface of the older units. Topographically, shield plains and regional plains occur at relatively low levels and fill the broad basins between elevated zones of groove and ridge belts. (III) Group III: This group forms the top of the regional stratigraphic column and consists of two material units, smooth plains (ps) and lobate plains (pl). Smooth plains have a featureless surface with uniform and preferentially low radar albedo, whereas lobate plains are characterized by distinctive internal flow-like features and have lobate and digitate boundaries. Both units are tectonically undeformed and embay most tectonic structures, including wrinkle ridges. Lobate plains are spatially associated with some coronae (e.g. Dunne-Musun). Individual flows of this unit extend down the regional slopes and partly fill the basin-like topographic lows.

Summary: Mapping in the V-57 quadrangle (Fig. 1) permits reconstruction of the major episodes characterizing the geologic and topographic evolution of the eastern portion of Lada Terra. Linear tectonic deformation patterns dominated during formation of the units of Group I at the early stages of observable geologic history. The most prominent tectonic features are still exposed in the deformational zones of ridge belts and in the corona-groove chains. The relationships between the older contractional and extensional structures suggest that the ridge belts are relatively older and the features of the corona-groove chains are younger. The tectonic components of coronae (annulae, fracturing in the core, etc.) appear to be partly synchronous with the linear segments of the groove swarms that connect the

coronae. The vast plains of the second group of units broadly embay the corona-groove complexes and, thus, are relatively younger. The most important topographic features in the map area, the broad topographic ridges and the basins, were formed during the earlier episodes of regional geologic history.

During the middle periods of geologic history, volcanic activity dominated in the Fredegonde region and the vast plains units were emplaced. Tectonic processes played a subordinate role at this time and produced low and widely distributed wrinkle ridge structures. The plains of the second group filled the broad basin-like topographic features between linear deformation belts, but left significant portions of the older topographic ridges (ridge belts and corona-groove chains) exposed. The topographic distribution of shield plains and regional plains suggests that the general topographic configuration of the midlands within the map area was established prior to emplacement of the units from the middle stratigraphic level. The early formation of major topographic features on Venus has also been observed at regional [13] and global [19] scales.

The youngest units (lobate plains) often represent a volcanic component of several coronae (e.g. Dunne-Musun). This association of the younger volcanic materials with the older tectonic structures suggests that some coronae were either reactivated or their volcanic activity occurred in the late stages of the history. The direction of the flows of lobate plains (from the broad topographic ridges toward the floor of the basins) and the topographic position of the earlier shield plains and regional plains (within the basins) suggest that the general topographic configuration of the region within the V-57 quadrangle has remained stable from the time of emplacement of the vast plains units through the latest stages of the geologic history in this area. The midlands thus appear to represent the result of early formation of linear deformation belts and lowland basins, followed by their filling and topographic preservation [e.g., 19].

References: 1) Masursky, H., et al., *JGR*, 85, 8232, 1980, 2) Pettengill, G.H., et al., *JGR*, 85, 8261, 1980, 3) Ford, P.G. and G.H. Petttengill, *JGR*, 97, 13103, 1992, 4) Barsukov, V.L., et al., *JGR*, 91, D399, 1986, 5) Frank, S.L. and J.W. Head, *EMP*, 50/51, 421, 1990, 6) Basilevsky, A.T. and J.W. Head, *PSS*, 48, 75, 2000, 7) Basilevsky, A.T. and J.W. Head, *JGR*, 105, 24583, 2000, 8) Stofan, E.R., et al., *Icarus*, 152, 75, 2001, 9) Bleamaster, L.F. and V.L. Hansen, *JGR*, 109, doi: 10.1029/2003JE002193, 2004, 10) Nunes, D.C., et al., *JGR*, 109, doi: 10.1029/2003JE002119, 2004, 11) Young, D.A. and V.L. Hansen, *JGR*, 110, doi: 10.1029/2004JE001965, 2005, 12) Herrick, R.R., et al., *JGR*, 110, doi: 10.1029/2004JE002283, 2005, 13) Ivanov, M.A. and J.W. Head, Geologic map of the Meskhent quadrangle (V-3), in edit, 2008, 14) Ivanov, M.A. and J.W. Head, *USGS Map I-2684*, 2001, 15) Ivanov, M.A. and J.W. Head, *USGS Map I-2792*, 2004, 16) Aubele J.C., *LPSC XXVI*, 59, 1995, 17) Addington, E.A., *Icarus*, 149, 16, 2001, 18) Ivanov, M.A. and J.W. Head, *JGR*, 109, doi: 10.1029/2004JE002252, 2004, 19) Ivanov, M.A. et al., The History of Topography on Venus, *Geology* (submitted), 2008.

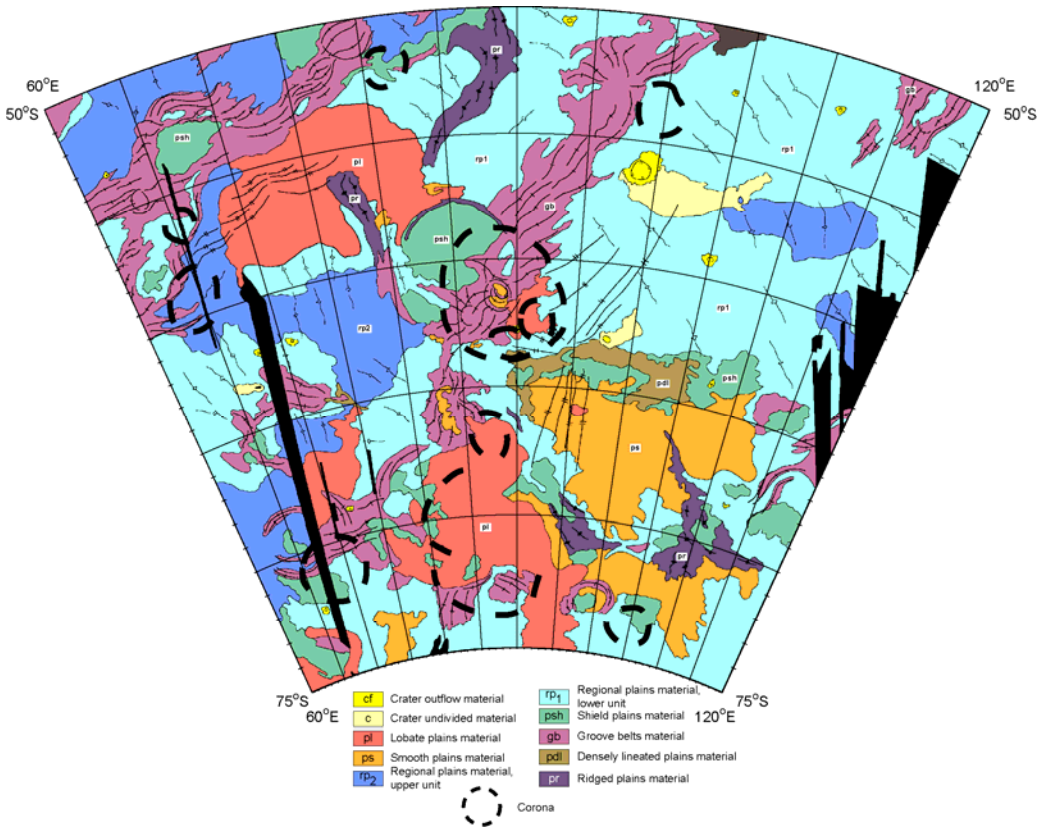

Fig. 1. Preliminary geological map of the Fredegonde (V-57) quadrangle

FORMATION AND EVOLUTION OF LAKSHMI PLANUM (V-7), VENUS: ASSESSMENT OF MODELS USING OBSERVATIONS FROM GEOLOGICAL MAPPING. M. A. Ivanov[1,2] and J. W. Head[2], [1]Vernadsky Institute, RAS, Moscow, Russia (Mikhail_Ivanov@brown.edu); [2]Department of Geol. Sci., Brown University, Providence, USA (James_Head@brown.edu).

Introduction: Lakshmi Planum is a high-standing plateau (3.5-4.5 km above MPR) surrounded by the highest mountain ranges on Venus [1-6]. Lakshmi represents a unique type of elevated region different from dome-shaped and rifted rises and tessera-bearing crustal plateaus. The unique characteristics of Lakshmi suggest that it formed by an unusual combination of processes and played an important role in Venus geologic history. Lakshmi was studied with Venera-15/16 [7-10,5,11] and Magellan data [12-14], resulting in two classes of models, divergent and convergent, to explain its unusual topographic and morphologic characteristics. Divergent models explain Lakshmi as a site of mantle upwelling [10,15-18] due to rising and subsequent collapse of a mantle diapir; such models explain emplacement of a lava plateau inside Lakshmi and, in some circumstances, formation of the mountain ranges. The convergent models consider Lakshmi as a locus of mantle downwelling, convergence, underthrusting, and possible subduction [19,11,20-29]. Key features in these models are the mountain ranges, high topography of Lakshmi interior, and the large volcanic centers in the plateau center. These divergent and convergent models entail principally different mechanisms of formation and suggest different geodynamic regimes on Venus.

Almost all models make either explicit or implicit predictions about the type and sequence of major events during formation and evolution of Lakshmi and thus detailed geological mapping can be used to test them. Here we present the results of such geological mapping (the V-7 quadrangle, 50-75N, 300-360E; scale 1:5M) that allows testing the proposed models for Lakshmi.

Material units: Eleven material units make up the V-7 quadrangle. (1) Tessera (t), exposed inside and outside Lakshmi appears to be the oldest material because it is embayed by most of the other units in the map area. (2) Densely lineated plains (pdl) postdate tessera and form one of the oldest units; patches occur outside Lakshmi Planum. (3) Ridged plains (pr) postdate pdl and occur outside Lakshmi. (4) Shield plains (psh) display abundant small shield-shaped features interpreted to be small volcanoes; embays the previous ones and occurs predominantly within lowlands around Lakshmi. (5) Pitted and grooved material (pgm) displays small pits and is cut by broad and shallow grooves with scalloped edges; occurs inside Lakshmi in association with mountain ranges. (6) Lower unit of regional plains (rp_1) has smooth surface, cut by wrinkle ridges; the most widespread unit that occurs inside and outside of Lakshmi Planum. (7) Upper unit of regional plains (rp_2) is also deformed by wrinkle ridges but has lobate boundaries and higher radar albedo than regional plains; occurs both inside and outside Lakshmi. (8) Lobate plains (pl_2) is characterized by lobate flows that embay most tectonic structures including wrinkle ridges; form fluctūs outside Lakshmi and surround Colette and Sacajawea Paterae inside the plateau. (9) Smooth plains (ps) have uniform and low radar albedo, embays wrinkle ridges; largest occurrence is in southern portion of Lakshmi. (10) Impact craters (c) and (11) crater outflow deposits (cf) are peppered throughout the quadrangle without any preferential concentrations.

Structures: Extensional structures. In places, fractures and graben are closely spaced and obscure underlying terrain; form belts (groove belts, gb) that extend for hundreds of kilometers mostly within the southern regional slope of Lakshmi where they cut pdl and pr and are embayed by shield plains and regional plains. Contractional structures. Wrinkle ridges mildly deform shield plains and regional plains; broader and more linear ridges dominate ridged plains (pr), which are largely equivalent to the ridge belts of [13,30]. The most important occurrences of contractional structures are mountain belts (unit mt) that surround the interior of Lakshmi and consist of densely spaced ridges 5-15 km wide, tens of km long. Regional plains usually embay the ridges.

Sequence of major events during evolution of Lakshmi Planum: Various plains units heavily embay fragments of tessera in all localities inside and outside Lakshmi. The consistent relationships of embayment and the complex and unique surface deformational pattern suggest that tessera represents the oldest material. Tessera distribution patterns suggest more extensive presence under younger plains units, forming basement.

Densely fractured plains (pdl) appear younger than tessera; the largest massifs of pdl occur in Atropos and Itzpapalotl Tesserae where plains are further deformed by broad ridges and to some degree resemble the tessera deformation patterns. The ridges are generally conformal to the strike of Akna/Freyja Montes and occur within large areas of densely lineated plains adjacent to the mountain ranges. The ridges are clearly related to the orogenic phase of formation of mountain belts [10,16-19,11,20-23,25,26,29]. Shield plains and regional plains embay mountainous ridges both outside and inside Lakshmi Planum, which implies that the orogenic phase was shifted toward earlier stages of the observable geological history of Ishtar Terra. Shield plains were emplaced after the main phase of mountain belt formation and before regional plains, but exclusively outside of the plateau.

The lower unit of regional plains (rp_1) postdates shield plains; occurrences are concentrated S of Lakshmi Planum (Sedna Planitia) and in the interior of Lakshmi. The thickness of unit rp_1 is small because outliers of older units occur within the broad regional plains. Youngest units in Ishtar, smooth/lobate plains, are su-

perposed on regional plains and undeformed by tectonic structures; they were emplaced after cessation of tectonic activity. Smooth/lobate plains form extensive lava aprons around Colette and Sacajawea Paterae, representing the latest volcanic activity inside Lakshmi Planum.

Testing models of Lakshmi Planum formation: Detailed geological analysis thus allows both definition of material units and tectonic structures and establishing the sequence of major events during its formation and evolution, and testing the suite of models proposed to explain the mechanisms of formation of this structure.

The interpreted nature of units and the sequence of events strongly contradict the predictions of divergent models: 1) The very likely presence of an ancient (craton-like) tessera massif in the core of Lakshmi; such a core is inconsistent with the rise and collapse of a mantle diapir [10,15,16]. 2) The absence of a rift zone in the interior of Lakshmi; these zones appear to be a natural consequence of growth of surface topography due to diapiric rise [e.g. 31]. 3) The apparent migration of volcanic activity toward the center of Lakshmi; divergent models are consistent with the opposite trend of volcanism. 4) The abrupt cessation of mountain range ridges at the edge and propagation over hundreds of kilometers outside Lakshmi in Atropos and Itzpapalotl Tesserae. Divergent models predict the opposite progression.

Convergent models of formation and evolution of Lakshmi Planum appear to be more consistent with the observations. The pure downwelling models [e.g. 23], however, face three important difficulties. 1) The possibly unrealistically long time span that can be required to produce the major features of Lakshmi [32]. 2) The strongly asymmetrical north-south topographic profile of Lakshmi and striking difference in the height and thickness of the mountain belts to the north-west and north (Akna and Freyja Montes) and to the south of Lakshmi (Danu Montes). The pure downwelling models would require formation of more symmetrical structures. 3) The absence of radial contractional structures (arches and ridges) in the interior of Lakshmi. These structures represent the necessary result of the downwelling models.

Convergence models are most consistent with observations and explain the structure by collision and underthrusting/subduction of lower-lying plains with the elevated and rigid block of tessera [20-22]. These models are capable of explaining formation of the major features (for example, mountain belts) and the sequences of events and principal trends in evolution of volcanism and tectonics. To explain the pronounced longitudinal asymmetry of Lakshmi, however, these models have to consider major axes of collision to be at the N and NW of the plateau in Atropos and Itzpapalotl Tesserae.

A plausible scenario for formation/evolution of Lakshmi Planum consists of the following stages: Stage 1: Pre-deformational configuration of western Ishtar; a layered suite of low-lying lava plains surrounded a tessera craton. Stage 2: Compression from the N led to deformation of plains against the tessera massif foreland and formation of higher mountain ranges; displacement of the craton may have caused formation of Danu Montes. Stage 3: Continued underthrusting finally caused limited uplift of N mountain ranges and the N portion of Lakshmi Planum, creating the Lakshmi asymmetry; two different events may have followed, one with and one without delamination [33]. Stage 4a: In the beginning of delamination, fertile mantle flowed toward the base of the massif, melted, and led to emplacement of rp_1 in the Lakshmi interior. Stage 5a: During more mature stages of delamination, the deepest portion of the slab would start to melt to form the youngest lava plains at Colette and Sacajawea Paterae. Stage 4b: If no delamination occurs then formation of unit rp_1 could be due to broad melting of the underthrust slab as it crosses the melting isotherm. Stage 5b: As underthrusting proceeded, the relatively colder slab deflected the isotherm downward and new deeper portions of the slab melted, producing the younger lavas near Lakshmi Planum center.

When either delamination or continued underthrusting waned, the thicker crust of the northern mountain ranges rose epirogenically, which led to additional elevation of the ranges and the northern portion of Lakshmi.

References: 1) Masursky, H., et al., 1980, *JGR*, 85, 8232; 2) Pettengill, G.H., et al., 1980, *JGR*, 85, 8261; 3) Campbell, D.B., et al., 1983, *Science*, 221 644; 4) Barsukov, V.L., et al., 1986, *JGR*, 91, D399; 5) Pronin, A.A., et al., 1986, *AV*, 20, 83 (in Russian); 6) Stofan, E.R., et al., 1987, *EMP*, 38, 183; 7) Solomon, S.C. and J.W. Head, 1984, *JGR*, 89, 6885; 8) Solomon, S.C. and J.W. Head, 1990, *GRL*, 17, 1393; 9) Sjogren W. L., et al., 1997, *In:* Venus II, 1125; 10) Pronin, A.A., 1986, *Geotectonika*, 20, 271 (in Russian); 11) Head, J.W., 1990, *Geology*, 18, 99; 12) Kaula, W.M., et al., 1992, *JGR*, 97, 16085; 13) Solomon, S.C., et al., 1992, *JGR*, 97, 13199; 14) Basilevsky, A.T. and J.W. Head, 1995, *SSR*, 29, 335; 15) Pronin, A.A., 1990, *LPSC 21*, 987; 16) Pronin, A.A., 1992, *In:* Venus Geology Geochemistry, and Geophysics, 68; 17) Grimm, R.E. and R.J. Phillips, 1990, *GRL*, 17, 1349; 18) Grimm, R.E. and R.J. Phillips, 1991, *JGR*, 96, 8305; 19) Head, J.W., 1986, *LPSC 17*, 323; 20) Head, J.W., et al., 1990, *GRL*, 17, 1337; 21) Roberts, K.M. and J.W. Head, 1990a, *GRL*, 17, 1341; 22) Roberts, K.M. and J.W. Head, 1990b, *EMP*, 50/51, 193; 23) Bindschadler, D.L., et al., 1990, *GRL*, 17, 1345; 24) Lenardic, A., et al., 1991, *GRL*, 18, 2209; 25) Hansen, V.L. and R.J. Phillips, 1993, *LPSC 24*, 603; 26) Hansen, V.L. and R.J. Phillips, 1995, Geology, 23, 292; 27) Keep, M. and V.L. Hansen, 1994, JGR, 99, 26015; 28) Ansan, V., et al., 1996, PSS, 44, 817; 29) Marinangeli, L., and M.S. Gilmore, 2000, JGR 105, 12053; 30) Squyres, S.W., et al., 1992, *JGR*, 97, 13579; 31) Condie, K.C., 2001, *Mantle plumes and their record in Earth history*, p. 306; 32) Kidder, J.G. and R.J. Phillips, 1996, JGR, 101, 23181; 33) Hess, P.C. and J.W. Head, 1990, EMP, 50/51, 57.

GEOLOGIC MAP OF THE MESKHENT TESSERA QUADRANGLE (V-3), VENUS: EVIDENCE FOR EARLY FORMATION AND PRESERVATION OF REGIONAL TOPOGRAPHY. M. A. Ivanov[1,2] and J. W. Head[2], [1]Vernadsky Institute, RAS, Moscow, Russia (Mikhail_Ivanov@brown.edu); [2]Department of Geol. Sci., Brown University, Providence, USA (James_Head@brown.edu).

Introduction: The area of the Meskhent Tessera quadrangle (V-3, 50-75°N, 60-120°E, Fig. 1) corresponds to a transition zone from the uplands of Ishtar Terra to the west to the lowlands of Atalanta Planitia to the east. The topographic configuration, gravity signature, and presence of large tesserae [1,2] in Ishtar Terra are consistent with extensive areas of thickened crust and tectonically stabilized lithosphere representing ancient and now extinct regimes of mantle convection [3,4]. The gravity and topographic characteristics of Atalanta Planitia have been cited as evidence for large-scale mantle downwelling [5-7]. Thus, the region of Meskhent Tessera quadrangle represents an important sample for the study of the regional history of long-wavelength topography (highlands, midlands, and lowlands), interaction between the downwelling and areas of thickened crust/lithosphere, formation of associated tectonic features, and emplacement of volcanic plains.

Stratigraphy: In the area of V-3 quadrangle we have defined and mapped one structural and ten material units. In order from older to younger they are as follows.

Tessera material (t, ~1.08 10^6 km^2 or ~14.1% of the quadrangle) is heavily deformed by intersecting ridges and grooves. *Densely lineated plains material* (pdl, ~0.19 x 10^6 km^2 or ~2.4%) is characterized by a relatively flat surface that is cut by densely packed subparallel lineaments. *Ridged plains material* (pr, ~0.35 10^6 km^2 or ~4.6%) is deformed by relatively broad (5-10 km wide) ridges tens of kilometers long after its emplacement. *Groove belts* (gb, structural unit, ~0.91 10^6 km^2 or ~11.9%) consist of long swarms of extensional structures, grooves. *Shield plains material* (psh, ~2.43 10^6 km^2 or about 31.7%) is characterized by abundant small shield-shaped features ranging from a few kilometers in diameter up to about 10-20 km. *Regional plains material* (rp, ~2.37 10^6 km^2). This unit is composed of morphologically smooth, homogeneous plains material complicated by wrinkle ridges. On the basis of its typical radar backscatter, regional plains material is subdivided into two units. The lower unit (rp_1, ~27.6%) has a homogeneous and relatively low radar albedo; the upper unit (rp_2 ~3.3%) appears to have slightly higher radar albedo and, in places, is characterized by lobate boundaries. *Smooth plains material* (ps, ~0.14 10^6 km^2 or 1.8%) is characterized by uniform and preferentially low albedo. *Lobate plains material* (pl, ~0.16 10^6 km^2 or 2.1%) has internal elements arranged in parallel to sinuous to lobate radar bright and dark strips and patches, and unit boundaries are typically lobate. Impact crater material was mapped as *undivided crater material* (cu) in some cases surrounded by *crater outflow deposits* (cf).

Topographic position of the mapped units: The major part of the map area is within the topographic province of the midlands and is mostly populated with material and structural units postdating tessera and predating regional plains material. Four elevated regions separated by elongated lower-lying areas characterize the overall topography of the map area (Fig. 2). Three of them, eastern Ishtar Terra, Tethus Regio, and in the arc of Dekla Tessera, all coincide with the large tessera occurrences that make up ~14% of the map area. The fourth region is the central-eastern portion of the quadrangle and corresponds to a zone of groove belts between Fakahotu Corona and Melia Mons.

The relatively old tectonized materials and deformational belts (gb, pr) are concentrated within regional slopes predominantly near the major tessera-bearing elevated regions. An exception is the ridge belts to the N of Dekla Tessera that occur in relatively low-lying Audra Planitia. There, the belts are broadly embayed by regional plains material. The most abundant unit in the quadrangle (psh) postdates tessera and the deformational belts, predates regional plains, and is clearly concentrated on the broad slopes away from the major elevated regions. Where the psh unit occurs within relatively low areas it is embayed by regional plains material. Regional plains material occurs throughout the map area (except for the major tesserae) but preferentially occupies the elongated lowlands where it embays all previous material and structural units. The youngest and relatively non-abundant material units such as the upper unit of regional plains (rp_2) and lobate/smooth plains materials (total ~7% of the map area) are related to distinct volcanic centers and their distribution appears to be governed by local slopes of older units.

Conclusions: The material and structural units within the V-3 quadrangle reveal not only the relative age relationships that are consistent throughout the map area but also good correlation with topography on the local and regional scales. The older units generally occupy the higher topographic levels, which is consistent with embayment by progressively younger units. This suggests two important characteristics of the regional-scale topography within the quadrangle and, by implication, within the broader surroundings. First, the actual regional-scale topographic pattern appears to have formed at the earlier stages of the observable geologic history, before emplacement of the lower unit of regional plains (rp_1). The areal distribution of this unit

appears to be controlled by the long-wavelength topographic features and the plains are clearly less abundant within elevated areas and concentrated in the regional lows. Second, although the vast plains units (e.g. psh and rp_1) were deformed after emplacement to some degree, the principal, regional-scale, topographic configuration of the area of the V-3 quadrangle remained stable since the time it was established prior to the regional plains. The apparent history of regional topography within the V-3 quadrangle is similar to the global-scale history of topography of Venus [8].

References: 1) Barsukov, V.L., et al., J*GR*, 91, D378, 1986; 2) Sukhanov, A.L., *in:* Venus geology, geochemistry, and geophysics, p. 82; 3) Grimm, R.E., *Icarus*, 112, 89, 1994; 4) Brown, C.D. and R.E. Grimm, *Icarus*, 139, 40, 1999; 5) Bindschadler, D.L. et al., *JGR*, 97, 13,495, 1992; 6) Konopliv, A.S. and Sjogren, W.L., *Icarus*, 112, 42, 1994; 7) Konopliv, A.S. et al., *Icarus*, 139, 3, 1999; 8) Ivanov, M.A. et al., Geology, 2008 (submitted).

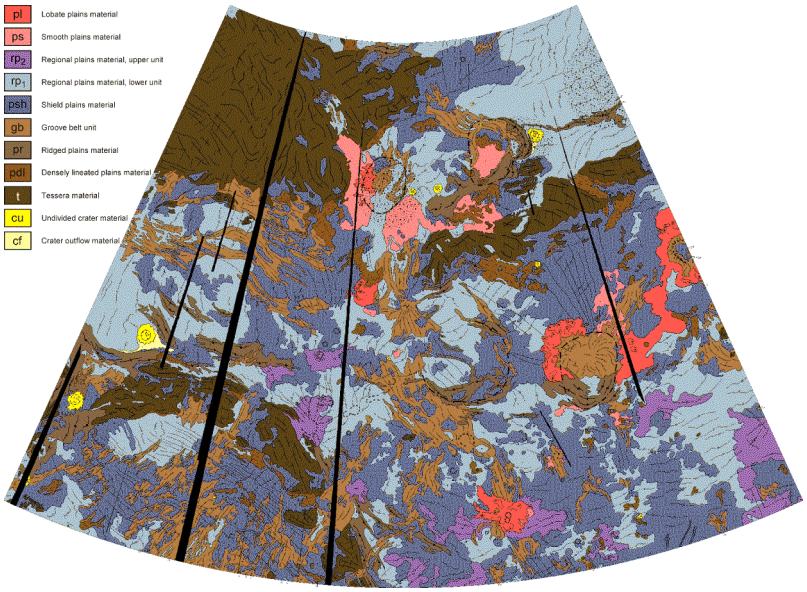

Fig. 1. Geological map of the V-3 Meskhent Tessera quadrangle

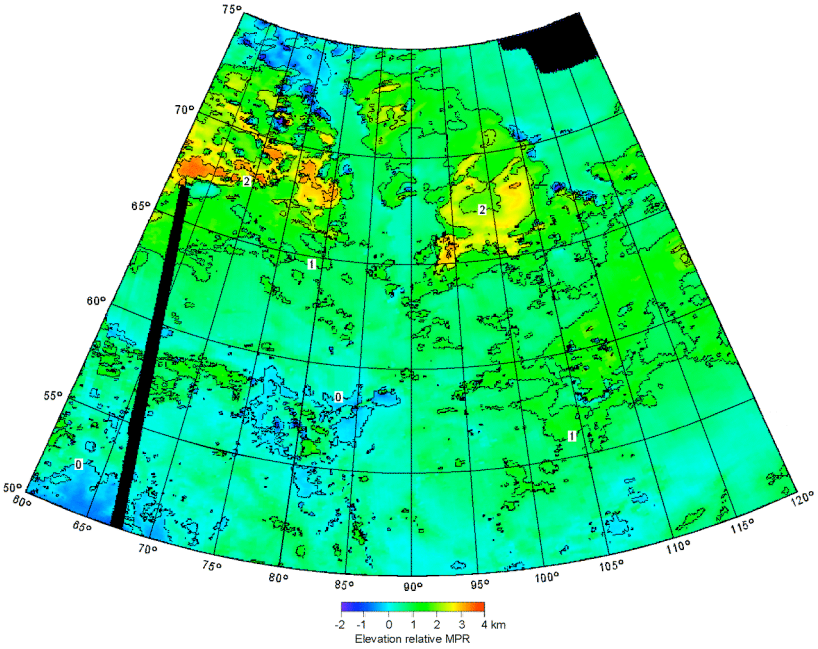

Fig. 2. Regional topography for the V-3 Meskhent Tessera quadrangle

GEOLOGICAL MAPPING OF THE LADA TERRA (V-56) QUADRANGLE, VENUS: A PROGRESS REPORT.

P. Senthil Kumar[1,2] and James W. Head III[2], [1]National Geophysical Research Institute, Hyderabad 500007, India, senthilngri@yahoo.com; [2]Department of Geological Sciences, Brown University, Providence, RI 02912, USA, james_head@brown.edu.

Introduction: Geological mapping of the V-56 quadrangle (Fig. 1) reveals various tectonic and volcanic features and processes in Lada Terra that consist of tesserae, regional extensional belts, coronae, volcanic plains and impact craters. This study aims to map the spatial distribution of different material units, deformational features or lineament patterns and impact crater materials. In addition, we also establish the relative age relationships (e.g., overlapping or cross-cutting relationships) between them, in order to reconstruct the geologic history. Basically, this quadrangle addresses how coronae evolved in association with regional extensional belts, in addition to evolution of tesserae, regional plains and impact craters, which are also significant geological units of Lada Terra.

Geologic mapping: We used 250-m-per-pixel Magellan SAR images to prepare a geologic map at a scale of 1:5,000,000. Wherever necessary, full-resolution (75-m-per-pixel) images are used for fine details. This quadrangle is bordered by Kaiwan Fluctus (V-44) [1] and Agnesi (V-45) [2] quadrangles in the north, and Mylitta Fluctus (V-61) [3,4], Fredegonde (V-57) [5] and Hurston (V-62) [2] quadrangles in the west, east, and south, respectively. From the geologic mapping, we report on the distribution of the following material and structural units, and reconstruct the geologic history.

Material and structural units: The oldest known material units are tesserae. They are radar bright areas characterized by multiple orientations of lineaments; two sets are dominant: NNW-SSE and ESE-WNW oriented lineaments. Tightly spaced ridges and troughs generally characterize tesserae. The third dominant lineaments are NNE-SSW and NNW-SSE oriented along rift zones, namely, Chang Xi Chasmata and Seo-Ne Chasma, but these are apparently restricted to the Cocomama Tessera. In the northeastern part of the quadrangle, terrains (TLT, Fig. 1) similar to tessera are found. They have NNE-SSW to NE-SW oriented ridges, which are cut by ESE-SNW to NW-SE oriented troughs. The spacing of these structures is greater than the structures of the tessera. The tessera units contain intra-tessera basins, which are filled by lava flows of different ages; most of them are derived from the units outside the tessera, and a few are from intra-tessera volcanism.

Regional plains units embay the tessera terrain; they have wrinkle ridges and a few young fracture systems. The oldest known plains (but younger than tessera) are lineated (LP, Fig. 1), and are closely associated with shield plains and the tessera. The LP is characterized by tightly spaced, NNW-SSE oriented fractures, which are also common in the tessera. Two types of shield plains are present: a few occur in the pre-regional plains areas, while others occur in the core of coronae and adjoining areas.

The older regional plains are cut by two regional extensional belts [6]: (1) NNW-SSE trending, 6000-km long and 50-200 km wide, Alpha-Lada (AL) belt, and (2) NNE-SSW trending, 2000 km long and 300 km wide, Derceto-Quetzalpetlatl (DQ) belt. These two belts are composed of fractures, rift basins and strike-slip zones. The DQ belt is punctured by Sarpanitum, Eithinoha and Quetzalpetlatl Coronae, while the Otygen, Demvamvit and Okhin-Tengri Coronae occur along the AL belt. A few coronae have a circular central dome and an outer concentric depression; they are defined by fractures, rift basins and ridge belts. Asymmetric and multiple coronae also occur in the southern part of the AL belt. Two other extensional belts branch from the AL belt. Dyamenyuo and Toyo-uke Coronae and Loo-wit and Kshumay Montes puncture these extensional belts. In many places, corona structures cut across the regional extensional belts, while in other places, the extensional belts cross the corona structures. There is a clear overlapping time relationship, as the one affects the formation of the other. Corona volcanism and tectonics are also closely related to one another. Lava flows erupt along the corona fractures, for example, in the Eithinoha Corona. Lava flows emanating from coronae travel several hundred kilometers across regional plains. Volcanism is also related to shield volcanoes in many places.

The DQ and AL belts separate the plains units of Lavinia Planitia, Aibarchin Planitia and Mugazo Planitia, where lava flows are abundant; principally there are four plains units, of which the oldest one appears to be common to all the planitia units. Most of the younger units are locally derived from the coronae. The regional plains occurring to the east of Otygen Corona have undergone intense fracturing and emplacement of graben (interpreted as dykes) after post corona-extensional belt deformation. These fractures occur in two directions: ENE-WSW and NW-SE. It appears that they represent the latest deformation, and could probably be related to the terrain uplift, as is evident in many terrestrial examples.

Impact craters are the youngest geologic units, except for one that is affected by the extensional belt deformation and the other embayed by regional plains. Most impact craters show a complex geometry and a

few are bowl-shaped. Many complex craters show run-out flows characteristic of oblique impacts.

Correlation of material units: Older tessera units are postdated by numerous plains units; areally, regional plains with wrinkle ridges are the most extensive, with shield plains generally predating these and some corona volcanism postdating them. Currently it is not clear whether coronae-related plains units formed contemporaneously or whether plains units originated from the tessera are coeval with those from coronae. Further detailed mapping is underway to understand the spatial and temporal evolution of the material units and deformation events. We are also linking this geologic history to the geodynamic processes implied by this surface evolution.

Acknowledgements: We thank Misha Ivanov for his help while initiating this mapping project, and Jay Dickson and Prabhat while working with the virtual wall image facility.

References: [1] Bridges, N.T., and McGill, M.E., *USGS Scientific Investigations Map I-2747*, 2002. [2] http://astrogeology.usgs.gov/Projects/PlanetaryMapping/MapStatus/VenusStatus/Venus_Status.html. [3] Ivanov, M.A., and Head, J.W., *USGS Scientific Investigations Map 2920*, 2006. [4] Ivanov, M. A., and Head, J. W., this volume. [5] Ivanov, M.A., et al., this volume. [6] Baer, G., et al., *J. Geophys. Res.*, 99, 8335-8369, 1994.

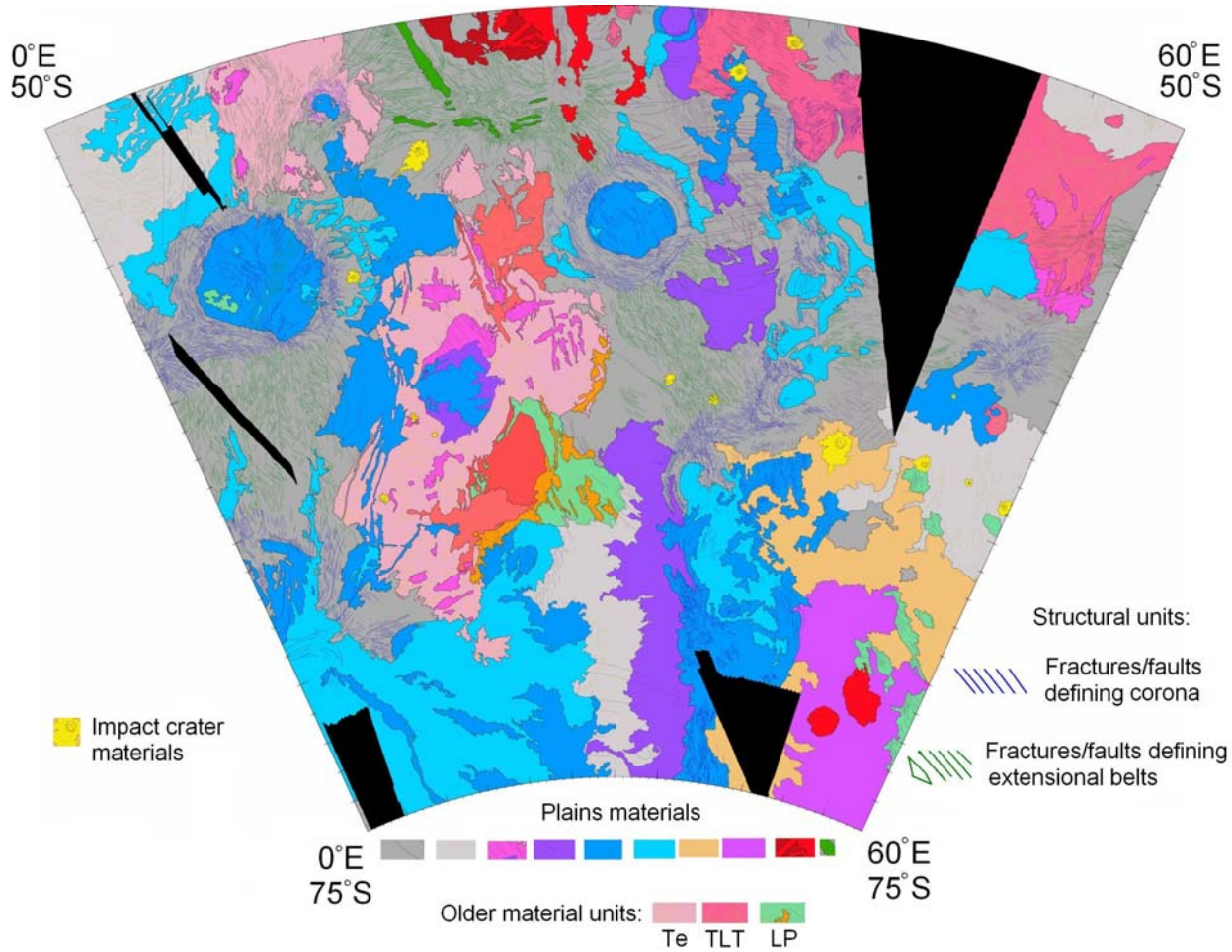

Fig. 1. Geological map of V-56 Lada Terra quadrangle (50°S-75°S; 0°E-60°E). Material units (from older to younger): tessera terrain (Te), tessera-like terrain (TLT), lineated plains (LP), plains units and impact craters. Lineament patterns defining the extensional belts (RZ) and coronae (C) are shown in different colors: green–extensional belts; dark blue–coronae. Many of the plains materials are related to volcanism associated with coronae.

GEOLOGY OF THE LACHESIS TESSERA QUADRANGLE (V-18), VENUS

George E. McGill

Department of Geosciences, University of Massachusetts, Amherst, MA 01003

The Lachesis Tessera Quadrangle (V-18) lies between 25^{o} and 50^{o} north, 300^{o} and 330^{o} east. Most of the quadrangle consists of "regional plains" (1) of Sedna and Guinevere Planitiae. A first draft of the geology has been completed, and the tentative number of mapped units by terrain type is:
Tesserae – 2; plains – 4; ridge belts – 1; fracture belts – 1 (plus embayed fragments of possible additional belts); coronae – 3; central volcanoes – 1; shield flows – 2; paterae – 1; impact craters – 1; undifferentiated flows – 1; bright materials – 1.

By far the areally most extensive materials are regional plains. These are mapped as two units, based on radar backscatter ("radar brightness"). The brighter unit appears to be younger than the darker unit. This inference is based on the common presence within the lighter unit of circular or nearly circular inliers of material with radar backscatter characteristic of the darker unit. The circular inliers are most likely low shield volcanoes, which are commonly present on the darker unit, that were only partially covered by the brighter unit. Clear cut examples of wrinkle ridges and fractures superposed on the darker unit but truncated by the brighter unit have not been found to date. These relationships indicate that the brighter unit is superposed on the darker unit, but that the difference in age between them is very small. Because they are so widespread, the regional plains are a convenient relative age time "marker." The number of impact craters superposed on these plains is too small to measure age differences (2), and thus we cannot estimate how much time elapsed between the emplacement of the darker and brighter regional plains units. More local plains units are defined by significantly lower radar backscatter or by a texture that is mottled at scores to hundreds of kilometers scale. A plains-like unit with a homogenous, bright diffuse backscatter is present as scattered exposures in the eastern part of the quadrangle. These exposures have been mapped as "bright material," but it is not clear at present if this is a valid unit or if it is part of the brighter regional plains unit.

Tessera terrain is primarily found along the western border of the quadrangle, where Lachesis Tessera refers to the southern exposures, and Zirka Tessera refers to northern exposures. A second tessera unit has been mapped with the symbol "t?." This unit appears to be deformed by the requisite 2 sets of closely spaced structures, but it is so extensively flooded by regional plains materials that the structural fabric is partially obscured. Tessera terrain is present in the adjacent V-17 quadrangle, where both Lachesis Tessera and Zirka Tessera are areally more extensive than in V-18.

Ridge and fracture belts are both present, but not as extensive as is the case in, for example, the Pandrosos Dorsa (3) and Lavinia Planitia (4) quadrangles. As is commonly the case, it is difficult to determine if the materials of these belts are older or younger than regional plains. A recent study using radar properties (5) demonstrated that at least most ridge belts appear to be older than regional plains. The materials of fracture belts probably are also older than regional plains, but the fractures themselves can be both older and younger than regional plains (e.g., 3).

Three named coronae are present, but only Zemire Corona has significant associated flows. An interesting nearly linear structure extends from the fracture belt Breksta Linea in the western part of the quadrangle east-southeastward through Zemire Corona to Pasu-Ava Corona. The tectonic significance of this composite structure is unclear at present. A feature named Jaszai Patera is very likely another corona.

Volcanic materials and landforms are abundant in the Lachesis Tessera quadrangle. In particular, small domes and shields are abundant and widespread. In places, small shields are not only exceptionally abundant, but they are associated with mappable materials, and thus help define a "shield flows" unit. Isolated flows are common, and where these are areally large enough they have been mapped as undifferentiated flows. Other volcanic features include two relatively large shield volcanoes, both with complete calderas and with flows extensive enough to map. A number of pancake domes occur in the Lachesis Tessera quadrangle. Various mechanisms for forming flat-topped domes such as these have been proposed, but none is really satisfactory. This quadrangle is not likely to provide breakthrough evidence for the genetic processes responsible for pancake domes.

The 13 impact craters in the Lachesis Tessera quadrangle range in diameter from 2.4 to 40 km. Four of these are actually doublets. Five of the craters have associated radar-dark halos or parabolas. Only 2 of the 13 craters are significantly degraded. All 13 craters are superposed on either regional plains or on flows that are, in turn, superposed on regional plains.

The fragmented record of tessera and some deformation belts suggests that flooding by regional plains materials has had a significant effect on the distribution of materials older than the regional plains. This, in turn, indicates that regional plains must be relatively thin in the Lachesis Tessera quadrangle, or else the tessera and deformation belts exhibit less relief than generally is the case.

References cited: (1) McGill, G.E., V-20 quadrangle, 2000; (2) Campbell, B.A., JGR 104, 21,951, 1999; (3) Rosenberg, E., and McGill, G.E., V-5 quadrangle, 2001; (4) Ivanov, M.A., and Head, J.W., III, V-55 quadrangle, 2001; (5) McGill, G.E., and Campbell, B.A., JGR 111, E12006, doi:10,1029/2006JE002705, 2006.

GEOLOGIC MAPPING OF THE JUNO CHASMA QUADRANGLE, VENUS: ESTABLISHING THE RELATION BETWEEN RIFTING AND VOLCANISM. D. A. Senske, Jet Propulsion Laboratory/California Institute of Technology, Pasadena, CA, 91109, dsenske@jpl.nasa.gov.

Introduction: To understand the spatial and temporal relations between tectonic and volcanic processes on Venus, the Juno Chasma region is mapped [1,2] (Fig. 1). Geologic units are used to establish regional stratigraphic relations and the timing between rifting and volcanism.

General Structure and Topography: Juno Chasma trends east to west along the crest of a 1.0 km high linear topographic rise. Located along the highest topography is a 60- to 90-km wide, 1.0- to 2.5-km deep, graben. A cluster of four coronae, Tai Shan, Gefjun, and two unnamed structures (31.8° S, 99.6° E; 29.8° S, 95.0° E) act to divide the rift into two main parts (Fig. 1). The first extends for 530 km between the 2.2-km high, 600-km diameter volcano Kunapipi Mons (outside the map area) and the cluster of coronae. The second lies between the corona cluster and an unnamed caldera-like structure centered at 30.6° S, 110.8°. To the east of the caldera-like structure, the rift branches into two arms, forming a "hub & spoke" pattern, the first segment trends N 55° E and the second S 60° E. This area corresponds to the highest topography and the rift is less well defined as a distinct graben, being made up of a series of depressions separated by local highs.

Geologic Units: Eight major units are identified (Fig. 1) based on patterns of radar backscatter and the presence of crosscutting and on-lapping relations. The units are divided into four classes: (1) those that form relatively localized systems of lava flows, (2) regional-scale plains forming materials, (3) tectonic units and (4) impact related materials. In addition to the sequence of events emplacing the geologic units, a number of episodes of tectonic activity have acted to shape the surface of this part of Venus.

Lava Flow Materials. Volcanic activity has produced a variety of structures that range from small shields (several to 10s of km in diameter), steep sided domes and channels to large constructs such as coronae, calderas, and regional-scale, greater than 100 km in diameter, edifices. The characteristics of units placed in the category of lava flow materials (*fa*,*fb*,*fc*, and *fd*) are distinguished by (1) lobate sets of deposits whose lengths exceed their widths, (2) the presence of distinct flow lobes both at the toe and along the margins of the flows and (3) a range of backscatter characteristics for different flows, producing a local mottled texture. Flow units are typically young stratigraphically and correspond to late-stage volcanism associated with coronae and calderas.

Plains Units. Regional plains (*pr, pha-b, pm, pl, pju*) make up a majority of the quadrangle. These units typically have homogeneous textures and are interpreted to be lava flood deposits. Their emplacement covers a major portion of the history of the region. The association of the oldest plains unit, lineated plains (*pl),* with outcrops of tessera suggests that some of the tessera forming tectonic events coincided with early plains formation. The association of homogeneous plains unit b (*phb*) with the Juno rift and its subsequent deformation by rift related faulting suggests that its emplacement is related to early chasma formation.

Tectonic Units. Located on the distal flanks of the Juno rift, but still associated with the elevated topography are areally extensive, elevated outcrops of material identified as tessera (*t*), Husbishag and Sudice Tesserae. Tessera represents the stratigraphically oldest terrain in this area.

Impact Crater Materials. Impact processes have modified the surface materials throughout the region. The 73-km diameter crater, Boulanger, and its associated dark surficial deposits (dark parabolas of low emissivity material) dominate the northwestern part of Juno Chasma. The Boulanger impact is relatively recent as its associated deposits superpose all other units in the northwest part of the quadrangle.

Geologic History: The relations between the units provide insight into the major geologic events, from oldest to most recent, in the formation of the Juno Chasma region: (1) tessera formation followed by extensive regional plains (*pr)* emplacement; (2) uplift and extension forming the Juno topographic rise and early faults; (3) emplacement of widespread homogeneous plains (*pha* and *phb*) on the flanks of the rise; (4) continued extension resulting in the removal of the source vents for the flanking flows; (5) volcanic activity forming Tai Shan and Gefjun Coronae and their associated deposits. Although impacts have occurred throughout the history of the region, the crater Boulanger appears to be geologically recent.

References: [1] Senske, D. A., *et al*., LPSC XXV, 1245-1246, 1994; [2] Senske, D. A., LPSC XXVII, 1171-1172, 1996; [3] Senske, D. A., Geologic Map of the Juno Chasma Quadrangle (V-47), Venus, in prep. for submittal to USGS, 2008.

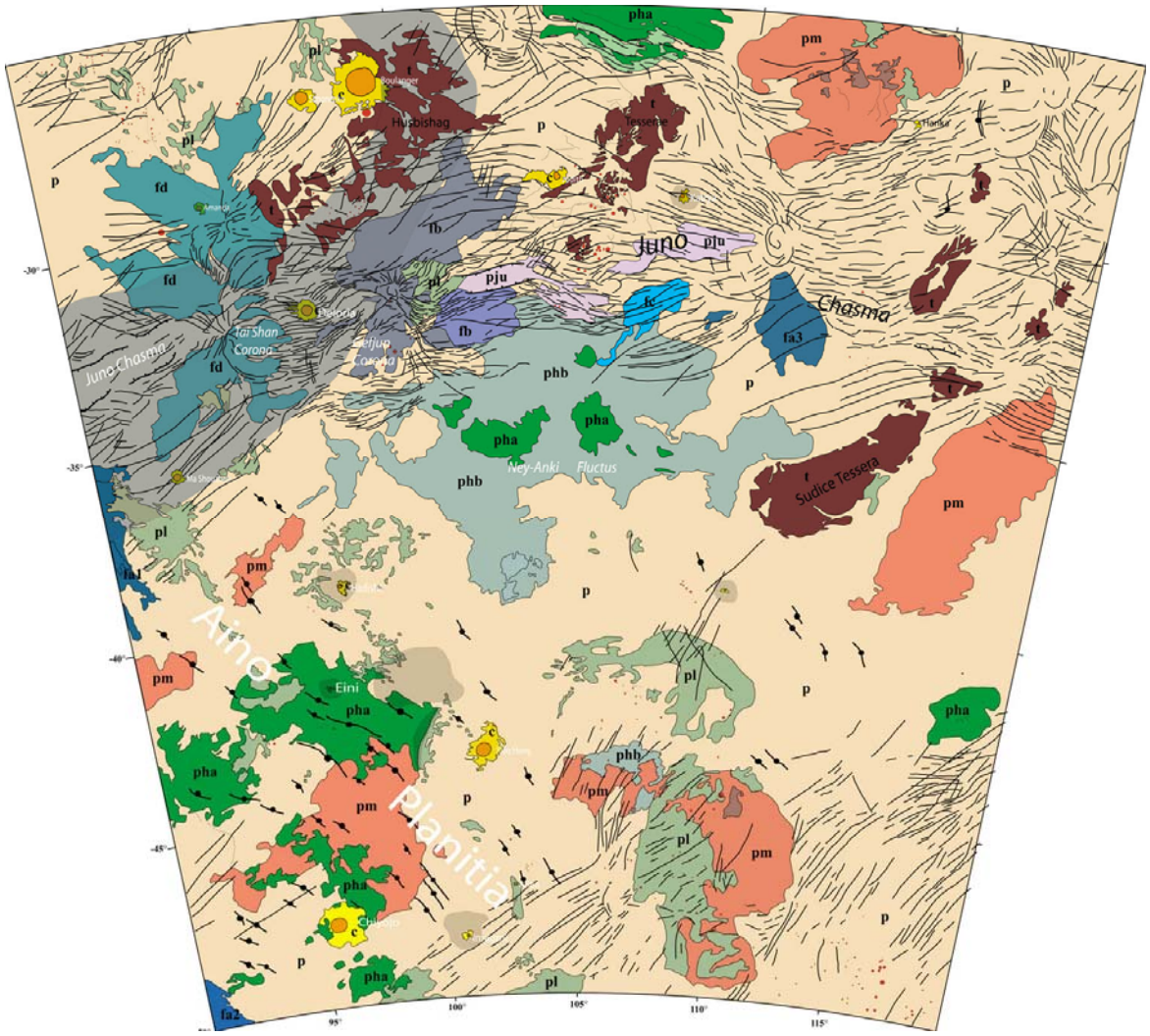

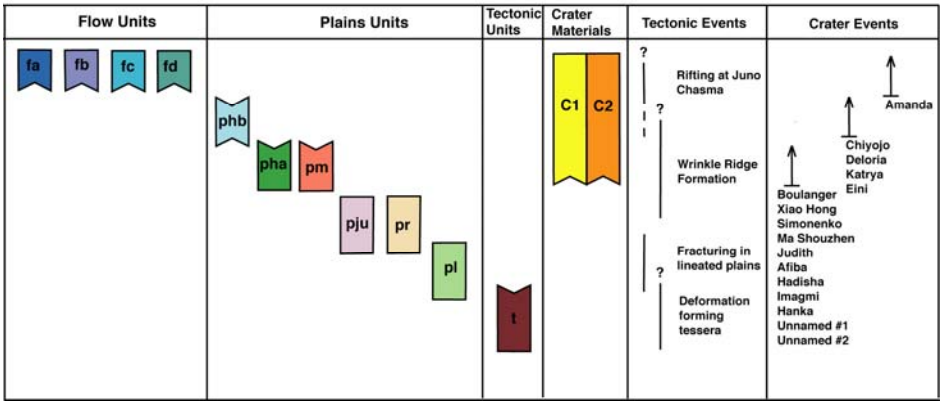

Figure 1. Regional-scale geologic map and correlation chart of the Juno Chasma Quadrangle (V-47). Units are defined on the basis of patterns in radar backscatter and cross-cutting and on-lapping relations.

GEOLOGIC MAPPING OF V-19, V-28 AND V-53. E. R. Stofan[1,2], P. Martin[3] and J. E. Guest[2], [1]Proxemy Research (20528 Farcroft Lane, Laytonsville, MD 20882, (ellen@proxemy.com), [2]Department of Geological Sciences, University College London, UK, [3]Department Earth Sciences, Durham University, Durham UK DH1 3LE.

Introduction: Geologic maps of Sedna Planitia (V-19), Hecate Chasma (V-28) and Themis Regio (V-53) quadrangles have been completed at the 1:5,000,000 scale as part of the NASA Planetary Geologic Mapping Program. V-53 has been reviewed once and will be resubmitted by fall, V-28 has undergone three reviews and will be resubmitted this summer, and V-19 will be submitted for review by August.

Quadrangle Overviews: V-19: The Sedna Planitia Quadrangle (V-19) extends from 25°N - 50°N latitude, 330° - 0° longitude. The quadrangle contains the northernmost portion of western Eistla Regio and the Sedna Planitia lowlands.

Seven plains materials units have been mapped in V-19, that range from relatively localized, limited extent units (unit pdS, densely fractured Sedna plains) to more regional plains units (unit phS, Sedna homogeneous plains). Sixteen units associated with volcanoes have been mapped, with multiple units mapped at Sif Mons, Sachs Patera and Neago Fluctūs. An oddly textured, radar-bright flow is also mapped in the Sedna plains, which appears to have originated from a several hundred kilometer long fissure. Six coronae have a total of eighteen associated flow units. In addition, impact crater materials and tessera materials are mapped.

Multiple episodes of plains formation and wrinkle ridge formation dominate the geologic history of the V-19 quadrangle, interspersed in time and space with edifice- and corona-related volcanism. The formation of Eistla Regio postdates most plains units, causing them to be deformed by wrinkle ridges and overlain by corona and volcano flow units.

V-28: The Hecate Chasma Quadrangle (V-28) extends from 0°-25° N. latitude, 240°-270° longitude. It contains a portion of the Hecate Chasma rift system, which is over 2000 km long and extends across a lowland region (Hinemoa Planitia). In V-28, we have mapped plains units, corona flow units, moderate and large volcano flow units, edifice field units, and tessera. The intermediate to large volcanoes include Nazit, Wyrd and Polik-mana Montes and Paoro, Nipa and Pajan Yan Tholi. There are fourteen coronae in the quadrangle, the largest of which is the 525 km diameter Taranga Corona. There are eight impact craters in the V-28 quadrangle. The ten plains materials units in V-28 are not very extensive and many are not in contact, resulting in a very horizontal stratigraphic column as we are unable to determine many clear stratigraphic relationships. Of the fourteen coronae in the quadrangle, ten have associated flow deposits, with several having multiple units. As is the convention with volcano units, we map corona flow units by naming them after their source (i.e., unit fT-flows from Taranga Corona). Other mappers have chosen to lump corona flows into a generic unit, which does not allow for as detailed a stratigraphic history for a given region. The other four coronae either deform plains units or are embayed by plains, volcano or other corona units.

The geologic history of V-28 is one of interleaved episodes of plains-forming volcanism, corona formation, and formation of intermediate to large volcanic edifices. The rift system is relatively young, but appears to have formed in stages, generally concurrent with corona formation.

V-53: The Themis Regio Quadrangle (V-53) extends from 25°S - 50°S latitude, 270° - 300° longitude. The quadrangle contains the southernmost portion of Parga Chasmata, the Themis Regio highland and surrounding plains. The topographically lowest points in the quadrangle (about 2 km below MPR) are within the Parga Chasmata rift and in the troughs around several coronae.

Six plains units have been mapped in V-53. The plains farthest from Parga Chasmata are more regional-scale plains units, unlike the more patchy plains units of V-28. Twenty corona materials units are mapped, and as in V-28, are named after their source. Nine units associated with specific named volcanic edifices have been mapped. Many flow units in V-53 are not in contact, or in contact with consistent plains units, making an overall stratigraphy difficult to determine. There are 12 impact craters within the quadrangle.

The geologic history of V-53 is dominated by corona and rift formation, with some coronae predating rifting, and some postdating it. Most coronae are interpreted to have formed synchronously with rifting. No clear progression in volcanism from coronae and volcanoes is observed.

Conclusions: In V-28 and V-53, more plains materials units have been mapped than in our previously mapped quadrangles, V-46 and V-39. V-19 is more comparable to these latter maps in terms of numbers of plains units. In V-28, all of the plains materials units to the south of the rift have an unusually high concentration of volcanic edifices, which both predate and postdate the units. A similar situation is seen in V-53 and V-19, where small edifice formation is not confined to any specific time period.

In the two chasma-related quadrangles, coronae are located along the rift, as well as to the north and the south of the rifts. Coronae in both quadrangles exhibit all forms of corona topographic shapes, including depressions, rimmed depressions, plateaus and domes. Most of the coronae formed synchronously with the rifting, although some predate the rifts and others postdate extensional deformation.

A strong association between volcanism and coronae along rifts has been noted elsewhere on the planet [1]. In V-28 and V-53, some coronae along the rift do not have much associated volcanism; coronae with the most volcanism in these quadrangles are located at least 500 km off the rifts or on the Themis Regio highland. While extension clearly plays a role in the amount of volcanism associated with coronae, it is not the only contributing factor. Coronae at Themis Regio may have greater than average associated volcanism owing to the possible mantle plume beneath the rise [2].

All three quadrangles have very horizontal stratigraphic columns, as limited contact between units prevents clear age determinations. While this results in the appearance that all units formed at the same time, the use of hachured columns for each unit illustrates the limited nature of our stratigraphic knowledge in these quadrangles, allowing for numerous possible geologic histories. The scale of resurfacing in these quadrangles is on the scale of 100s of kilometers, consistent with the fact that they lie in the most volcanic region of Venus.

References: [1] Magee, K.P. and J.W. Head, 1995. *J. Geophys. Res*. **100**, 1527-1552. [2] Stofan, E.R., S.E. Smrekar, D.L. Bindschadler, and D.A. Senske, 1995. *J. Geophys. Res*. 100: 23,317-23,327.

LUNAR GEOLOGIC MAPPING PROGRAM: 2008 UPDATE. L. Gaddis[1], K. Tanaka[1], J. Skinner[1], and B.R. Hawke[2], [1]U.S. Geological Survey, Astrogeology Program, 2255 N. Gemini Drive, Flagstaff, AZ (lgaddis@usgs.gov); [2]PGD/SOEST, Univ. Hawaii, Honolulu, HI.

Introduction: The NASA Lunar Geologic Mapping Program is underway and a mappers' handbook is in preparation. This program for systematic, global lunar geologic mapping at 1:2.5M scale incorporates digital, multi-scale data from a wide variety of sources. Many of these datasets have been tied to the new Unified Lunar Control Network 2005 [1] and are available online. This presentation summarizes the current status of this mapping program, the datasets now available, and how they might be used for mapping on the Moon.

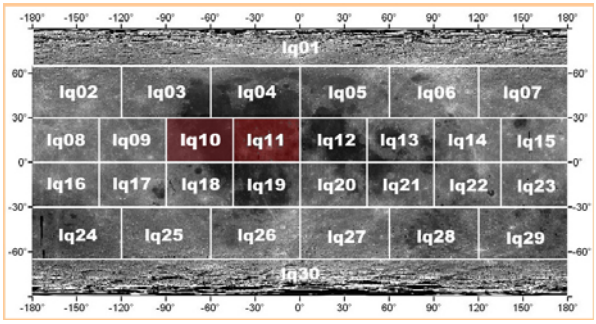

Figure 1. Mapping quad scheme for lunar geologic maps at 1:2.5 M scale. Image base is Clementine 750-nm albedo. Quads lq10 and lq11 have been assigned to mappers.

Background: The primary image bases for early lunar geologic mapping were photographic prints (~400 to 2 m ground resolution) from the five Lunar Orbiter (LO) missions in 1966 and 1967 [2-4]. Forty-four geologic maps at 1:1 M scale were made using the LO data, followed by 1:5 M near side, north, south, east, west and central far side geologic maps [5-10]. These maps were based upon the foundation established by Shoemaker and Hackman [11], who applied well established stratigraphic methods to map materials observed in and near Copernicus crater (~90 km dia.). This new mapping program builds further on this foundation by incorporating new digital datasets and mapping methods that enable far more detailed identification and mapping of geologic units on the Moon.

Mapping Status: Two quadrangles have thus far been assigned (Figure 1) and several more have been proposed to NASA. Quad lq11 was the first in this series, centers on Copernicus crater, and is now in draft form in preparation for review [12]. Quad lq10 was assigned recently and is now in the early stages of development [13].

Digital Image Bases: Following the early spacecraft observations of the Moon in the 1960s and 70s, a second era of global observation began in the 1990s. The global color, elemental abundance, and topographic datasets from these missions (including Galileo, Clementine, and Lunar Prospector or LP) have led to the development of a newer generation of digital data products that are tied to an updated global geodetic control network [14, 15]. Two major projects to scan and process photographic data from Lunar Orbiter [16] and Apollo [17] missions have produced digital products that can be analyzed in the context of the new generation of global datasets. Further, the LO and Apollo metric and panoramic digital data can be used to make controlled, high-resolution digital terrain models (DTMs) and image mosaics that will be useful for both local and regional scale mapping. When used with data from the next generation of lunar observing instruments [including the micro-Imager (AMIE) from SMART-1, Europe; Lunar Imager/Spectrometer from Kaguya (SELENE), Japan; the Stereo Camera and Laser Altimeter from Chang'e-1, China; the Terrain Mapping Camera, Hyperspectral Imager, and Moon Mineralogy Mapper from Chandrayaan-1, India; and the camera and laser altimeter from Lunar Reconnaissance Orbiter, United States] the collection of digital image data for the Moon will soon exceed the volume of data for all previous lunar and planetary missions combined. Effective use of these data for lunar geologic mapping will require (a) creation of cartographic mapping products that can readily be integrated, (b) advances in storage, manipulation, and analysis of high-volume, multidimensional data, and (c) expertise in use of advanced methods of data interpretation and digital mapping.

Many of the available digital lunar image bases are described on the Lunar Geologic Mapping site (see http://astrogeology.usgs.gov/Projects/PlanetaryMapping/Lunar/) and are available on the PDS

Map-a-Planet site (http://www.mapaplanet.org/explorer/moon.html) and/or the USGS 'Planetary Interactive GIS on the Web Interactive Analyzable Database' (PIGWAD) site (http://webgis.wr.usgs.gov/). Primary image bases for lunar geologic mapping are the global Clementine mosaic of "albedo" at 750-nm [18] and the highly complementary Lunar Orbiter mosaic [16]. Additional mapping layers include the global Clementine multispectral mosaic (available at 100 m/pixel for five ultraviolet-visible or UVVIS wavelengths [19]: 415, 750, 900, 950, and 1000 nm; and six near-infrared or NIR wavelengths [20]: 1100, 1250, 1500, 2000, 2600, and 2780 nm) and Clementine topography and shaded relief data [21]. Derived maps of Clementine 'standard' color-ratio (e.g., R=750/415; G=750/950; B=415/750), optical maturity, FeO, and TiO_2 content [22-25], 'rock types' [26], and LP measured elemental abundance maps [27-32] are also available at these sites. An alternative method for deriving FeO content and removing the effects of maturity differences among lunar soils [33] is also available for application to the Clementine 11-band data and for comparison to other methods. Use of these digital data and derived products support image manipulation and enhancement, and further derivation of products such as spectral band-depth maps, slope and image texture maps, density-sliced albedo and color, as well as other 2- and 3-D analyses and visualizations for geologic mapping. Derived maps of optical maturity of lunar soils have been used to refine stratigraphic assignment of several impact craters in the Copernicus quadrangle (lq11; [34]) and will be very helpful in modifying the lunar stratigraphic column [35, 36] as needed based on new mapping.

In recognition of the extreme importance of coregistered image products for geologic mapping, mosaics of Clementine UVVIS and NIR data and derived products, as well as the global mosaic from Lunar Orbiter, have been warped to the latest lunar control network [1, 14, 15] and are online at the PIGWAD site. Reconstruction of the Clementine 750-nm map mosaic using the 2005 lunar control network is now underway at USGS [37] and is expected to result in a more spatially accurate product than the warped version. Construction of the other Clementine UVVIS and NIR bands is not currently planned but is being considered at USGS and elsewhere. Further improvements of the lunar control network are underway and can be applied directly to these products when available.

Summary: The Lunar Geologic Mapping Program is continuing to progress and to make use of the new lunar data that have recently and will soon become available. We are working with the Lunar Geodesy and Cartography working Group [38] to ensure that these data will be useful for geologic mapping applications. Proposals for participation in this mapping program can be submitted to the NASA Planetary Geology and Geophysics Program science research opportunity that is included in the annual NASA Research Opportunities in Space and Earth Sciences (ROSES) announcement on the NSPIRES web site (see http://nspires.nasaprs.com/external/).

References: [1] Archinal et al., 2006, USGS OFR 2006-1367. [2] Hansen, 1970, NASA SP-242. [3] Kosofsky and El-baz, 1970, NASA SP-200. [4] Bowker and Hughes, 1971, NASA SP-206. [5] Wilhelms and McCauley, 1971, USGS I-703. [6] Lucchitta, 1978, USGS I-1062. [7] Wilhelms et al., 1979, USGS I-1162. [8] Wilhelms and El-baz, 1977, USGS I-946. [9] Scott et al., 1977, USGS I-1034. [10] Stuart-Alexander, 1978, USGS I-1047. [11] Shoemaker and Hackman, 1962, Symp. 14 IAU, 289-300. [12] Gaddis et al., 2006, LPS XXXVII, #2135. [13] Gregg, Tracy, Pers. Comm. [14] Archinal et al., 2008, LPS XXXIX, #2245. [15] Hare et al., 2008, LPS XXXIX, #2337. [16] Becker et al., 2008, LPS XXXIX, #2357. [17] Apollo Image Archive, see http://apollo.sese.asu.edu/index.html. [18] Eliason et al., 1999, LPS XXX, #1933. [19] Eliason et al., 1999, Clementine UVVIS Mosaic, PDF Volumes USA_NASA_CL_4001-4078. [20] Gaddis et al., 2008 (in review), The Clementine NIR Global Lunar Mosaic, PDS Volumes USA_NASA_PDS_CL_5001 through 5078. [21] Rosiek et al., 2002, LPS XXXIII, #1792. [22] Lucey et al., 1995, Science 268, 1150. [23] Lucey et al., 1998, JGR 103, 3679-3699. [24] Lucey et al., 2000a, JGR 105, 20,297-20,305. [25] Lucey et al., 2000b, JGR 105, 20,377-20,386. [26] Pieters et al., 2001, JGRP, 106, 28001. [27] Lawrence et al., 2002, JGR 107, 2001JE001530, 13-1 to 13-26. [28] Elphic et al., 2000, JGR 105, 20,333-20,346. [29] Gillis et al., 2003, JGR 108, 3-1 to 3-18. [30] Lawrence et al., 2000, JGR 105, 20,307-20,332. [31] Prettyman et al., 2002a, LPS XXX, #2012. [32] Feldman et al., 2002, JGR 107, E3. [33] Le-Mouelic et al., 2000, JGRP, 105, 9445. [34] Hawke et al., LPS XXXIX, #1902. [35] Wilhelms, 1987, USGS Prof. Paper 1348, 302 pp. [36] Hiesinger et al., 2003, JGR, 108, doi:10.1029/2002JE001985. [37] Lee, E.M., Pers. Comm. [38] Archinal et al., 2008, submitted to the First Lunar Science Conference.

GEOLOGIC MAPPING OF THE MARIUS QUADRANGLE, THE MOON. Tracy K.P. Gregg[1] and Aileen Yingst[2], [1]Department of Geology, 876 Natural Sciences Complex, University at Buffalo, Buffalo, NY 14260, (tgregg@geology.buffalo.edu), [2]Natural and Applied Sciences, University of Wisconsin-Green Bay, Green Bay, WI 54311-7001 (yingsta@uwgb.edu).

Introduction: We will construct a 1:2,500,000-scale map of Lunar Quadrangle 10 (hereinafter called "LQ10" and/or the "Marius Quadrangle") to address outstanding questions about the Moon's volcanologic history and the role of impact basins in lunar geologic evolution. The selected quadrangle contains Aristarchus plateau and the Marius hills (informal names), Reiner Gamma, and Hevelius crater. By generating a geologic map of this region, we can constrain the temporal (and possibly genetic) relations between these features, revealing more information about the Moon's chemical and thermal evolution. Although many of these individual sites have been investigated using Lunar Orbiter, Clementine, Lunar Prospector and Galileo data, no single investigation has yet attempted to constrain the stratigraphic and geologic relationships between these features. Furthermore, we will be able to compare our unit boundaries on the eastern boundary of the proposed map area with those already mapped in the Copernicus Quadrangle [1-3].

Outstanding Questions to be Answered through Geologic Mapping: Geologic mapping of the Marius Quadrangle would provide insight to the following questions [4].

1) What are the origin, evolution, and distribution of mare volcanism?

The Marius Quadrangle contains superlatives of lunar volcanism. Aristarchus plateau contains the widest sinuous rille on the Moon, Vallis Schröteri [5], and the highest concentration of sinuous rilles on the Moon [5-7]. The Marius hills represent the largest concentration of domes and cones yet found on the Moon [8]. Surrounding these features are the maria of Oceanus Procellarum, containing some of the youngest examples of lunar volcanism [7, 9–11]. Any model for mare volcanism must take into account the range of volcanic behavior displayed within the Marius Quadrangle, and geologic mapping will provide clues as to how these volcanic features are related in space and time. Furthermore, the Procellarum KREEP terrain [12-14] is roughly centered within the proposed map area. It is unlikely to be mere coincidence that the high abundance of heat-producing thorium [12] is concentrated in this region of nonpareil volcanism on the Moon [cf. 14]. However, the precise relation between the Procellarum KREEP terrain and the surficial geology must be examined in detail to constrain cause and effect. A geologic map of LQ10 will directly address this outstanding question.

2) What were the timing and effects of the major basin-forming impacts on lunar crustal stratigraphy?

Orientale basin is one of the youngest impact basins on the Moon [5], and much of its structure is not flooded by younger maria. The western portion of LQ10 is dominated by highlands that are modified by Orientale impact ejecta [5,15]. The boundary between the ejecta-covered highlands and the Procellarum maria has an interesting topographic expression (Fig. 2), revealing that the lavas are quite thin where they embay the highlands, and that the underlying ejecta patterns locally control the lava emplacement. Examining the Orientale ejecta, its distribution and composition, could reveal important information about ejecta emplacement and basin excavation. Mustard and Head [16] identified abundant cryptomaria identified in the region affected by Orientale ejecta, indicative of volcanism within Oceanus Procellarum prior to the Orientale impact. Furthermore, they state that the relation between geomorphology and composition is not always clear-cut on the Moon. It has been proposed [5,17,18] that Oceanus Procellarum is the site of an ancient impact basin. However, there is not a general consensus about the existence of such a basin [5,10,11,19,20]. Generating a geologic map, including structural features and mare thickness, would provide additional data to constrain the presence of such a basin. As noted below, the most up-to-date lunar topographic data [21] will be used to characterize the current expression of impact craters and their deposits.

3) What are the Moon's important resources, where are they concentrated, and how can they be accessed?

How "important resources" are precisely defined would shape the answer to this question. Here, we define "important resources" as those that would assist the human presence on the Moon. Oxygen is obviously a vital resource, and most proposals to extract oxygen from lunar materials require a source of FeO [22-24]. Ilmenite ($FeTiO_2$) has been identified on the Moon, and is the most likely source for abundant TiO_2 and FeO. Recently, the Hubble Telescope imaged the Apollo 17 landing site and Aristarchus crater, and ilmenite was identified as a likely component in both locations [http://www.nasa.gov/vision/universe/solarsystem/hubble_moon.html]. Volcanic glass could be a viable FeO source [25]. McEwen et al. [26] identified ~200 km^3 of pyroclastic deposits (i.e., iron-bearing

volcanic glass) mantling the Aristarchus plateau; similar deposits are found on the Marius hills [8]. By analogy with materials collected at the Apollo 17 landing site, these pyroclastics were likely generated by the fragmentation of lava by magmatic volatiles [cf. 27,28], and so their surficial distribution is related to their subsurface distribution. Identifying and mapping pyroclastic deposits within the Marius Quadrangle will provide information about the distribution of these materials through space and time. Constraining the timing, volumes, and distributions of pyroclastic deposits within the map area further constrains the volatile history, and provides insight as to the volatile abundance through time—and possibly identifies additional resources for lunar development.

Mapping Progress: Although funding has been approved, it has not yet been received. The PIs will meet this summer to begin test-mapping subregions in July, 2008.

References: [1] Gaddis, L.R., J. Skinner, Jr., K. Tanaka, B.R. Hawke, P. Spudis, B. Bussey, C. Pieters and D. Lawrence, 2006a, *LPSC 37th*, Abstract #2135. [2] Gaddis, L.R., J. Skinner, Jr., T. Hare, K. Tanaka, B.R. Hawke, P. Spudis, B. Bussey, C. Pieters and D. Lawrence, 2006b, *USGS Open-File Report 2006-1263*. [3] Skinner, J.A., Jr., L.R. Gaddis and K.L. Tanaka, 2006, *USGS Open-File Report 2006-1263*. [4] Joliff, B.L., 2006, *Rev. Min. Chem. 60*:v-xv. [5] Wilhelms, D.E., 1987, *USGS Prof. Paper 1348*. [6] Guest, J.E. and J.B. Murray, 1976, *J. Geol. Soc. London 132(3)*:251. [7] Whitford-Stark, J.L. and J.W. Head, 1977, *Proc. Lun. Planet. Sci. 8th*:2705. [8] Weitz, C.M. and J.W. Head, 1999, *J. Geophys. Res. 104(E8)*:18,933. [9] Whitford-Stark, J.L. and J.W. Head, 1980, *Proc. Conf. Multi-ringed basins*, pp. 105. [10] Hiesinger, H., J.W. Head, U. Wolf, R. Jaumann and G. Neukum, 2003, *J. Geophys. Res. 108(E7):*5065. [11] Hiesinger, H. and J.W. Head, 2006, *Rev. Min. Geochem. 60*:1. [12] Haskin, L.A., J.J. Gillis, R.L. Korotev and B.L. Jolliff, 2000, *J. Geophys. Res. 105(E8)*:20,403-20,415. [13] Jolliff, B.L., J.J. Gillis, L.A. Haskin, R.L. Korotev and M.A. Wieczorek, 2000, *J. Geophys. Res. 105(2)*:4197. [14] Wieczorek, M.A. and R.J. Phillips, 2000, *J. Geophys. Res. 105(E8):*20,417. [15] Scott, D.H., J.F. McCauley and M.N. West, 1977, *USGS Misc. Invest. Ser. I-1034*. [16] Mustard, J.M. and J.W. Head, 1996, *J. Geophys. Res. 101(E8):*18,913. [17] Wilhelms, D.E. and J.F. McCauley, 1971, *USGS Misc. Invest. Series I-703*. [18] Feldman, W.C., O. Gasnault, S. Maurice, D.J. Lawrence, R.C. Elphie, P.G. Lucey and A.B. Binder, 2002, *J. Geophys. Res. 107(3*):1. [19] Spudis, P.D., 1993, Cambridge University Press, 263 pp. [20] Spudis, P.D. and P.H. Schultz, 1976, *NASA Tech. Mem. 88-383:203*. [21] Archinal, B.A., M.R. Rosiek, R.L. Kirk and B.L. Redding, 2006, *USGS Open-File Report 2006-1367*. [22] Coombs, C.R., B.R. Hawke and C.C. Allen, 1998, *Proc. 6th Int. Conf. Exposition Eng. Const. Ops*, 608. [23] Rosenberg, S.D., 1998, *Proc. 6th Int. Conf. Exposition Eng. Const. Ops*, 622. [24] Duke, M.R., L.R. Gaddis, G.J. Taylor and H.H. Schmidt, 2006, *Rev. Min. Geochem. 60*:597. [25] Hawke, B.R., C.R. Coombs and B. Clarke, 1990, *PLPSC 20th*:249. [26] McEwen, A.S., M.S. Robinson, E.M. Eliason, P.G. Lucey, T.C. Duxbury and P.D. Spudis, 1994, *Science 266*:1858. [27] Wilson, L. and J.W. Head, 1981, *J. Geophys. Res. 86(4)*:2971. [28] Wilson, L. and J.W. Head, 2003, *Geophys. Res. Lett. 30(12*):1605.

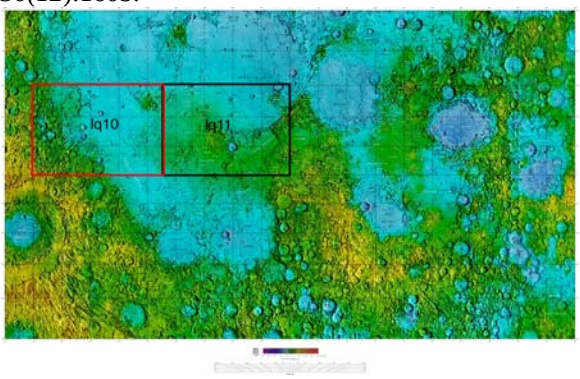

Figure 1. Location of Lunar Quadrangle 10 outlined in red in this topographic map of the lunar near side [Archinal et al., 2006]. Lunar Quadrangle 11, outlined in black, is currently being mapped at 1:2.5 million by Gaddis and others [1, 2].

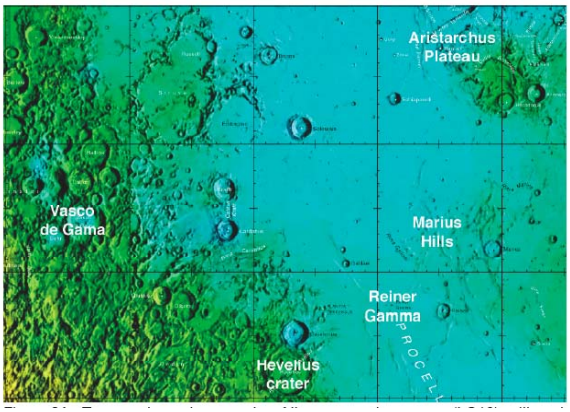

Figure 2. Topography and geography of the map area (LQ10), with major geographic features labeled. Topographic color scale is the same as in Fig. 1.

GEOLOGIC MAPPING ALONG THE ARABIA TERRA DICHOTOMY BOUNDARY: MAWRTH VALLIS AND NILI FOSSAE, MARS: INTRODUCTORY REPORT. Leslie F. Bleamaster III[1,2], and David A. Crown[1], Planetary Science Institute, [1]corporate address - 1700 E. Ft. Lowell Rd., Suite 106, Tucson, AZ 85719; [2]mailing - 3635 Mill Meadow Dr., San Antonio, TX 78247, lbleamas@psi.edu.

Introduction. Geologic mapping studies at the 1:1M-scale will be used to characterize geologic processes that have shaped the highlands along the Arabia Terra dichotomy boundary. In particular, this mapping will evaluate the distribution, stratigraphic position, and lateral continuity of compositionally distinct outcrops in Mawrth Vallis and Nili Fossae as identified by spectral instruments currently in orbit. Placing these landscapes, their material units, structural features, and unique compositional outcrops into spatial and temporal context with the remainder of the Arabia Terra dichotomy boundary will provide the ability to: 1) further test original dichotomy formation hypotheses, 2) constrain ancient paleo-environments and climate conditions, and 3) evaluate various fluvial-nival modification processes related to past and present volatile distribution and their putative reservoirs (aquifers, lakes and oceans, surface and ground ice) and the influences of nearby volcanic and tectonic features on hydrologic processes in these regions.

The result will be two 1:1M scale geologic maps of twelve MTM quadrangles (Mawrth Vallis - 20022, 20017, 20012, 25022, 25017, and 25012; and Nili Fossae - 20287, 20282, 25287, 25282, 30287, 30282).

Figure 1. Merged 128 pixel/degree MOLA digital elevation model, THEMIS IR mosaic, and Viking MDIM 2.1 of the Arabia Terra dichotomy boundary. Cyan-colored boxes show mapping regions with respect to other mapping areas and regions of interest for this investigation. Simple Cylindrical projection, 5 degree graticule.

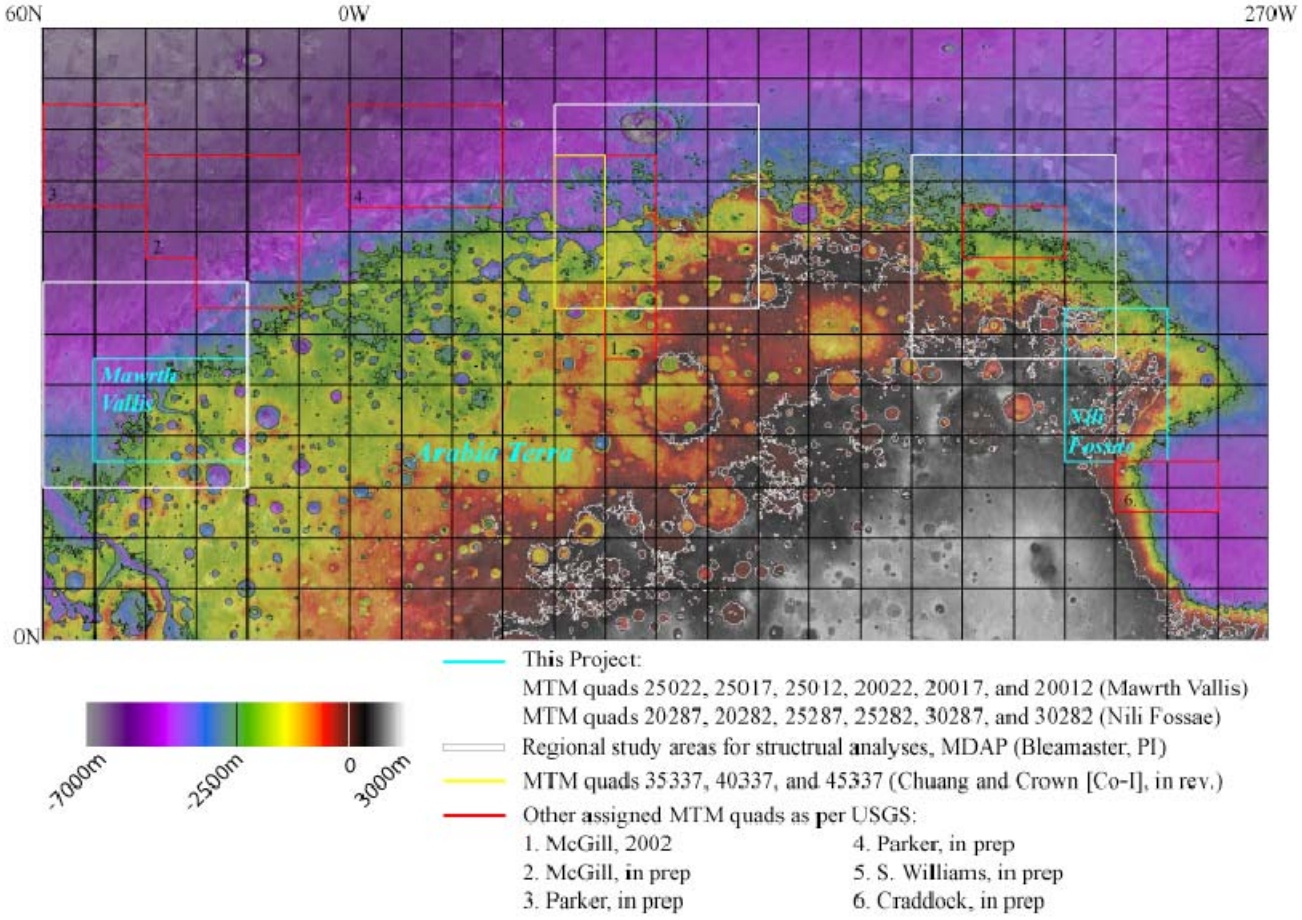

Mawrth Vallis, an extensive (500 km long) sinuous channel that dissects the heavily cratered surface of Arabia Terra, is located near the western extent of the Arabia Terra plateau. Considered one of the oldest of the outflow channels, along with Ares Vallis [1], this easternmost circum-Chryse Planitia channel may represent remnant scours of catastrophic outflow often attributed to failure of a subterranean aquifer and/or by persistent groundwater sapping. Mawrth Vallis, however, does not exhibit typical outflow channel source region characteristics [2] and may have resulted from a more protracted hydrologic history [3]. Mawrth's source region is highly degraded and appears to head from a degraded crater (18°N, 13°W) but loses definition in both the up and down gradient directions and preserves few pristine bedforms suggesting that significant modification has taken place since its formation. MOLA topography displays subtle southeastern extensions towards Meridiani Planum that may be related to paleo-Mawrth Vallis headwaters. Mawrth Vallis displays no evidence of surface water contributions or linkages with Noachian valley networks, and preserves little evidence (streamlined islands, inner channels, etc.) of sustained flow along its length in high-resolution images. Although it is difficult to discount that Mawrth Vallis was at one time an active fluvially derived feature, a conclusion based on its macro-scale, plan-form morphology and spatial association with the other outflow channels, much of the geologic evidence of its origin appears to have been degraded, modified, and reworked into what we observe today, a complex amalgam of geologic materials.

Mawrth Vallis' mouth is also coincident with a portion of the putative Arabia shoreline [4, 5]. The juxtaposition of considerable amounts of aqueous-altered rock (phyllosilicates) with what may have been an ancient Mars shoreline is compelling. The widespread nature of layered deposits throughout the region, the mineralogic assemblages observed, and a terrain that displays such variety in state of burial and exhumation, all suggest a highly active sedimentary history, which could potentially have involved several phases of deposition and erosion related to episodic transgressions and/or major climatic variations.

Nili Fossae, located north of Syrtis Major volcano and west of Isidis basin, contains a series of curved depressions, which are oriented roughly concentric to the Isidis basin. The largest trough originates from Hesperian age volcanic flows, extends northward through Noachian etched and cratered units, and ends near the dichotomy boundary [6, 7] and most likely manifests as the surface expression of an outer ring fault related to the reasonably sized topographic and structural basin created by the Isidis impact into the underlying Noachian crust. Crosscutting and embayment relationships of the primary Nili Fossae trough with materials that span the Noachian to late Hesperian, as well as intersecting with structural elements potentially related to original dichotomy formation, suggest that Isidis has long been an influence on local geologic evolution.

Although masked in regions by volcanic flows from Syrtis Major, aeolian and fluvial deposition, and potential coastal deposits related to an ancient Martian ocean [4], subsequent stripping has revealed outcrops of significant geochemical importance. Like those observed in the Mawrth Vallis region, several outcrops of phyllosilicate-bearing Noachian materials have been revealed by the MEX OMEGA instrument [8, 9]. Phyllosilicates in this location point to the ancient history of Mars when the stability of ground and/or surface water was present for significant periods of time, facilitating the widespread aqueous alteration observed.

Final Remarks. Because of the landing site selection process, much attention has been given to these two areas. The increase of overall data coverage (and their respective increases in spatial- and spectral-resolutions) of these very localized areas complicates the original study, but also necessitates the broader geologic framework that this study intends to provide. Upon completion of GIS database compilation, this investigation will proceed with mapping of the Nili Fossae region.

References. [1] Nelson and Greeley, 1999: JGR, v. 104, no. E4, p. 8653-8669. [2] Parker, 2000: Mars Polar Science, abstract 4039. [3] Rodrogiuez et al., 2005: Icarus, v. 175, p. 36-57. [4] Parker, 1989: Icarus, v. 82, p. 111-145. [5] Webb, V.E., 2004: JGR doi:10.1029/2003JE002205. [6] Greeley and Guest, 1987: US Geol. Surv. Misc. Invest. Ser. Map I-1802B. [7] Craddock, 1994: LPSC XXV, pp. 291-292. [8] Poulet et al., 2005: Nature, v. 438, doi:10.1038/nature04274. [9] Mustard et al., 2005: Science, v. 307, p. 1594-1597.

NEW GEOLOGIC MAP OF THE ARGYRE REGION OF MARS.

J.M. Dohm[1], K.L. Tanaka[2], T.M. Hare[2]; [1]Dept. of Hydrology and Water Resources and Lunar and Planetary Laboratory, Univ. of Arizona, Tucson, AZ 85721, [2]USGS, 2255 N. Gemini Dr., Flagstaff, AZ 86001 (dohm@hwr.arizona.edu).

Introduction: The new generation of Mars orbital topographic and imaging data justifies a new mapping effort of the Argyre impact basin and surroundings (-30.0° to -65.0° lat., -20.0° to -70.0° long; Fig.1). Our primary objective is to produce a geologic map of the Argyre region at 1:5,000,000 scale in both digital and print formats. The map will detail the stratigraphic and crosscutting relations among rock materials and landforms. These include Argyre basin infill, impact crater rim materials and adjoining highland materials of Noachis Terra, valleys and elongated basins that are radial and concentric about the primary Argyre basin, faults, enigmatic ridges, lobate debris aprons, and valley networks. Such information will be useful to the planetary science community for constraining the regional geology, paleohydrology, and paleoclimate. This includes the assessment of: (a) whether the Argyre basin contained lakes [1], (b) the extent of reported flooding and glaciation, which includes ancient flows of volatiles into the impact basin [2-4], (c) existing interpretations of the origin of the narrow ridges located in the southeast part of the basin floor [2,5], and (d) the extent of Argyre-related tectonism and its influence on the surrounding regions. Whereas the geologic mapping investigation of Timothy Parker focuses on the Argyre floor materials at 1:1,000,000 (MTMs -50036, -50043, -55036, -55043; see Fig. 1 for approximate corners of the area), our regional geologic mapping investigation includes the Argyre basin floor and rim materials, the transition zone that straddles the Thaumasia plateau, which includes Argyre impact-related modification [6], and the southeast margin of the Thaumasia plateau using important new data sets (Fig. 1). Our mapping effort will incorporate the map information of Parker if it is made available during the project.

This mapping effort, which has received seed money during the first year, will complement the new global mapping effort spearheaded by K.L. Tanaka. As a state-of-the-art digital, GIS-based product, the map will be easily archived, distributed, and ingested into various research and mission-planning efforts and can be readily updated by us or by others when the need arises. Skinner et al. [7] renovated and GIS-formatted the Scott et al. [8] Viking-based global geologic map in a global projection with the MOLA DEM, and this has already been distributed widely. In addition to delivering a digital map, we hope to publish the map at 1:5,000,000 scale as a printed USGS map.

Science Objectives and Approach: The primary science objective will be to update our Viking-era understanding of the geologic history of the Argyre region [e.g., 8], which will include many new findings since the previous Viking-based maps [e.g. 8] were published, as well as other discoveries that will be made during the course of the mapping using the new data sets. As more data continue to pour in from Mars, the complexity of this planet becomes better appreciated. Interactions between volcanism, tectonism, cratering, hydrology, climate, and atmosphere in a variety of topographical, latitudinal, and other settings are the subjects of investigation by a large host of researchers. We intend to compile detailed geologic information for a first-order regional assessment by us and other investigators pertaining to stratigraphy and structural, impact, hydrologic, aeolian, and climate histories and reconstructions.

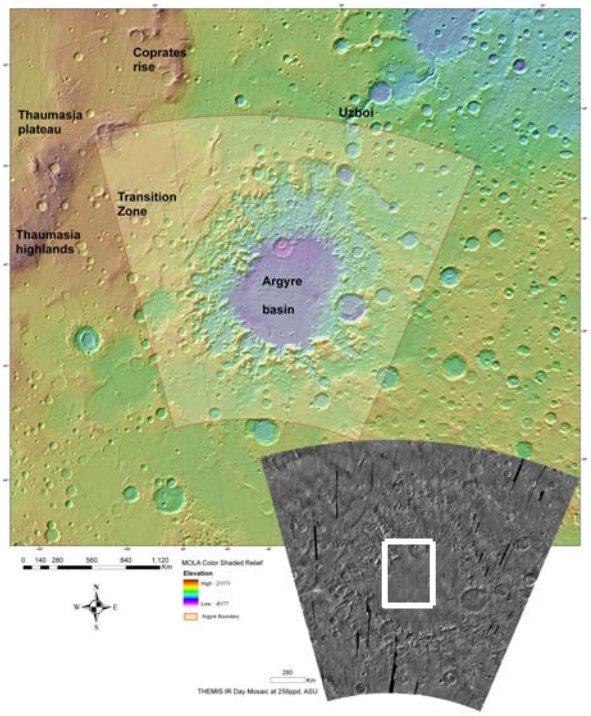

Fig. 1. MOLA color shaded relief map centered on the Argyre region (transparent outline). The image on the bottom right shows a 256 pixels/degree THEMIS IR day mosaic, to show the coverage available for mapping. Also shown is the approximate boundary (white box) of the 1:1,000,000-scale mapping investigation of Timothy Parker (MTMs -50036, -50043, -55036, -55043) originally funded to use Viking data to map mainly floor materials. Our regional 1:5,000,000-scale mapping investigation will include the Argyre floor and rim, transition zone, and the southeast margin of the Thaumasia plateau [6].

Stratigraphic mapping: We intend to apply various methods, including use of geologic and stratigraphic terminologies that will effectively communicate mapping results to the research community. We will follow the lead of Tanaka et al. [9] in mapping complex units as allostratigraphic units [10], also known as unconformity-bounded units [11-12]. These units include rocks and sediments of multiple, intimately mixed lithologies, a geologic scenario common to the Martian surface. Our strategy thus inherently avoids the splitting of lithologically similar materials without strong evidence for a hiatus in material emplacement activity. Stratigraphic units will be differentiated chiefly on the basis of both stratigraphic (crosscutting, overlap, and embayment) and contact relations and primary (that is, when the unit formed), morphologic characteristics.

Crater counting: Comprehensive crater counts for Martian geologic units in the Argyre region have not been obtained since the Mariner 9- and Viking-based geologic mapping [6, 13-19]. MOC, THEMIS, HRSC, CTX, and HiRISE images allow a major improvement. Careful interpretation of crater density data is required due to the following factors: (a) resurfacing activity causes degraded and/or embayed craters as well as inflections and roll-offs in crater-size distributions due to crater obliteration [e.g., 14, 20-21]; (b) possible secondary and non-impact craters, particularly at smaller diameters, which can alter crater size-frequency distributions [22]. We intend to produce detailed summary crater counts for all map units, as well as multiple counts for more broadly occurring units. These should help establish ranges and spatial variability of ages of surface and near-surface units, as well as resurfacing ages.

Structural and feature mapping: Features associated with unit formation will be mapped, including Argyre impact-induced, structurally-controlled valleys and basins, as well as impact crater rims. However, we intend to avoid the common practice of delineating degraded craters from other Noachian units, whose materials are already considered to include crater ejecta [e.g., 8]. We will restrict our mapping of a crater unit to those having well-preserved ejecta blankets extending >50 km (>1 cm on a 1:5M scale map), following the approach of Tanaka et al. [18]. We will also map features such as wrinkle ridges, lobate scarps, faults, fluvial channels, enigmatic ridges, lobate debris aprons, polygons, and valley networks to help unfold the geological history. Detailed structural mapping of the Thaumasia region, for example, which included producing paleotectonic and paleoerosional maps, as well as determining fault, fault-length, channel, and channel-length densities, was significant to describing and interpreting its geological evolution [6]. Thaumasia rift structures were also correlated spatially and temporally with the heads of fluvial channels in the region [23]. Using the newly available data will lead to improved mapping, characterization, and interpretation. For example, reassessing Viking-based published geologic information of parts of the Thaumasia region using MGS and MO data [24-25] has yielded several determinations, including: (a) an increase in the total number of mapped structures, (b) improved differentiation of fault segments and fault scarps of complex rift systems, (c) more structural trends and enhanced structural detail, and (d) a greater geologic perspective using multiple data types based largely on factors such as structural orientation, look direction of the acquired image, sun angle, and atmospheric conditions.

We will be conservative in feature interpretation. We will constrain the ages of structural and modification features where possible using crosscutting relationships and crater counts. Our structural mapping approach will be consistent with that of Dohm et al. [6], which provided a comprehensive digital paleotectonic and paleoerosional data set of the Thaumasia region, enhancing other geologic investigations [e.g., 26-27].

Summary: The primary objective of the mapping effort is to produce a geologic map of the Argyre region at 1:5,000,000 scale in both digital and print formats. We will present the progress and preliminary mapping information at the meeting.

References: [1] Parker, T.J. and D.S. Gorsline, 1993, *Am. Geophys. Union Spring Meeting*, 1pp. [2] Kargel, J.S., and Strom, R.G., Ancient glaciation on Mars, *Geology*, 20, 3-7, 1992. [3] Parker, T.J., et al., 2000, *LPSC* 31, abstract 2033. [4] Hiesinger, H., and J.W. Head, 2002, P&SS 50, 939-981. [5] Kargel, J.S., 1993, LPSC 24, 753-754. [6] Dohm, J.M., et al., 2001a, *USGS Map I-2650*. [7] Skinner, J.A., et al., 2006, *LPSC 37, abstract* #2331. [8] Scott, D.H., et al., 1986-87, *USGS Map I-1802-A-C*. [9] Tanaka, K.L., 2005, *Nature 437*, 991-994. [10] North American Commission on Stratigraphic Nomenclature, 1983, *Amer. Assoc. Petrol Geol. Bull., 67*, 841-875. [11] Salvatore, A., 1994, The International Union of Geological Sciences, GSA, 214 p. [12] Skinner, J.A., and K.L. Tanaka, 2003, *LPSC 34, Abstract* #2100. [13] Scott, D.H., and M.H. Carr, 1978, *USGS Map I-1083*. [14] Neukum, G. and K. Hiller, 1981, *JGR* 86:3097-3121. [15] Barlow, N.G., 1990a, *JGR* 95, 14191-14201. [16] Tanaka, K.L., 1986, *Proc. Lunar Planet. Sci. Conf., 17th, Part 1, JGR. 91,* suppl., E139-158. [17] Craddock, R.A., and T.A. Maxwell, 1990, *JGR 95*, 14,265–14,278. [18] Tanaka, K.L., et al., 2005, *USGS Map SIM-2888*. [19] Werner, S.C., 2005, Ph.D thesis, Freien Universität, Berlin, 160 p., appendices. [20] Scott, D.H., and K.L. Tanaka, 1981, *Icarus*, *45*, 304-319. [21] Tanaka, K.L., et al., 2006, Workshop on Surface Ages and Histories, LPI, Abstract #6014. [22] McEwen, A.S., et al., 2005, *Icarus 176*, 351-381. [23] Kreslavsky, M.A., and J.W. Head, 2002, *JGR 107*, 5121. [24] Dohm, J.M., and T.M. Hare, 2007, *LPSC 38*, Abstract #1403. [25] Dohm, J.M., and T.M. Hare, 2008, *LPSC 39*, Abstract #1935. [26] Anguita, F., and seven others, 2006, *Icarus* 185, 331-357. [27] Grott, M., et al., 2007, *Icarus*, *186*, 517-526.

GEOLOGIC EVOLUTION OF THE MARTIAN HIGHLANDS: MTMS -20002, -20007, -25002 AND -25007. C. M. Fortezzo[1] and K. K. Williams[2], [1]United States Geological Survey, Astrogeology Team, Flagstaff, AZ, 86001, cfortezzo@usgs.gov; [2]Buffalo State University, Buffalo, NY.

Introduction: As part of a continuing study to understand the relationship between valleys and highland resurfacing through geologic mapping, we are continuing to map seven 1:500,000-scale MTM quads in portions of the Margaritifer, Arabia, and Noachis Terrae. Results from this mapping will also help constrain the role and extent of past water in the region. The MTMs are grouped in two different areas (Figure 1, red boxes with black text) within the region and compliment previous mapping in adjacent areas (Figure 1, red boxes with hatch pattern) [1-5].

Three western quads focus on Jones crater and the Himera, Samara, and Loire Valles systems (central portion of Figure 1). This abstract focuses on the four eastern quads wherein a large, ancient impact structure, Noachis basin, is flanked on its south and east by a series of valley networks. A solitary valley drains this basin and stretches north-northeast for ~450 km, transporting materials into Arabia Terra.

Methods: We have imported and registered all pertinent raster and vector data using ESRI's ArcMap GIS software. Using this digital environment, we have nearly completed digitizing lines (e.g., contacts, structures, etc.) and polygons (e.g., units and craters). Arc extensions provide robust tools for (1) analyzing spatial relationships across multiple data layers, (2) attributing and updating digital linework, (3) building and analyzing vector topologies, and (4) importing new data as they are released. To inspect and quantify stratigraphic relations, we are compiling crater counts in ESRI's ArcView GIS software to make use of crater counting tools [6] specifically developed for planetary mappers [7].

Datasets: For these maps, we began using MDIM 2.1 and MOLA (128 pix/deg) datasets as the initial mapping bases. In year 3, we continued processing THEMIS daytime and nighttime infrared images and the visible range images and produced mosaics covering ~99%, ~ 95%, and ~50%, respectively. Due to their scale-compatible resolution and coverage, we are using the THEMIS daytime and nighttime IR mosaics as the basemaps for this region.

New datasets from the Mars Reconnaissance Orbiter including 4 CTX images (~6 m/pix), 31 CRISM multispectral pushbroom images (165 m/pix) and 4 HiRISE (0.25 m/pix) images were incorporated into the project during the third year. CTX provides both high-resolution, local details with regional context ideal for mapping. The multi-spectral CRISM data provides mineralogical context for mafic, ferric, and hydrated

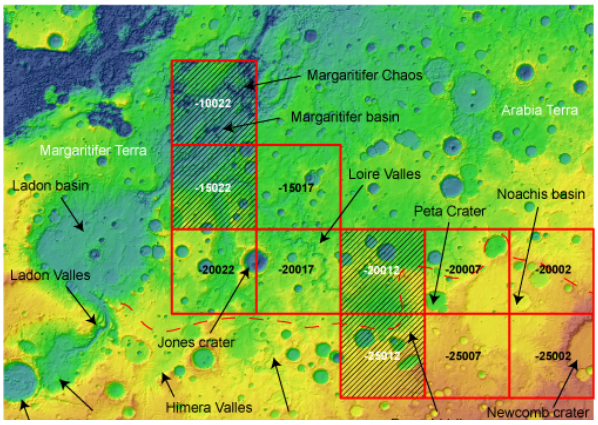

Figure 1: Shaded relief overlain by MOLA 128 pix/deg of Margaritifer Terra. Arrows point to feature locations. The red boxes indicate individual MTM quads. Red boxes with black numbers are the 7 quads currently being mapped and boxes with a hatch pattern and white numbers indicate quads in review and press. The red dashed line is an approximate boundary for the HMTZ. The HMTZ intersects the southeastern mapping area along the northern flanks of Peta crater, Newcomb crater, and Noachis basin.

minerals using summary parameters [8]. The HiRISE images provide detail to further describe the geomorphology of units and describe localized erosion. However, HiRISE is limited to three small locations in this region so descriptions using HiRISE images may be aerially limited.

Local Physiography: MTMs -20002, -20007, -25002 and -25007 contain portions of Noachis and Arabia Terrae and lie on the eastern border of Margaritifer Terra (Figure 1). The area slopes downward from southeast to northwest following the regional trend of the northwest portion of the circum-Hellas rise in the highlands. Two large impact basins, Newcomb crater and Noachis basin, control the local topography (Figure 2). Valley orientation is controlled by topographic lows. In the west, valleys trend west towards Paraná basin. In the south, valleys flow into the relatively flat-floored Noachis basin. In the north, valleys flow towards southern Arabia Terra, the Highland-Midland Transition Zone (HMTZ).

The HMTZ is represented in MOLA as a northwest-facing, southwest northeast trending slope from the Holden crater region in the southwest to the western flank of the Terra Sabaea rise in the northeast. The transition zone appears less densely cratered than the adjacent Noachis and Arabia Terrae [9]. Based on the abundance of partially buried and flat-floored craters, the apparent younger age is likely due to resurfacing

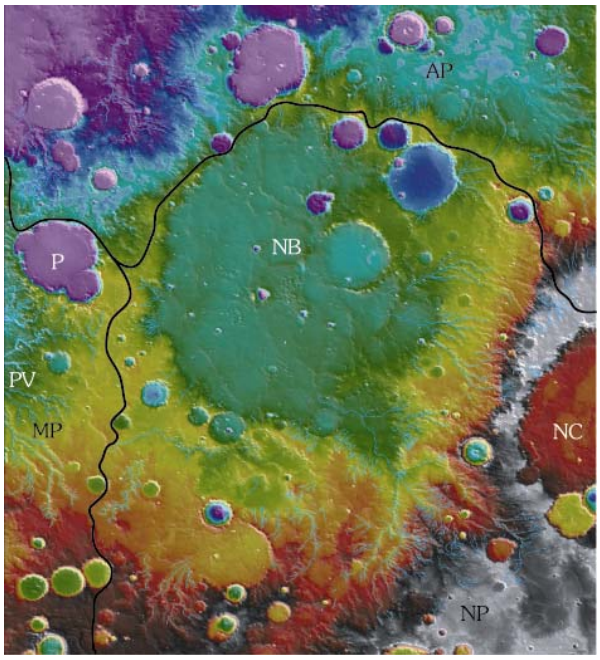

Figure 2: MOLA topography draped on shaded relief with highs=hot colors and lows=cool colors. Blue lines indicate valleys and black lines indicate province borders. Black letters are province names: NP=Noachis province, AP=Arabia province and MP=Margaritifer province. White letters are geographic names: P=Peta crater, NB=Noachis basin, PV=Paraná Valles and NC=Newcomb crater.

from deposited materials sourced from the southern highlands

Provinces: In an attempt to conform to terrestrial geologic mapping techniques [10], geographic names are used to describe location in the unit descriptions and abbreviations. The units of this mapping area have been divided into the Margaritifer, Noachis, and Arabia provinces based on topographic drainage divides and named after the terrae in which the valleys debouch. (Figure 2). The valleys and catchments that drain and transport materials into Paraná basin (Figure 1) comprise the Margaritifer province. Noachis basin, Newcomb crater and the southern and eastern valley networks transporting material into Noachis basin are designated as the Noachis province. The area north of Noachis basin and valleys forming on the northwestern flanks of Newcomb crater are designated as Arabia province.

Initial CRISM Results: The CRISM multi-spectral pushbroom dataset uses summary parameters [8] with thresholds to select targets for the high-resolution datasets. The benefit for mappers is the extensive coverage and general compositional information. The CRISM Analysis Tool (CAT), running in the

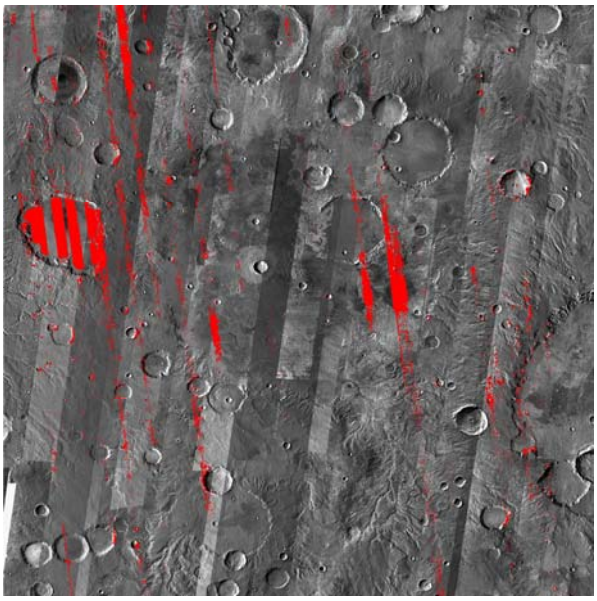

Figure 3: THEMIS daytime IR mosaic (100 m/pix) with CRISM multi-spectral pushbroom threshold olivine index summary parameter absorptions overlain. Note the high density of absorptions throughout Peta crater, and in the eastern and southwestern portions of Noachis basin.

IDL ENVI software package, destripes, mixes bands, and map projects the data for use in GIS.

The results of a cursory analysis show strong mafic (olivine, and low- and high-calcium pyroxene, LCP and HCP, respectively) absorptions in the floors of Peta crater and Noachis basin (Figure 3). LCP absorptions occur more often than olivine; however, olivine tends to be denser than both pyroxenes. LCP is expected in this region, as it is indicative of ancient Noachian materials [11] and is likely a common component of the local mantle. Olivine and HCP may indicate relatively younger rocks, which is supported by the occurrence of wrinkle ridges associated with high olivine and HCP absorptions in the Peta crater and Noachis basin floors.

References: [1] Grant J.A. & D.A. Clark, (2002) Planet. Map. Mtg. (abst.). [2] Williams, K.K. and J.A. Grant, (2003) Planet. Map. Mtg. (abst.). [3] Fortezzo, C.M. and J.A. Grant, (2004) Planet. Map. Mtg. (abst.). [4] Grant, J.A., et al., (2005) Planet. Map. Mtg. (abst.). [5] Grant, J.A., et al., *in press*, USGS Map. [6] Hare, T. et al., (2006) *LPSC XXXVII*, 2398 (abst.). [7] Barlow, N., (2006) *LPSC XXXVII*, 1337 (abst.). [8] Pelky, S.M., et al., (2007) *Jour. Geophys. Res, 112.* [9] Anguita, F., et al., (1997) *Earth, Moon, and Planets*, 77. [10] Tanaka, K.L., et al., (2005) USGS Map 2888. [11] Mustard, J., et al., (2005) *Sci., 307.*

MAPPING HESPERIA PLANUM, MARS. Tracy K.P. Gregg[1] and David A. Crown[2], [1]Department of Geology, 876 Natural Sciences Complex, University at Buffalo, Buffalo, NY 14260, tgregg@geology.buffalo.edu; [2]Planetary Science Institute, 1700 E. Ft. Lowell Rd., Suite 106, Tucson, AZ 85719, crown@psi.edu.

Introduction: Hesperia Planum, characterized by a high concentration of mare-type wrinkle ridges and ridge rings [1-4], encompasses > 2 million km^2 in the southern highlands of Mars (Fig. 1). The most common interpretation is that the plains were emplaced as "flood" lavas with total thicknesses of <3 km [4-10]. The wrinkle ridges on its surface make Hesperia Planum the type locale for "Hesperian-aged ridged plains" on Mars [e.g., 9], and recent investigations reveal that wrinkle-ridge formation occurred in more than one episode [4]. Hesperia Planum's stratigraphic position and crater-retention age [e.g., 9, 11-12] define the base of the Hesperian System. However, preliminary results of geologic mapping reveal that the whole of Hesperia Planum is unlikely to be composed of the same materials, emplaced at the same geologic time. To unravel these complexities, we are generating a 1:1.5M-scale geologic map of Hesperia Planum and its surroundings (Fig. 1). To date, we have identified 4 distinct plains units within Hesperia Planum and are attempting to determine the nature and relative ages of these materials (Fig. 2) [13-15].

Hesperia Planum Plains Materials: Geologic units within Hesperia Planum can be broadly classified as those associated with Tyrrhena Patera, and those that are not (Fig. 2). Crown and others [14] discuss the characteristics and relative ages of the Tyrrhena Patera materials [see also 16-20]. The plains materials to the south and southeast of Tyrrhena Patera are heavily affected by fluvial, ice, and possibly lacustrine processes [16, 21, 22], making interpretations of the original nature of the materials difficult. Here, we discuss previously unidentified plains units within eastern Hesperia Planum and the adjacent highlands.

The region of Hesperia Planum located to the east of Tyrrhena Patera (Fig. 2) is the typical "Hesperian ridged plains" [7, 9]. Aside from Tyrrhena Patera, no obvious volcanic vents have been found within Hesperia Planum [cf. 4, 12, 17, 19-21]. Lava flows can be seen at available image resolutions in the Tyrrhena Patera lava flow field [17] that post-dates the ridged plains, but they are not readily apparent within the ridged plains. In eastern Hesperia Planum, we have identified the following plains units: *highland knobby plains*, *smooth plains*, *highland smooth plains*, and *knobby plains*. MOLA data reveal that the east and west boundaries of the continuous topographic basin that defines Hesperia Planum closely follow the 2-km contour, and most of what has been geologically defined as Hesperia Planum [cf. 1, 7] is contained within that contour line. In contrast, highland plains occur in isolated outcrops surrounded by highlands material (Fig. 3). Units with the descriptor "highlands" are found at elevations above 2 km [15]. Jones and others [15] discuss the potential for these basins to have been sites of temporary lakes, fed by highland valley networks.

Highlands Materials: As part of her M.S. thesis, Jones [23] identified 3 distinct units within the highlands subregion located in the extreme northwest corner of the map area. These units are characterized primarily on the basis of erosional morphology: the density and size of gullies and channels; the crispness of topographic crests and troughs; the degree of outcrop isolation (an individual massif surrounded by plains deposits versus a part of a broader highlands region). It is not yet clear whether these are appropriate distinguishing characteristics for highlands geologic map units; however, their spatial distributions may reveal significant information about the erosional history of the region.

Mapping Progress: Units have been identified and are being mapped across the region. Preliminary crater size-frequency distributions have been calculated using Barlow's crater database for craters ≥5 km in diameter. The plains-forming materials are mapped; we are currently working on mapping the highlands materials and comparing our results with those found in published 1:500K-scale maps of the region.

References: [1] Scott, D.A. and M. Carr (1978) *USGS Misc. Series I-1083*. [2] Chicarro, A.F., P.H. Schultz and P. Masson (1985) *Icarus 63*:153. [3] Watters, T. and D.J. Chadwick (1989) *NASA Tech. Rpt. 89-06*:68. [4] Goudy, C., R.A. Schultz and T.K.P. Gregg, *J. Geophys. Res. 110*: E10005 10.1029/2004JE002293. [5] Potter, D.B. (1976) *USGS Misc. Series I-941*. [6] King, E.A. (1978) *USGS Misc. Series I-910*. [7] Greeley, R. and P. Spudis (1981) *Rev. Geophys. 19*:13. [8] Scott, D.A. and K. Tanaka (1986) *USGS Misc. Series I-1802A*. [9] Greeley, R. and J. Guest (1987) *USGS Misc. Series I-1802B*. [10] Leonard, J.G. and K. Tanaka (2001) *USGS Misc. Map Series I-2694*. [11] Tanaka, K.L. (1986) Proc. LPSC 17th, JGR Suppl. 91, E139-E158. [12] Tanaka, K. (1992) in *Mars*, U. Arizona Press, p. 345. [13] Gregg, T.K.P. and D.A. Crown

(2007) *Lun. Planet. Sci. Conf. 38th*, Abstract #1190. [14] Crown, D.A., D.C. Berman and T.K.P. Gregg (2007) *Lun. Planet. Sci. Conf. 38th*, Abstract #1169. [15] Jones, T.K., T.K.P. Gregg and D.A. Crown (2007) *Lun. Planet. Sci. Conf. 38th*, Abstract #2156. [16] Mest, S. and D.A. Crown (2001) *Icarus 153*:89. [17] Greeley, R. and D.A. Crown (1990) *J. Geophys. Res. 95*:7133. [18] Gregg, T.K.P., D.A. Crown and R. Greeley (1998) *USGS Misc. Series I-2556*. [19] Gregg, T.K.P. and M.A. Farley (2006) *J. Volcanol. Geophys. Res. 151*:81-91. [20] Farley, M.A., T.K.P. Gregg and D.A. Crown (2004) *USGS Open File Rpt. 2004-1100*. [21] Ivanov, MA et al. (2005) JGR 110, E12S21. [22] Crown, D.A., L.F. Bleamaster III and S.C. Mest (2005) *J. Geophys. Res. 110, E12S22*, doi:10.1029/2005JE002496. [23] Jones-Krueger, T. (2007) *M.S. Thesis*, University at Buffalo, Buffalo, NY, 94 pp.

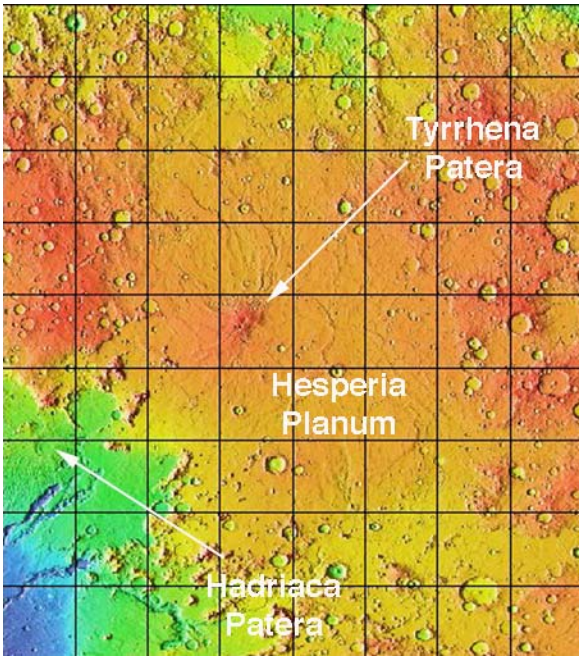

Figure 1. Gridded MOLA data (128 pixels/degree) of the area being mapped at 1:1.5 million. Reds are topographic highs (Tyrrhena Patera summit is ~3 km above mean planetary radius) and blues are lows.

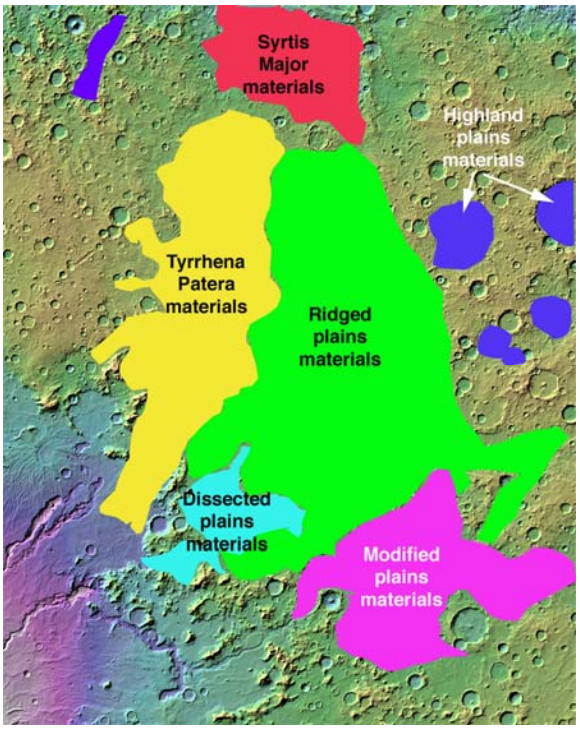

Figure 2. Rough boundaries of identified plains materials within Hesperia Planum. Portions of these materials were originally mapped as "Hesperian-aged ridged plains" at 1:15 million [9].

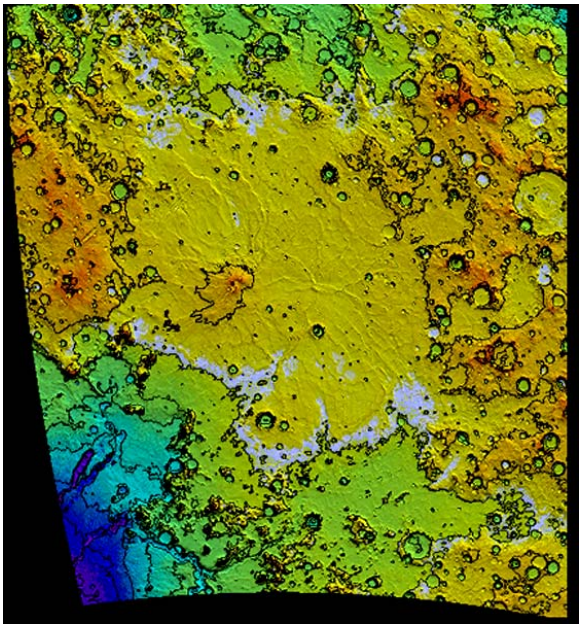

Figure 3. Hesperia Planum with 1-km-interval contour lines. The boundary of Hesperia Planum [9] roughly corresponds with the 2-km elevation line [21].

GEOLOGIC MAPPING OF THE MERIDIANI REGION, MARS. B.M. Hynek, Laboratory for Atmospheric and Space Physics and Department of Geological Sciences (392 UCB, Univ. of Colorado, Boulder, CO 80309) hynek@lasp.colorado.edu.

Introduction: The light toned bedrock that has been observed at the Mars Exploration Rover Opportunity landing site is an upper layer in a sequence >600 m thick in places. These outcrops contain mineral and textural signatures that require interaction of, and possibly formation from, water. Many distinct layers are visible in the remote sensing data (e.g. Figure 1) and no work has ever characterized the full set of these materials that cover an area $>3 \times 10^5$ km^2 spanning 20º of longitude. Thus, whatever water-related process(es?) altered, and possibly formed, the rocks at the Opportunity landing site extended over a vast region of Mars. Yet many questions remain to be answered, such as: (1) in what capacity did water form and alter the deposits?, (2) what are the temporal and spatial relations with other major events known from ancient Mars?, and (3) would this type of environment have been conducive to the development of life?

To address these questions we are completing a detailed geologic, stratigraphic, and thermophysical properties study of this widespread terrain. Specifically, we are drafting a 1:2M-scale geological map covering the full extent of these water-related deposits. In tandem with the mapping, Hynek and Phillips [1] have conducted a preliminary stratigraphic analysis of the stack of materials. After mapping is complete, we will study the thermophysical properties of the varied layers to derive possible compositional information of the materials. These tasks serve several purposes including gaining an understanding of the complex nature of these materials, their potential source region(s), and their timing of emplacement. All of these efforts are necessary to place the observations by the Opportunity Rover in a broader context and prepare for potential future landed missions to the region. Understanding the large-scale paleohydrology of Mars is central to NASA's goals and vital for determining if life ever arose on the planet.

Geologic Mapping: PI Hynek and Collaborators Roger Phillips (SwRI), Ken Tanaka (USGS) and Bruce Jakosky (CU/LASP) are currently funded to complete detailed geologic mapping at 1:2,000,000-scale in the Meridiani region, defined here as 5°S-15°N, 15°W eastward across the prime meridian to 15°E. This covers portions of the quadrangles MC-11 (Oxia Palus), MC-12 (Arabia), MC-19 (Margaritifer Sinus), and MC-20 (Sinus Sabaeus). The area encompasses the entire suite of light toned outcrops within the Meridiani region, which will be the primary focus of this map. In places of particular interest with sufficient data coverage, we will map the terrain at a larger scale to truly detail the local geology. The numerous units in the study area will be refined from recent works [2-6].

Formal geological mapping has not yet begun. The large geographic area has resulted in delays in the production of a 100-m-resolution THEMIS base map, which was just completed by the USGS Flagstaff. We have acquired many other data sets, formatted them for GIS, and coregistered them (Figure 1). This includes MOC WA images, THEMIS daytime and nighttime IR data, some THEMIS visible data, MOLA topography, some MOC NA images, TES and THEMIS thermal inertia, and mineral abundance maps from TES and OMEGA. We have completed mapping of regional valley networks to understand their potential link to the layers. We have produced generalized sketch maps of key units within the region (Figure 1) but are just beginning formal mapping with the newly-acquired high resolution THEMIS base map.

Stratigraphic and Thermophysical Analyses: PI Hynek has been working with Collaborator Roger Phillips to map out the largest stratigraphic markers across the Meridiani region. We extracted the individual MOLA elevation data points along their exposures, tried to fit planes to the data, and then analyzed their orientations relative to the regional tilt. Our results show that most of these benchmark horizons: (1) are planar and coherent over at least a 100-km scale, and (2) have dip azimuth and magnitudes that are similar to the underlying regional slope, which was emplaced by 3.7 Ga. Mapping relations with nearby ancient river valleys suggest that these deposits also formed near this time and without significant contributions from precipitation-fed surface runoff. THEMIS thermal inertia data and erosional expressions imply that significant physical compositional differences exist within the stratigraphy, and these likely reflect a changing paleodepositional environment and/or chemical alteration histories. Any hypothesis for the origin of these regional-scale materials must be consistent with all these observations. This work is helping to elucidate the timing, origin, and nature of the Meridiani region layered deposits and we have placed significantly greater constraints on the layers' characteristics and history. A manuscript detailing this work has been written and is in review for publication [1].

Summary: In our first six months of funding, significant progress has been made on acquiring data for

geologic mapping and initial delineation of major units. With the newly-produced base map we plan to begin formal mapping. A large stratigraphic analysis of the region has already been completed and we have found that most of the benchmark horizons identified are coherent over the 100-km-scale and are similar in dip azimuth and direction to the underlying long wavelength topography [1]. This work has helped test hypotheses regarding the origin of the layered materials and their timing relative to other events that shaped ancient Mars.

References: [1] B. M. Hynek and R. J. Phillips, *Earth and Plan. Sci. Lett.*, 2008 (submitted). [2] B. M. Hynek et al., *J. Geophys. Res.*, doi:10.1029/2002JE 001891, 2002. [3] Edgett, K. S., and M. C. Malin, *Geophys. Res. Lett.*, doi:10.1029/2002GL016515, 2002. [4] Hynek, B. M., *Nature*, doi:10.1038/nature02902, 2004. [5] Edgett, K. S., *Mars*, doi:10.1555/mars.2005.0002, 2005. [6] R. E. Arvidson et al., *Science*, doi:10.1126/science.1109509, 2005.

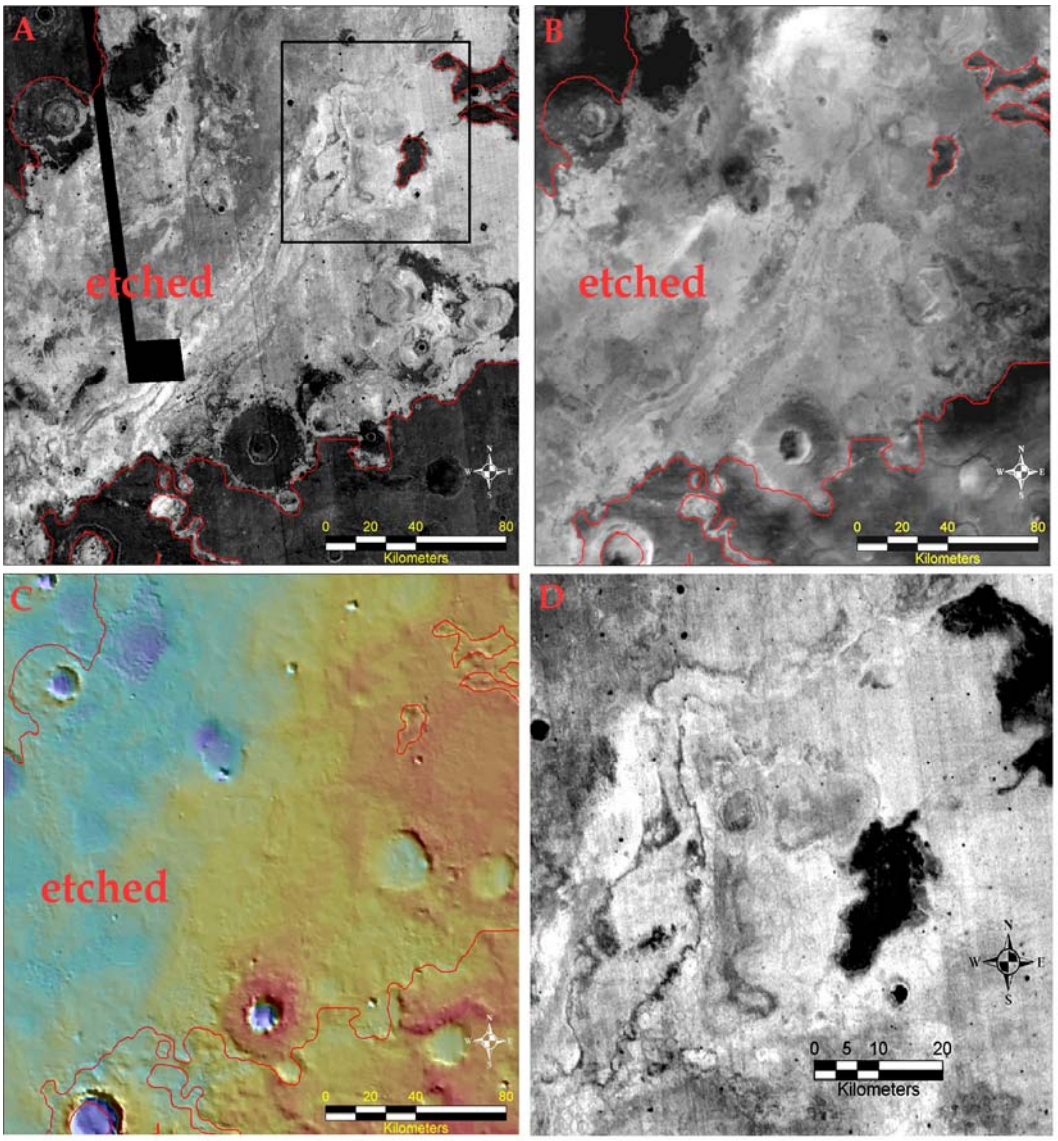

Figure 1. Examples of the data sets being used in the analyses. Figures 1A and 1D are THEMIS-derived thermal inertia (dark = low values); Figure 1B is a MOC WA mosaic (credit: MSSS); Figure 1C is MOLA elevation colors on MOLA shaded relief (blue = low, red = high, ~1 km relief). Red lines denote the generalized extent of a prominent light toned etched unit and Figure 1D is a zoomed in view of the black box in Figure 1A. To date, we have mapped out the major "etched" unit but diverse subunits are clearly visible in all the data sets. Figures 1A-1C cover the same geographic extent and are centered near 2ºN, 5ºE.

GEOLOGY OF HOLDEN CRATER AND THE HOLDEN AND LADON MULTI-RING IMPACT BASINS, MARGARITIFER TERRA, MARS. R. P. Irwin III and J. A. Grant, Center for Earth and Planetary Studies, National Air and Space Museum, Smithsonian Institution, MRC 315, 6th St. at Independence Ave. SW, Washington DC 20013-7012, irwinr@si.edu, grantj@si.edu.

Introduction: Geologic mapping at 1:500K scale of Mars quads 15s027, 20s027, 25s027, and 25s032 (Fig. 1) is in progress to constrain the geologic and geomorphic history of southwestern Margaritifer Terra. This work builds on earlier maps at 1:5M [1] and 1:15M scales [2], recent to concurrent 1:500K-scale mapping of adjacent areas to the east [3–5], and studies of drainage basin evolution along the Uzboi-Ladon-M (ULM; the third valley in the sequence has no formal name) Valles basin overflow system and nearby watersheds [6–9]. Two of the six landing sites under consideration for the Mars Science Laboratory rover are in this map area, targeting finely layered, phyllosilicate-rich strata and alluvial fans in Holden crater [10–12] (26°S, 34°W, 150 km diameter) or deposits southeast of a likely delta in Eberswalde crater [13–16] (24°S, 33°W, 50 km in diameter). Diverse processes including larger and smaller impacts, a wide range in fluvial activity, and local to regional structural influences have all affected the surface morphology.

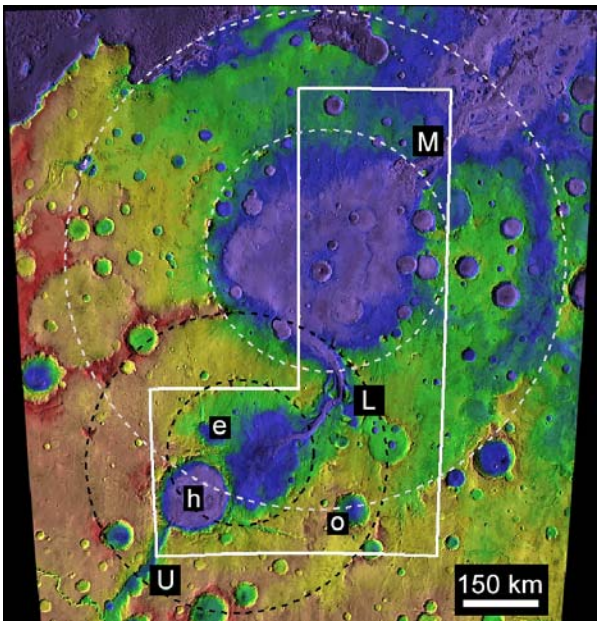

Fig. 1. Map area outline (white) with Ladon (gray) and Holden (black) basin rings dashed. Labels are Uzboi (U), Ladon (L), and a third unnamed valley (M); Holden (h), Eberswalde (e), and Ostrov (o) craters.

Large Impact Basins: The Early Noachian Ladon and Holden multi-ring impact basins (distinguished from the younger Holden crater), with inner/outer ring diameters of ~500/1000 and ~300/600 km, respectively (Fig. 1), are the oldest evident structures in the map area. Holden ring structures overprint those of Ladon [17], and the combination of the two structures oriented basin overflow floods and lesser fluvial activity over ~95% of the map area (Fig. 1). ULM segments follow the regional gradient to the NE and are radial to basin centers, except where the outer ring of Holden basin diverts Ladon Valles to the NW as it enters Ladon basin. Drainage from the southeastern margin of the study area was similarly confined within the outer Ladon basin ring (Fig. 1), wherein it joined lower Samara Valles and debouched to Margaritifer basin outside the NE corner of the area [7]. Eberswalde crater lies within the inner ring of Holden basin, which defines much of its watershed margin. Holden crater's location on the inner Holden basin ring created an asymmetry in the crater rim height, with a lower but less eroded eastern rim inside the older basin.

Intercrater Plains: Intercrater surfaces evolved during the Noachian Period with reduction of short-wavelength topographic relief, resurfacing, infilling and loss of impact craters as new ones formed, and partial infilling of the Ladon and Holden basins [7]. This terrain forms the cratered and subdued cratered units of [2] and the Noachis Terra unit of [18]. Eberswalde and other highly degraded craters formed and were modified during this time.

ULM Activity: A large supply of water to Holden basin via Uzboi Vallis led to overflow and incision of an outlet breach (Ladon Valles) [6]. The larger Ladon basin then filled and overflowed, forming unnamed valleys labeled M in Fig. 1. Multiple hanging channels in these outlets record large discharges that the initial topography could not confine. These flows coalesced with incision of the outlet breach, abandoning some higher channels [19]. The water volume needed to overflow Ladon basin was on the order of 10^4–10^5 km^3. Preservation of ULM valleys suggests that they postdate much of the intercrater plains development.

Holden Crater: The Holden crater impact destroyed and dammed the lower reach of Uzboi Vallis where it debouched to Holden basin. Holden crater is late Noachian in age, and some of its textured ejecta

are preserved along with extensive chains of secondary craters to the north [1].

Holden crater stratigraphy. Megabreccia forms the base of the stratigraphic sequence in Holden crater and is overlain by >100 m of light-toned, layered deposits (LTLD) [12] (Fig. 2). These strata are poorly resistant to wind and rich in phyllosilicates, with bedding that is often <1 m thick and continuous for kilometers. These features suggest distal alluvial or lacustrine deposition [12]. Holden crater was initially an enclosed drainage basin with no external contributing valleys. The walls of Holden and Ostrov craters became deeply eroded, and alluvial fans of gravel and fines accumulated along the base of the interior walls [11]. These fans prograded over and now protect LTLD outcrops, which may be coeval. Alluvial fans are concentrated along the higher western wall of Holden crater but are well-developed throughout Ostrov. The alluvial deposit or delta in Eberswalde crater overlies Holden ejecta and is likely contemporary [14].

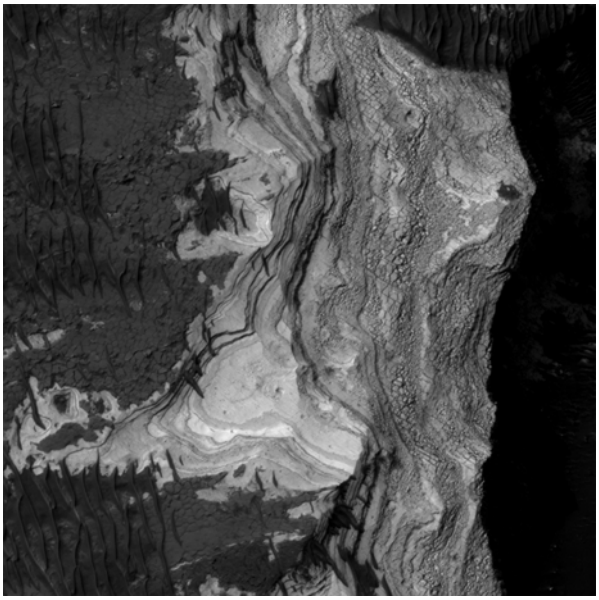

Fig. 2. Light-toned strata on the Holden crater floor, from the High Resolution Imaging Science Experiment.

Late Fluvial Activity: The Bond and Holden impacts created an enclosed basin in Uzboi Vallis, which drainage from the Nirgal Vallis tributary appears to have filled and overflowed. Full breaching of the SW Holden crater rim rapidly flooded the crater floor, incised channels, and deposited lobes of gravel and boulders over the LTLD. A small channel in lower Uzboi Vallis may represent the later stage of flow [12].

Structural Geology: Minor compressional faults striking N/S occur in several locations throughout the map area, whereas roughly concentric and radial normal faulting disrupted low-standing surfaces mostly in the northern half of the area. The latter modification is concentrated in deeper impact craters and basin floors within the inner Holden and Ladon basin rings, including the southern part of the Holden crater floor. Extensional faults typically do not extend into adjacent upland surfaces or intercrater plains, and they crosscut wrinkle ridges where the two faults intersect. Grabens cut the ejecta and floors of some fresh impact craters, whereas other craters superimpose the troughs, suggesting Hesperian or later faulting.

Chaotic or knobby terrains formed in Holden basin, upper Ladon Valles, and the upper reach of the valleys labeled M in Fig. 1 after basin overflows incised the outlet valleys [7]. The floor of Ladon basin is severely faulted near the margin of the chaotic terrain, which may be coeval with the grabens. In lower Ladon Valles, the upper reach of valleys labeled M in Fig. 1, and Holden crater, chaotic terrain or grabens are associated with uplifted areas in the floors. These structural features may be contemporary with outflow channel activity in Ares Vallis and elsewhere.

Recent Features: More recent modifications are largely aeolian and differentially affected basin floors. A dark dune field occurs in east-central Holden crater, and most fluvial deposits therein have etched surfaces. The floor of Ladon basin is also etched in places. A number of small impact craters have ejecta blankets that are distinct in infrared imaging, likely the most recent impacts in the map area.

References: [1] Saunders R. S. (1979) *USGS I-1144*, 1:5M. [2] Scott D. H. and Tanaka K. L. (1986) *USGS I-1802-A*, 1:15M. [3] Williams K. K. et al., submitted map, USGS. [4] Grant J. A. et al., map in press, USGS. [5] Fortezzo C. M. et al. (2006) *Planet. Geol. Mappers Meeting*, Nampa, ID. [6] Parker T. J. (1985) M. S. thesis, Calif. State Univ. [7] Grant J. A. (1987) *NASA TM 89871*, 1–268. [8] Grant J. A. (2000) *Geology*, *28*, 22–227. [9] Grant J. A. and Parker T. J. (2002) *JGR*, *107*(E9), 5066, doi:10.1029/ 2001JE001678. [10] Malin M. C. and Edgett K. S. (2000) *Science*, *290*, 1927–1937. [11] Moore J. M. and Howard A. D. (2005) *JGR*, *110*, E04005, doi:10.1029/ 2004JE002352. [12] Grant J. A. et al. (2008) *Geology*, *36*, 195–198. [13] Malin M. C. and Edgett K. S. (2003) *Science*, *302*, 1931–1934. [14] Moore J. M. et al. (2003) *GRL*, *30*(24), 2292, doi:10.1029/ 2003GL019002. [15] Bhattacharya J. P. et al. (2005) *GRL*, *32*, L10201. [16] Wood L. J. (2006) *GSAB*, *118*, 557–566. [17] Schultz P. H. et al. (1982) *JGR*, *87*, 9803–9820. [18] Tanaka K. L. et al. (2005) *USGS SIM 2888*, 1:15M. [19] Irwin III R. P. and Grant J. A. in *Megaflooding on Earth and Mars*, in press.

GEOLOGIC MAPPING OF ATHABASCA VALLES. L. P. Keszthelyi[1], W. L. Jaeger[1], K. Tanaka[1], and T. Hare[1], [1]U.S. Geological Survey, Astrogeology Team, 2255 N. Gemini Dr., Flagstaff, AZ 86001.

Introduction: We are approaching the end of the second year of mapping the Athabasca Valles region of Mars. The bulk of the linework has been completed and we are on schedule to submit the 4 MTM quads (05202, 05207, 10202, 10207) and accompanying paper by the end of the 3rd (and final) year of funding.

Previous Work: The study area is of special interest for several reasons: (a) it is central to the controversial and now disproven "Elysium Sea" [1,2]; (b) it is the location of the best preserved outflow channel [2-4]; (c) it also covers the confluence of lavas from the Elysium rise, multiple small vents, and vast flood lavas [5-8]; (d) and it contains the long-puzzling Medusae Fossae Formation (MFF). Moreover, the remnant knobs of ancient highlands in this region may help constrain the current nature of the Highlands-Lowlands Boundary (HLB).

Mapping Methodology: Two factors drive us to map the Athabasca Valles area in unusual detail: (1) the extremely well-preserved and exposed surface morphologies and (2) the extensive high resolution imaging. In particular, the near-complete CTX coverage of Athabasca Valles proper and the extensive coverage of its surroundings have been invaluable.

The mapping has been done exclusively in ArcGIS, using individual CTX, THEMIS VIS, and MOC frames overlying the THEMIS IR daytime basemap. MOLA shot points and gridded DTMs are also included. It was found that CTX images processed through ISIS are almost always within 300 m of the MOLA derived locations, and usually within tens of meters, with no adjustments to camera pointing. THEMIS VIS images appear to be systematically shifted to the southwest of their correct positions and MOC images are often kilometers off. The good SNR and minimal artifacts make the CTX images vastly more useful than the THEMIS VIS or MOC images.

The bulk of the mapping was done at 1:50,000 scale on CTX images. In more complex areas, mapping at 1:24,000 proved necessary. The CTX images were usually simultaneously viewed on a second monitor using the ISIS3 qview program to display the full dynamic range of the CTX data. Where CTX data was not available, mapping was often done at 1:100,000 and most contacts are mapped as approximate.

The Expected: Jaeger et al. [2] showed that Athabasca Valles is coated by a thin layer of lava left behind after an extremely voluminous flow passed through it. The mapping provides the detailed observations that back up the statements in [2] that the lavas then filled Cerberus Palus and drained through smaller channels to the southeast and southwest. We also detail the multiple lava sources along the Cerberus Fossae and the array of distributaries that fed lava beyond Athabasca Valles proper. As indicated in [2], the lava coats all possible locations of flood sediments. This flood lava is a proper lithochronologic unit that we have called the Athabasca Valles Lava (Aav).

The various sheet flows show the expected morphologic transitions from drained channels near-vent to platy-ridged surfaces in the medial portion to inflated pahoehoe at the distal margins. The most difficult contacts to identify are where the marginal inflated pahoehoe from different eruptions intermingle.

The Unexpected: The most surprising aspect of the Athabasca Valles Lava is the exposure of young lava, indistinguishable from Aav, in a window through the MFF. This suggests that some parts of Aav may have been exhumed from underneath ~100 m of mantling deposits. There is also a lobe of young flood lava in the southeastern part of the map whose source may be buried underneath the MFF.

Some of the tectonic features in the study area record young deformation. Near the northern limit of Aav, a lava-coated channel cuts into, and is cut by, the same strand of the Cerberus Fossae. Similarly, a wrinkle ridge near the western edge of the mapped extent of Aav is coated by lava but also appears to have deformed it.

There are fewer craters than might be expected on the knobs mapped as remnant ancient highlands. Part of this is undoubtedly due to the steep slopes with active mass wasting that quickly erases small (<1 km diameter) craters.

Remaining Work: The major mapping tasks that remain are (1) adding geologic structures, especially fissures and wrinkle ridges, (2) attempting to subdivide the Elysium rise lavas which exhibit may distinct lobes, (3) refining the correlations between the young lavas underneath Aav, (4) finish mapping the small craters and other km-scale features, (5) correlation of map units and description of map units, and (6) JGR/Icarus manuscript preparation.

References: [1] Murray J. B. et al. (2005) *Nature, 434*, 352-356. [2] Jaeger W. L. et al. (2007) *Science, 317*, 1709-1711. [3] Tanaka and Scott (1986) *LPS XVII*, 865. [4] Burr D. M. et al. (2002) *Icarus, 159*, 53-73. [5] Plescia J. B. (1990) *Icarus, 88*, 465-490. [6] Lanagan P. D. (2004) *Ph.D Thesis*, Univ. Arizona. [7] Keszthelyi, L. et al. (2004) *G*^{3}, 5, 2004GC000758.

Figure 1. Draft geologic map of the Athabasca Valles region of Mars. Transverse Mercator projection with center longitude of 150° E, center latitude of 0°. Latitude range is 2.4-12.6° N, longitude range is 149.9-160.1° E.

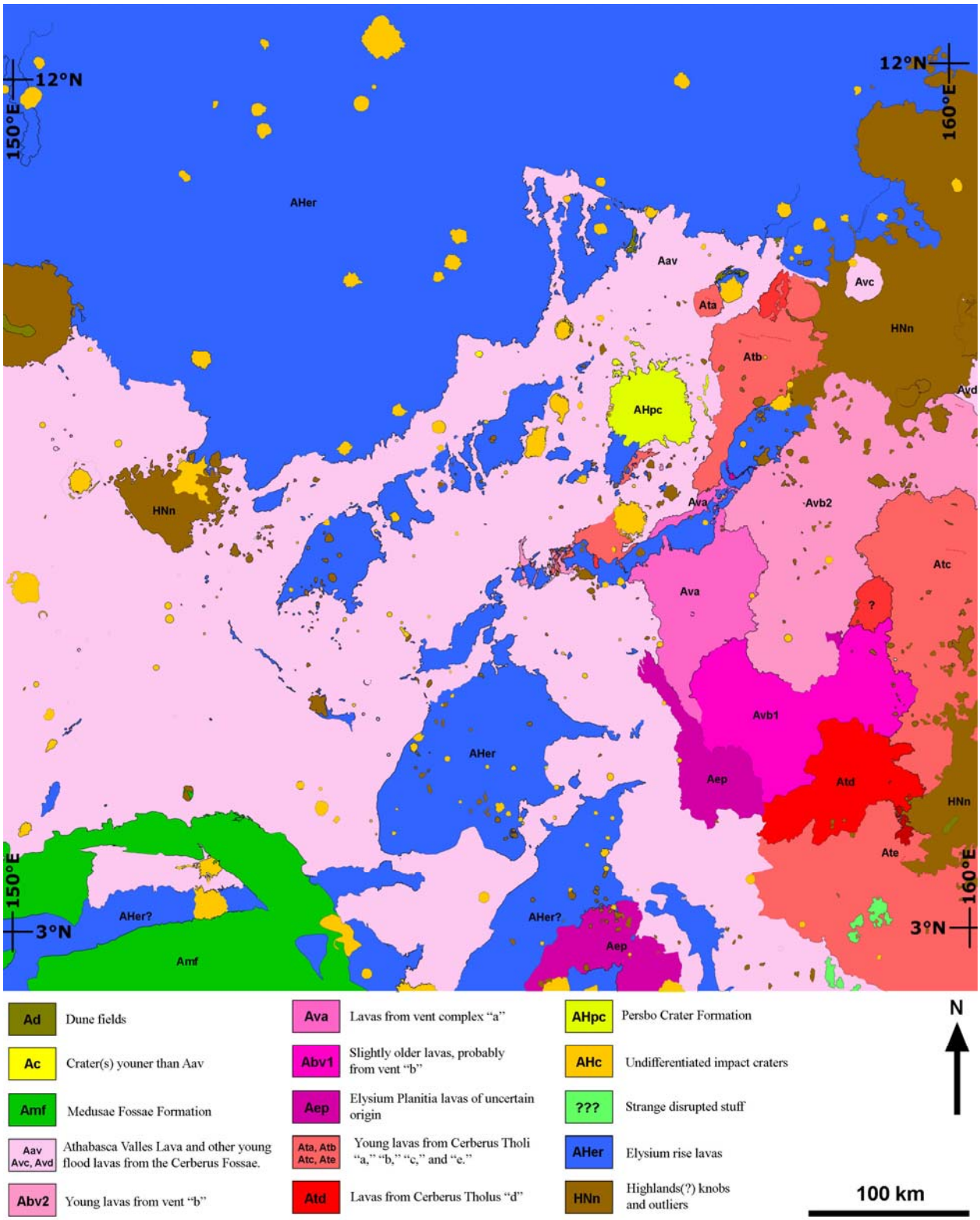

GEOLOGIC MAPPING OF MTM -30247, -35247 AND -40247 QUADRANGLES, REULL VALLIS REGION OF MARS. S.C. Mest[1,2] and D.A. Crown[1], [1]Planetary Science Institute, 1700 E. Ft. Lowell Rd., Suite 106, Tucson, AZ 85719-2395, mest@psi.edu; [2]Planetary Geodynamics Lab, NASA GSFC, Greenbelt, MD 20771.

Introduction: Geologic mapping and stratigraphic analyses of MTM -30247, -35247, and -40247 quadrangles are being used to characterize the Reull Vallis (RV) system and to determine the history of the eastern Hellas region of Mars. Studies of RV examine the roles and timing of volatile-driven erosional and depositional processes and provide constraints on potential associated climatic changes. This study complements earlier investigations of the eastern Hellas region, including regional analyses [1-6], mapping studies of circum-Hellas canyons [7-10], and volcanic studies of Hadriaca and Tyrrhena Paterae [11-13]. Key scientific objectives for these quadrangles include 1) characterization of RV in its "fluvial zone," 2) analysis of channels in the surrounding plains and potential connections to and interactions with RV, 3) examination of young (?), presumably sedimentary plains along RV that embay the surrounding highlands, and 4) determination of the nature of the connection between segments 1 and 2 of RV.

Project Status: This analysis of RV includes preparation of the geologic map of MTM quadrangles -30247, -35247, and -40247 (compiled on a single 1:1M-scale base). The current map area is included in previous Viking-based mapping efforts at regional [5,6] and local (1:500K; MTM -30247) scales. Crater size frequency distributions compiled for the regional analysis of RV [5,6] will be used in conjunction with newly generated crater statistics for units mapped in the current study using the new datasets (e.g., MOC, THEMIS, CTX and HiRISE). This mapping effort will synthesize past results and new analyses, completing MTM-scale mapping of the entire RV system.

Mapping Results: This section describes results derived from mapping of MTMs -30247, -35247, and -40247 combined with results from previous regional [5,6] and local mapping efforts of this area.

Highland degradation: Small valley networks and channels dissect highland terrains in this area. Most fluvial features are found in low-lying areas and appear to erode a sedimentary unit that fills intermontane areas [5-8]. These networks consist of narrow (<1 km) valleys up to several tens of kilometers in length and exhibit rectilinear patterns. Valley and network morphologies suggest they could have formed by combinations of runoff and sapping processes.

Several large craters in the map area exhibit degraded rims, parallel interior gullies, and eroded ejecta blankets. Several craters also contain debris aprons that extend from the craters' interior walls onto their floors. Most craters in the map area are partially filled by smooth or hummocky deposits. The range of crater preservation and the presence of gullies and debris aprons suggest that a combination of fluvial processes and mass wasting is responsible for erosion and degradation of highland craters [2,5-8,14-18].

Tectonism: Wrinkle ridges and ridge rings are the most prominent tectonic features, found predominantly in the northern part of the map area within ridged plains. Two dominant trends are observed—NE–SW (Hellas radial) and NW–SE (Hellas concentric)—indicating either multiple stress regimes were active concurrently or the stress regime shifted over time [19-21]. Crosscutting relationships suggest that ridge formation occurred after plains emplacement (Early Hesperian) and prior to collapse events and fluvial dissection associated with the formation of upper RV (mid-Hesperian?) [5,6].

Reull Vallis System: Segment 1 (S1) and part of Segment 2 (S2) of RV are found within the map area. S1 (~240 km long, 8–47 km wide, 110–600 m deep) is found in the eastern part of the map area within MTMs -30247 and -35247 and displays erosional scarps, scarp-bounded troughs, small theater-headed channels that converge at a large (~50 km across) depression, streamlined inliers of ridged plains material, and scour marks on the canyon floor. To the south, RV narrows then opens into a series of irregular scarp-bounded basins that also contain blocks of ridged plains material on their floors. Floor materials are generally smooth within S1 and likely include fluvial deposits, as well as debris contributed by collapse of the vallis walls. The overall morphology of S1 suggests formation by a combination of subsurface and surface flow and collapse of ridged plains material; this segment is believed to be the source area for at least some of the fluids that carved RV downstream [5,6,22].

An obvious surface connection between S1 and S2 is not apparent. Recent work using HRSC data suggests that the intersection of S1 and S2 marks the site of the Morpheos basin that formed in an early stage of RV's evolution [23,24]. It is believed that water flowing south from S1 accumulated in the Morpheos basin and was released to carve S2.

Segment 2 consists of morphologically distinct upper (S2-U) and lower (S2-L) parts. Contained within MTM -40247, S2-U displays sinuous morphology and extends for ~240 km through degraded highlands. S2-U (6 to 13 km wide, 110 to 650 m deep) exhibits features indicative of surface flow including layering or terracing along canyon walls, and braided gullies incised in floor material [5,6].

A portion of S2-L occurs in the southwest part of the map area, and begins where a narrow (1–2 km wide), shallow (~100 m deep) gully downcuts into the canyon floor [5,6]. This part of S2-L extends for ~70

km before opening into a large basin west of the map area [7,8]. Here, S2-L displays steep walls and a relatively flat floor, and is narrower (6 km) and shallower (140–350 m) than the remainder of S2-L to the west [7,8]. Unlike S2-U, S2-L does not display features on its floor indicative of fluvial erosion, though the canyon contains small-scale layering or terracing (tens to hundreds of meters thick) along its walls near the transition. Floor material consists of debris infilling the canyon from fluvial deposition and wall collapse, and exhibits pits and lineations that parallel the vallis walls similar to lineated valley fill in fretted terrain.

The morphology of S2 suggests initial formation by fluvial processes and subsequent modification by collapse and mass wasting. Several narrow, steep walled and flat-floored channels enter S2-U suggesting fluvial contributions to RV. These tributaries begin within and cut through various units including the basin–rim unit and smooth plains [5,6].

Regional Stratigraphy: The northern part of the map area is composed primarily of ridged plains material, initially believed to have been emplaced as flood lavas [25-27], although no obvious flow fronts are visible. Subsequent fluvial activity and deposition of sediments have significantly modified portions of the ridged plains in this area. Inter-ridge areas display relatively smooth and featureless surfaces except for the presence of low-relief scarps and small sinuous channels, interpreted to be fluvial in origin. MOC images show that inter-ridge areas contain dune features indicating eolian redistribution of sediments [5,6].

Analyses of the map area to date indicate that highland materials are surrounded and embayed by at least two plains units identified in previous mapping studies: dissected and smooth plains [5,6]. Dissected plains material, previously mapped as ridged plains [27], is found in MTM -35247 along the western edge of the map and between S1 and S2, and in the southeast part of the map area. This unit is characterized by a smooth surface dissected by narrow sinuous channels and low-relief scarps, and displays a few eroded wrinkle ridges. The contact between the ridged plains and dissected plains is gradational in most places, but the lack of high concentrations of pristine wrinkle ridges in dissected plains material allows it to be distinguished from ridged plains material [5-8]. Dissected plains material is interpreted to consist of volcanic and/or sedimentary materials eroded by fluvial processes.

Smooth plains material, originally mapped as part of the smooth plateau unit [27], is found adjacent to S2 of RV, embays highland units where they are in contact, and exhibits lobate terminations in some locations [5-8]. In high-resolution images, smooth plains display low-relief scarps, small channels, pits and small-scale undulations suggesting sublimation and collapse of volatile-rich material, as well as modification by fluvial and eolian processes. Along S2-U of RV, smooth plains material shows a fluted scarp boundary, whereas along most of S2-L, smooth plains material extends to the canyon wall [7,8]. Smooth plains are interpreted to be a mixture of sediments deposited from overflow of RV and at the termini of valley networks, and may also include materials deposited via mass wasting [5-8].

Mass wasting formed some of the youngest deposits in the map area. Debris aprons [1,5-8,16-18] and other viscous flow features [28,29] are found along highland massifs and crater walls, and are interpreted to consist of debris mass-wasted from steep slopes. Massif-associated features typically have uniform or mottled albedo, lobate frontal morphologies, and appear to be composed of multiple coalescing flows. Crater-associated features are relatively small and display mottled albedo, relatively featureless surfaces, and arcuate to lobate fronts. Some crater floor deposits contain rings concentric to the crater walls, similar to concentric crater fill [30,31].

References: [1] Crown, D.A., et al. (1992) Icarus, **100**, 1-25. [2] Crown, D.A., et al. (2005) JGR, **110**, E12S22, doi:10.1029/2005JE002496. [3] Tanaka, K.L. and G.J. Leonard (1995) JGR, **100**, 5407-5432. [4] Leonard, G.J. and K.L. Tanaka (2001) *Geologic map of the Hellas region of Mars*, USGS. Geol. Inv. Ser. Map I-2694. [5] Mest, S.C. (1998) M.S. Thesis, Univ. of Pittsburgh. [6] Mest, S.C., and D.A. Crown (2001) Icarus, **153**, 89-110. [7] Mest, S.C. and D.A. Crown (2002) *Geologic map of MTM -40252 and -40257 quadrangles, Reull Vallis region of Mars*, USGS Geol. Inv. Ser. Map I-2730. [8] Mest, S.C. and D.A. Crown (2003) *Geologic map of MTM -45252 and -45257 quadrangles, Reull Vallis region of Mars*, USGS Geol. Inv. Ser. Map I-2763. [9] Price, K.H. (1998) *Geologic map of the Dao, Harmakhis and Reull Valles region of Mars*, USGS Misc. Inv. Ser. Map I-2557. [10] Bleamaster, III, L.F. and D.A. Crown (2008) *Geologic Map of MTM -40277, -45277, and -45272 Quadrangles, Hellas Planitia Region of Mars*, USGS, in review. [11] Greeley, R. and D.A. Crown (1990) JGR, **95**, 7133-7149. [12] Crown, D.A. and R. Greeley (1993) JGR, **98**, 3431-3451. [13] Gregg, T.K.P., et al. (1998) *Geologic map of part of the Tyrrhena Patera region of Mars (MTM Quadrangle -20252)*, USGS Misc. Inv. Ser. Map I-2556. [14] Craddock, R.A., and T.A. Maxwell (1993) JGR, **98**, 3453–3468. [15] Grant, J.A., and P.H. Schultz (1993) JGR, **98**, 11,025–11,042. [16] Pierce, T.L., and D.A. Crown (2003) Icarus, **163**, 46-65, doi:10.1016/S0019-1035(03)00046-0. [17] Crown, D.A., et al. (2006) LPSC XXXVII, abstract **1861**. [18] Berman, D.C., et al. (2006) LPSC XXXVII, abstract **1781**. [19] King, E.A. (1978) *Geologic map of the Mare Tyrrhenum quadrangle of Mars*, USGS Misc. Inv. Ser. Map I-1073. [20] Watters, T.R., and D.J. Chadwick (1989) Tech. Rpt. 89-06, LPI, Houston. [21] Porter, T.K., et al. (1991) LPSC XXII, 1085–1086. [22] Crown, D.A. and S.C. Mest (1997) LPSC XXVIII, 269-270. [23] Ivanov, M.A., et al. (2005) JGR, **110**, doi:10.1029/2005JE002420. [24] Kostama, V.-P., et al. (2006) LPSC, XXXVII, abstract **1649**. [25] Potter, D.B. (1976) *Geologic map of the Hellas quadrangle of Mars*, USGS Misc. Inv. Ser. Map, I-941. [26] Greeley, R. and P.D. Spudis (1981) Rev. Geophys., **19**, 13-41. [27] Greeley, R., and J.E. Guest (1987) *Geologic Map of the Eastern Equatorial Region of Mars.* USGS Misc. Inv. Ser. Map I-1802B. [28] Mustard, J.F., et al. (2001) Nature, **412**, 411-414. [29] Milliken, R.E., et al. (2003) JGR, **108**, E6, doi:10.1029/2002JE002005. [30] Squyres, S.W., and M.H. Carr (1986) Science, **231**, 249-252. [31] Carr, M.H. (1996) Water on Mars, Oxford Univ. Press, NY.

Geologic Mapping of the Martian Impact Crater Tooting. Peter Mouginis-Mark and Joseph M. Boyce, HIGP/SOEST, University of Hawaii, Honolulu, HI 96822. <pmm@higp.hawaii.edu> and <jboyce@higp.hawaii.edu>

Introduction: Tooting crater is ~29 km in diameter, is located at 23.4°N, 207.5°E, and is classified as a multi-layered ejecta crater [1]. Tooting crater is a very young crater, with an estimated age of 700,000 to 2M years [2]. The crater formed on virtually flat lava flows within Amazonis Planitia where there appears to have been no major topographic features prior to the impact, so that we can measure ejecta thickness and cavity volume [2]. In the past 12 months, we have: (1) Published our first detailed analysis of the geometry of the crater cavity and the distribution of the ejecta layers [2]; (2) Refined the geologic map of the interior of Tooting crater through mapping of the cavity at a scale of 1:100K (Figure 1); and (3) Continued the analysis of an increasing number of high resolution images obtained by the CTX and HiRISE instruments [3].

Science Questions: We are trying to resolve several science issues that have been identified during this mapping, including:

1) What is the origin of the lobate flows on the NW and SW rims of the crater? We have produced a digital elevation model from a stereo pair of HiRISE images of the western rim of the crater that has enabled us to determine the slope and thickness of a prominent lobe on the outer SW wall. These measurements support the idea that these flows are sediment flows (potentially similar to terrestrial lahars) rather than being flows of impact melt or lava.

2) How did the ejecta curtain break apart during the formation of the crater, and how uniform was the emplacement process for the ejecta layers? We have identified three different types of ejecta layers: (1) layers that have massive, circumferential ridges on the surface; (2) smoother ejecta layers with faint radial striations; and (3) crenulated terrain close to the maximum radial extent of the ejecta layer, but closer to the primary than the distal rampart. This subdivision of the ejecta layers may have particular importance for the formation of individual ejecta layers at Tooting, and also has importance for the formation of ejecta layers at other, older, Martian multi-layered craters [1, 4-6]. This emplacement process appears to be quite different from the mode of emplacement of ejecta at double-layered craters [7] and our hope is that our mapping at scales of 1:50K or 1:100K may help us better understand the process at Tooting.

3) Can we infer physical characteristics about the ejecta? CTX and HiRISE images have revealed that there are a large number of pits, often aligned as chains of many dozen individual craters, within the ejecta layers. These pits seem to be preferentially concentrated at the crest of the distal ramparts, or as long (5 – 10 km) chains of craters that form on the outermost layer of ejecta. In several instances, we also see chains of craters extending beyond the visible outer boundary of the ejecta. We also find a few (<10) places where the ejecta ramparts appear to have been remobilized, suggesting that the fluidization process continued even after the ejecta came to rest for the first time. We

continue to study these higher resolution data sets in order to better define the number of sub-units that define the flow properties of the ejecta.

Plans for Year 3:

a) Complete a draft geologic map of Tooting crater and submit this map to the U.S. Geological Survey for preliminary review.

b) Publish a second research paper (either in *JGR-Planets* or *Meteoritics and Planetary Science*) on the detailed geology of the crater cavity, and the distribution of the flows on the crater rim.

c) Complete the accompanying map text.

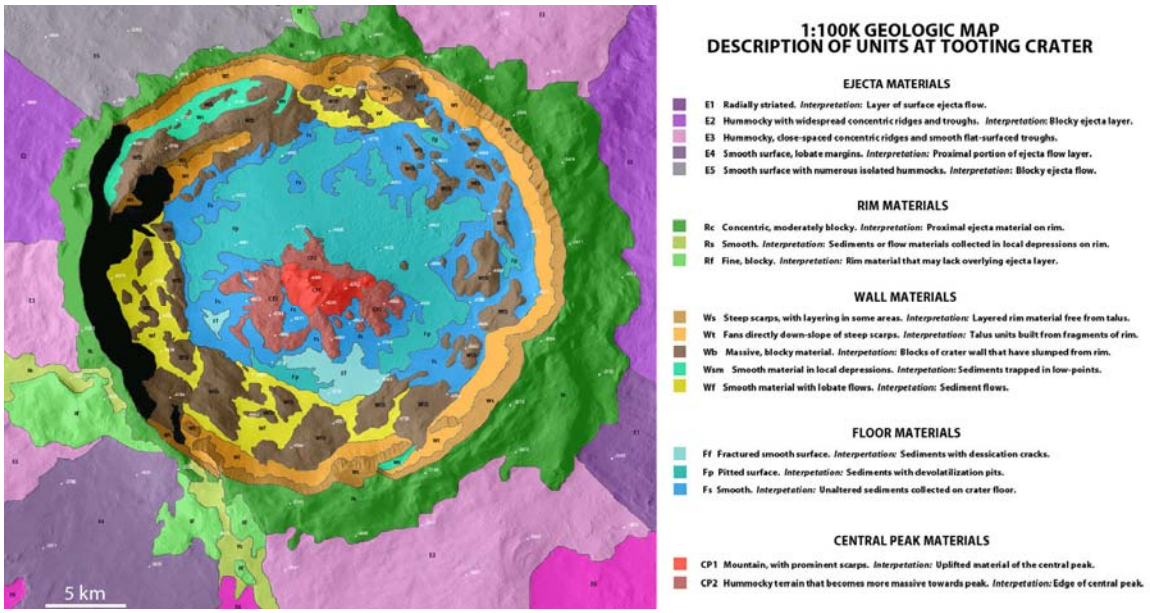

Figure 1: Revised draft of the geology of the cavity of Tooting crater, produced from analysis of THEMIS VIS and HiRISE images. The white labels give the elevation of the crater and ejecta relative to the MOLA datum for Mars.

References: [1] Barlow N.G. et al. (2000). Standardizing the nomenclature of Martian impact crater ejecta morphologies. *Journal of Geophysical Research* 105: 26,733 - 26,738. [2] Mouginis-Mark, P.J. and H. Garbeil (2007). Crater geometry and ejecta thickness of the Martian impact crater Tooting. *Meteoritics and Planetary Science*, 42: 1615 – 1626, 2007. [3] Mouginis-Mark, P.J., L.L. Tornabene, J.M. Boyce, and A.S. McEwen (2007). Impact melt and water release at Tooting Crater, Mars. *7th Int. Conf. On Mars. Abs #3039.* [4] Mouginis-Mark P.J. and Baloga S.M. (2006). Morphology and geometry of the distal ramparts of Martian impact craters. *Meteoritics and Planetary Science* 41: 1469 – 1482. [5] Baloga, S.M., S.A. Fagents, and P.J. Mouginis-Mark (2005). Formation of rampart ejecta deposits around Mars impact craters. *Journal of Geophysical Research* 110, E10001, doi: 10.1029/2004JE002338. [6] Barnouin-Jha O.S., Baloga S., and Glaze L. (2005). Comparing landslides to fluidized crater ejecta on Mars. *Journal of Geophysical Research* 110, E04010, doi: 10.1029/2003JE002214. [7] Boyce, J.M. and P.J. Mouginis-Mark (2006). Martian craters viewed by the THEMIS instrument: Double-layered ejecta craters. *J. Geophysical Research*, 111, E10005, doi: 10.1029 /2005JE002638.

GEOLOGY OF THE SOUTHERN UTOPIA PLANITIA HIGHLAND-LOWLAND BOUNDARY PLAIN: FIRST YEAR RESULTS AND SECOND YEAR PLAN. J. A. Skinner, Jr., K. L. Tanaka, and T. M. Hare, Astrogeology Team, U. S. Geological Survey, 2255 N. Gemini Drive, Flagstaff, AZ 86001 (jskinner@usgs.gov).

Introduction: The southern Utopia highland-lowland boundary (HLB) extends >1500 km westward from northern Nepenthes Mensae to the topographic saddle that separates Isidis and Utopia Planitiae. It contains bench-like platforms that contain depressions, pitted cones (some organized into arcuate chains and thumbprint terrain), isolated domes, lineated depressions, buried circular depressions, ring fractures, polygonal fractures, and other locally- to regionally-dispersed landforms [1]. The objective of our mapping project is to clarify the geologic evolution of the southern Utopia Planitia HLB by identifying the geologic, structural, and stratigraphic relationships of surface materials in MTMs 10237, 15237, 20237, 10242, 15242, 20242, 10247, 15247, and 20247.

Datasets and methods: The chief map base is a USGS-produced THEMIS daytime IR mosaic (100 m/px). We supplement this base with image and topography datasets, including the Viking MDIM 2.1 (231 m/px), MOLA DEM (463 m/px) (and ancillary products), MOC WA mosaic (231 m/px), and internet-hotlinked image footprints (*e.g.*, MOC NA, THEMIS VIS and IR, HiRISE, and CTX). We are applying "classical" and updated planetary mapping methods [1-4]. Because many of the materials that form the southern Utopia Planitia HLB are likely to be dispersed sedimentary sequences [1, 5-7], daytime and nighttime thermal data provide critical information for defining unit boundaries (where not covered by dust), particularly as such sequences may laterally grade into other materials [*e.g.*, 8].

Mapping bases are co-registered to one another and global datasets in ArcGIS®, which serves as our primary mapping environment. We have found that a maximum scale of 1:200,000 is adequate for units and landforms resolvable in the THEMIS base map resolution. We can confidently delineate and describe surface features >500 meters in diameter. We digitally stream vector linework into the GIS project using a WACOM® tablet. Vertex spacing for vector data is 250 meters. Lines are smoothed and line attributes (*e.g.*, contacts, linear structures) are committed on-the-fly. Unit polygons are periodically built from digitized contacts and iteratively revised, as necessary. Metadata for all vector information is being periodically inputted in order to (1) document mapping stages, and (2) ease production of the final map product.

Accomplishments: Proposed project runs January, 2007 to December, 2009. The project was awarded in April, 2007 and work commenced immediately. Year 1 (1/07 to 12/07) accomplishments included: (1) collation of relevant datasets (including construction of THEMIS daytime IR basemap by USGS cartography staff), (2) construction of GIS project with current data releases, (3) processing of HRSC and CTX images, (4) geologic and structure mapping, beginning with Amazonian units and superposed impact crater materials, (5) catalog of impact craters ≥ 1 kilometer in diameter, and (6) nomenclature updates (three impact crater names). A PGG-funded undergraduate student assisted on project goals during the summer 2007.

Year 2 accomplishments (to date) include the geologic delineation and characterization of the Amazonian-age VB unit margin, results and scientific perspectives of which were presented at LPSC 38 [8]. In addition, impact craters, structures, and Hesperian-age units have been delineated and described, providing first-cut geologic units and correlation of map units (COMU). The remainder of the project year will be committed to the completion of all geologic vector information (contacts, units, and tectonic and erosional structures) and compilation of the geologic history.

Results: Geologic mapping tasks are progressing well and are (generally) ahead of the proposed schedule. Based on the efforts to date, our most notable results include: (1) detailed characterization of the Vastitas Borealis (VB) unit margin, (2) mapping of overlapping sequences of Hesperian lobate materials, and (3) the delineation of impact crater ejecta facies and their temporal relationships. In the following sections, we briefly outline these results and provide interpretations on how they help gauge the regional geologic history.

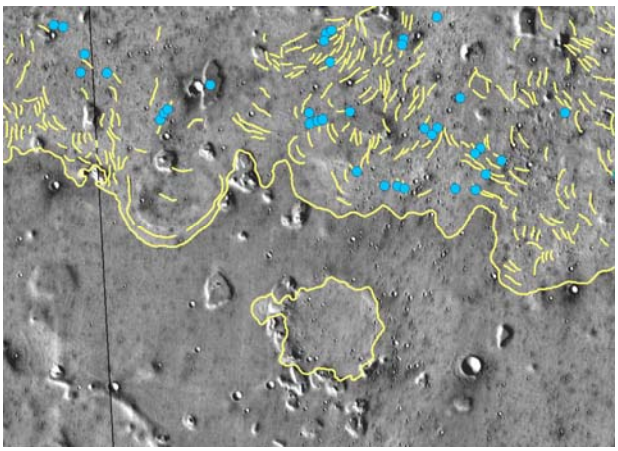

Figure 1. THEMIS base map showing the VB margin (continuous yellow line), arcuate ridges (short yellow lines), and pitted cones (blue dots). Note isolated occurrence of VB material located within an eroded crater south of the VB margin.

Amazonian VB unit margin. The regional VB margin is composed of overlapping, south-facing lobes (**Fig. 1**), often accompanied by km-long shallow troughs. The lobe-forming VB margin in southern Utopia Planitia is traceable for >2800 km and varies only slightly in elevation (–3569±318). The VB margin characteristically ramps onto (or terminates against) small knobs and plateaus. North of the VB margin, the unit contains a series of km-spaced, convex-southward arcuate ridges; these roughly parallel to the marginal lobes (**Fig. 1**). The ridges are composed of small (<80-m-wide) pitted cones and hummocks exist where the ridges intersect. We observe several subdued ridges south of the A_{Bv_m}/H_{Bu_2} contact, though these are discontinuous and not clearly delineable.

Based on current mapping results, we suggest that the regional VB margin formed through the soft-sediment deformation related to seismicity [8] (and not by an ocean shoreline [*e.g.*, Parker et al., 1989]). We attribute characteristic landforms to shoaling effects of a seismic wave and the detachment and southward movement of surficial units. This hypothesis implicates major variation in the near subsurface (within the uppermost tens of meters), perhaps due to grain size, lithification, and/or water or ice content. Older surfaces may indicate higher stands of subsurface volatiles and/or different layers of liquefied lowland materials. We speculate that the source of the seismic energy was one or more lowland impacts, whereby lowland material was conducive to wave propagation.

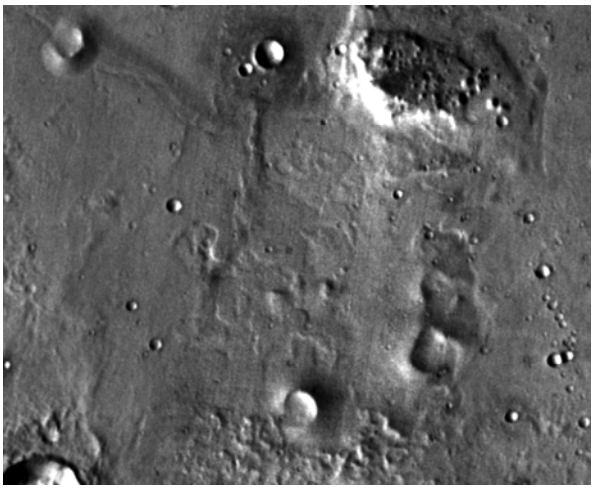

Figure 2. THEMIS base map showing lobate materials and the source constructs (pitted cones). Note cross-cutting relationships between the lobate materials within which the pitted cones are located.

Hesperian lobate plains. Our mapping shows that the Hesperian plains located between the VB margin (to the north) and the HLB scarp (to the south) are predominantly composed of discretely overlapping lobate materials with characteristic smooth and rugged surfaces (**Fig. 2**). Though texture alone is inadequate criteria to delineate geologic units [3], the cross-cutting relationships between these units are superb, perhaps indicative of discrepant viscosities of erupted material. Lobate flows are commonly traceable to isolated or coalesced pitted cones. Lobate materials are generally confined to the region between Amenthes Cavi and the higher-standing knobby plains located adjacent to the HLB scarp to the south. The formation of the lobate plains appears coincident with the formation of Amenthes Cavi; the depressions deform and are filled by lobate deposits.

We find evidence that the HLB plains in southern Utopia Planitia were both emplaced and deformed through volatile-related processes, perhaps akin to terrestrial soft sediment deformation [7]. This runs counter to previous interpretations, which defined these as volcanic materials [*e.g.*, 5]. We suggest the lobate flows were perhaps related to seismically- and/or tectonically-induced extrusion of fluidized regolith. We further suggest that Amenthes Cavi formed in tandem with the lobate plains, perhaps via compaction of underlying sequences and extrusion of pore-space fluids as breccia flows.

Impact crater materials. We have opted to abandon age-related impact crater units in favor of delineating impact facies, similar to those employed in lunar geologic maps [*e.g.*, 9]. This is particularly relevant to the study area, where crater ejecta morphologies are pervasively diagnostic of the ejection processes. We currently identify six mappable impact facies, as follows: (1) lobate ejecta, located distal to the crater, (2) hummocky ejecta, locate proximal to the crater, (3) interior wall material, (4) hummocky floor materials, (5) smooth floor materials, and (6) interior peaks. These materials will be divided by relative age. Facies can be applied (at least in part) to craters >20 km diameter. We currently differentiate secondary crater chains (polygons) and low-albedo ejecta material (points for crater <1 km diameter, stippled polygon for craters >1), as these provide insight into subsurface characteristics.

References: [1] Tanaka *et al.*, (2005) *USGS SIM 2888*, 1:15M scale. [2] Wilhelms, D.E., (1990) in *Planetary Mapping* (R. Greeley and R.M. Batson (eds.)), Cambridge U. Press. [3] Hansen, V.L. (2000) *EPSL*, *176*, 527-542. [4] Skinner and Tanaka (2003) *LPSC XXXIV*, abs. #2100. [5] Greeley, R. and Guest, J.E., (1987) *USGS I-1802-B*, 1:15M scale. [6] Tanaka, K.L. *et al.*, (2003a) *JGR*, *108*, (E4). [7] Skinner, J.A. Jr. *et al.*, (2007) *Icarus*, *186*, 41-59. [8] Skinner, J. A. Jr. *et al.*, (2008) *LPSC XXXIX*, abs. #2418. [9] Schmidt, H. H. *et al.,* (1967) *USGS I-515*, 1:1M scale. [10] Parker, T.J., *et al.*, (1989), *Icarus*, *82*, 111-145.

MARS GLOBAL GEOLOGIC MAPPING: AMAZONIAN RESULTS. K.L. Tanaka[1], J.M. Dohm[2], R. Irwin[3], E.J. Kolb[4], J.A. Skinner, Jr.[1], and T.M. Hare[1], [1]U.S. Geological Survey, Flagstaff, AZ, ktanaka@usgs.gov, [2]U. Arizona, Tucson, AZ, [3]Smithsonian Inst., Washington, DC, [4]Google, Inc., CA.

Introduction: We are in the second year of a five-year effort to map the geology of Mars using mainly Mars Global Surveyor, Mars Express, and Mars Odyssey imaging and altimetry datasets. Previously, we have reported on details of project management, mapping datasets (local and regional), initial and anticipated mapping approaches, and tactics of map unit delineation and description [1-2]. For example, we have seen how the multiple types and huge quantity of image data as well as more accurate and detailed altimetry data now available allow for broader and deeper geologic perspectives, based largely on improved landform perception, characterization, and analysis. Here, we describe early mapping results, which include updating of previous northern plains mapping [3], including delineation of mainly Amazonian units and regional fault mapping, as well as other advances.

Northern plains: One of the first steps in re-drawing Amazonian contacts within and around the Martian lowlands includes the adaptation of the recent geologic map of the northern plains [3], which ranges from 1:7.5M scale at the equator to 1:15M scale at the north pole due to its polar stereographic projection. Our new map will be compiled at 1:20M scale in either Lambert Equal-area Azimuthal (as proposed) or another planet-wide projection, such as Mollweide (as used in [4]). This reduction in scale has led us to (1) eliminate units whose outcrop extents are not readily viewable at 1:20M scale and (2) merge units having broadly correlative ages and similar regional occurrences (e.g., several Amazonis Planitia units). For contact types, we have eliminated "inferred" and "inferred, approximate" and added "time-transgressive." We also expect some contacts to shift in significant ways. In particular, the outer margins of the Vastitas Borealis interior and marginal units were based on only a handful of released Thermal Emission Imaging System (THEMIS) infrared (IR) images available at the time; we now have ~100% coverage of the planet with this data set, including global mosaics of day time and night time images. The thermal characteristics of the marginal unit are commonly distinctive, especially when coupled with kilometer-scale surface textures (e.g., as observed in Mars Orbiter Laser Altimeter (MOLA) digital elevation models (DEMs) and THEMIS visible (VIS) images).

Highlands: Several changes to previous mapping efforts [e.g., 5-7] are being made in the cratered highlands, although some consistency with older mapping is not uncommon. Where tenable, we are defining units on the basis of primary morphologic characteristics, relative age, and composition at 1:20M scale rather than post-depositional features, such as faults and valley networks; the latter are being mapped as secondary (superposing) geologic features. To substantiate this approach, we have begun assessing methods of dividing highland terrains into discrete geologic units. This includes analysis of overlapping impact crater materials of variable age. These assessments are improved by simple qualitative application of THEMIS and Mars Reconnaissance Orbiter (MRO) Compact Reconnaissance Imaging Spectrometer for Mars (CRISM) spectral data sets. The combination of spectral and morphologic information may be a critical method to differentiating impact units within the highlands. This tactic is still being explored.

Amazonian highland features and rock materials thus far include the ice-rich debris aprons that are commonly seen on hill slopes along the eastern Hellas rim and much of the upper part of Reull Vallis. In addition, the western floor sections of Hellas basin contain mapped Amazonian mantles; these mantles are also assumed to be ice-rich based on THEMIS VIS images showing mild flow deformation features in mantle sections that overlie locally steep terrain. The relative-age assignments for the Argyre basin floor materials (mostly Noachian and Hesperian in Viking-era mapping [5]) is being re-evaluated to see whether Amazonian resurfacing also occurred in this Noachian highland impact basin [8].

Wind-eroded layered deposits and alluvial fans are also noted. A few large dune fields occur inside impact basins. Smooth plains material in a broad trough SE of Isidis basin may also be Amazonian [5]. Finally, Amazonian layered materials comprise the south polar plateau, Planum Australe.

Tharsis: For Tharsis, we include an expanded number of tentative geologic contact types mapped, as well as specification of where they are used, including: (1) certain (e.g., older outcrops that are deformed by tectonic structures are clearly onlapped by younger flow materials); (2) approximate (e.g., individual outcrops at mappable scale that are embayed by flow materials such as the margins of the aureole deposits of the large shield volcanoes, Tharsis Montes and Olympus Mons); (3) gradational (e.g., flows that lack lobate flow margins which transition into plains-forming materials such as in the case of flows that drape parts of the eastern basal scarp of Olympus Mons); and (4) buried (e.g., parts of shield-forming basal scarp materials of Olympus Mons that are draped by lavas). Other improvements of previous, Viking-based mapping [5, 7] consist of: (1) enhanced stratigraphic and cross-cutting relations among rock materials and structures [9]; (2) an increase in the types and number of mapped structures, including improved differentiation of fault segments,

fault scarps of complex rift systems, and ridge types [9, 10].

Summary: We have completed preliminary mapping of most Amazonian materials as defined in previous mapping. Yet to be explored in detail, however, is Amazonian mantling. For example, a meters-thick mantle ~<150,000 years old covers mid-latitude parts of Mars [12], but is difficult to recognize in global-scale datasets. Also, there may be vestiges of earlier mantling such as the Astapus Colles unit mapped in NW Utopia Planitia [3]. Where highland mantles are thin, the highland materials will be mapped based on the materials that define the surface topography at mapping resolution. The character and relative age of the local mantling and its affect on surface appearance will be discussed in the map-unit descriptions. Extensive yet thin mantles such as described in [12] can be portrayed in digital-only map layers and in figures in the printed map. On the other hand, where the mantles are thicker and more extensive, they will be mapped and attributed as Amazonian units.

Notable improvements in technique over previous work include (1) improved delineation and differentiation of rock materials, (2) more sophisticated use of digital tools to portray in more detail various types of geologic contacts, structural landforms, and stratigraphic and cross-cutting relations among rock materials and structures, and (3) significant refinement in how the stratigraphic correlations among map units are depicted (adapting some of the techniques shown in [11]). Additional questions will need to be addressed as we deal with crater units, secondary crater fields, units resulting from extensive reworking of older materials (e.g., as in chaotic terrains), and other issues.

References: [1] Tanaka K.L. et al. (2007) *7th Intl. Conf. Mars* Abs. #3143. [2] Tanaka K.L. et al. (2008) *LPSC XXXIX*, Abs. #2130. [3] Tanaka K.L. et al. (2005) *USGS Map SIM-2888*. [4] Nimmo F. and Tanaka K. (2006) Ann. Rev. Earth Planet. Sci. 33, 133-161. [5] Scott D.H. et al. (1986-87) *USGS Maps I-1802-A, B, C*. [6] Leonard G.J. and Tanaka K.L. (2001) *USGS Map I-2694*. [7] Dohm J.M. et al. (2001) *USGS Map I-2650*. [8] Dohm J.M. et al., this meeting. [9] Dohm, J.M., and T.M. Hare (2007) *LPSC 38*, Abstract #1403. [10] Dohm, J.M., and T.M. Hare (2008) *LPSC 39*, Abstract #1935. [11] Geological Survey of Queensland (1975) *Mines Dept. State Series: Map 2*. [12] Mustard J.F. et al. (2001) Nature 412, 411-414.

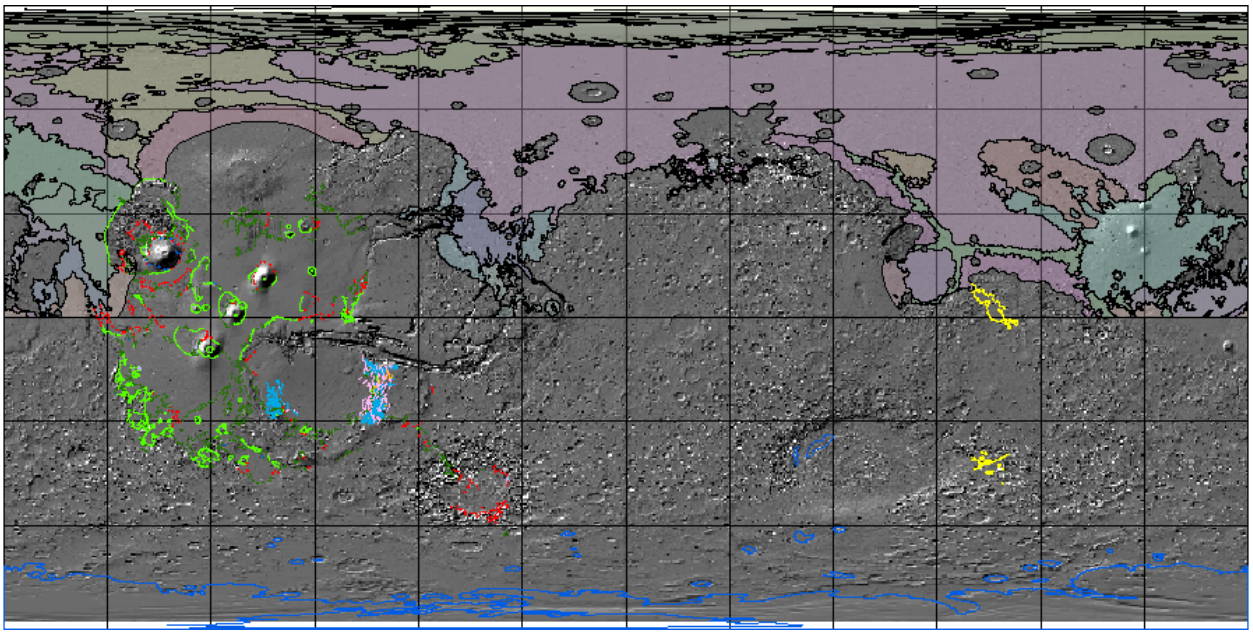

Figure 1. Current status of the global geologic map of Mars (in progress). The colored outcrops of Amazonian and Hesperian materials in the northern hemisphere are adapted from [3] by mapper JAS (see text for details). Tharsis and Argyre region mapping by JMD includes contacts of most Amazonian units (certain, bright green solid lines; approximate, dark green dashed lines; gradational, red dashed lines; buried, blue dashed lines) and some of the SE Tharsis tectonic structures (fault, medium blue lines; narrow ridge, orange lines; wrinkle ridge, pink lines). Southern highland Amazonian unit contacts are shown as mapped by EJK (dark blue lines) and RI (yellow lines). MOLA shaded relief base, Simple Cylindrical projection, 30° grid.

RECENT GEOLOGIC MAPPING RESULTS FOR THE POLAR REGIONS OF MARS. K.L. Tanaka[1] and E.J. Kolb[2], [1]Astrogeology Team, U.S. Geological Survey, Flagstaff, AZ 86001, ktanaka@usgs.gov, [2]Google, Inc., Mountain View, CA 94043, ekolb@google.com.

Introduction: The polar regions of Mars include the densest data coverage for the planet because of the polar orbits of MGS, ODY, and MEX. Because the geology of the polar plateaus has been among the most dynamic on the planet in recent geologic time, the data enable the most detailed and complex geologic investigations of any regions on Mars, superseding previous, even recent, mapping efforts [e.g., 1-3]. Geologic mapping at regional and local scales is revealing that the stratigraphy and modificational histories of polar materials by various processes are highly complex at both poles. Here, we describe some of our recent results in polar geologic mapping and how they address the geologic processes involved and implications for polar climate history.

North polar stratigraphy: The exposed geologic record for the north polar region appears largely limited to the Amazonian Period, as redefined by [3]. The north polar plains are made up of the *Vastitas Borealis units*, perhaps emplaced as fluvial sediments and (or) periglacially reworked material at the beginning of the Amazonian following cessation of outflow-channel discharges from the Chryse region [3].

Thereafter, the *Scandia region unit* was emplaced in the form of circular plateaus and irregular hilly complexes of Scandia Tholi and Cavi and planar deposits that have since eroded into knobs and mesas, forming Scandia Colles. This unit may have once covered ~1.5 x 10^6 km^2 of the plains north of Alba Patera to Planum Boreum to an average thickness of 100 m. We interpret that the material represents deposits related to mud-diapir-like processes, possibly redistributed by wind. In this scenario, the north polar gypsum discovered by the OMEGA instrument [4] may relate to Alba Patera magmatism [5].

Possibly coeval with and following formation of the Scandia region unit was emplacement of evenly to wavy-bedded material forming the *Rupes Tenuis unit* (ABrt) [6-7]. This material forms the base of much of Planum Boreum. West of Chasma Boreale, along the Rupes Tenuis scarp, the unit includes more than 20 beds and is >1000 m thick. A number of large impact craters on the unit indicate that it is a fairly ancient polar deposit. In spite of the unit's great thickness, it appears to be completely eroded back to an abrupt margin. Possibly correlative is the mantle material that forms the bases of >1800 pedestal craters in surrounding plains [8].

Perhaps during much of the Amazonian, dark, (possibly made up of weathered basalt [9]) dune fields migrated across the circum-polar plains mainly north of 70ºN where dunes are presently common. We map the current dune fields as the *Olympia Undae unit*, after the largest dune field. Some of the present dune fields originate from steep scarps exposed on the margins of Abalos Mensa, from Boreum and Tenuis Cavi at the head of Chasma Boreale, and from reentrants of Olympia Cavi into Planum Boreum. The bases of the scarps include dark, cross-bedded bright and dark layered material mapped as the *Planum Boreum cavi unit* (ABb_c) [7, 10]. Some of the dunes of Olympia Undae are embayed by the young mid-latitude mantle [11] and the youngest polar layered deposits (Planum Boreum unit 2).

The Planum Boreum cavi unit grades upwards into *Planum Boreum 1 unit* (ABb_1), which forms the majority of what are commonly referred to as "polar layered deposits" (however, other polar deposits are also layered, thus the term is now ambiguous). The unit includes dozens of unconformities as seen in MOC images, which may be related to changing patterns of spiral-trough development and (or) local variations in topographically controlled depositional environments [12]. Correlation of layer sequences exposed in various troughs is challenging, but rhythmic sequences of layers ~30-m-thick have been detected [13]. Deformation within this unit is rarely observed, such as near Udzha crater [14].

Within Chasma Boreale and troughs and adjacent plains of Planum Boreum, several dark layers form a sequence as much as 200 m thick and forms the *Planum Boreum 2 unit* (ABb_2). This unit is sculpted with yardangs and within Chasma Boreale is embayed by dozens of bright layers of the *Chasma Boreale unit* (ABcb). This unit also includes yardangs. In turn, the youngest layered deposits, *Planum Boreum 3 unit* (ABb_3), consists of several layers as much as a few tens of meters thick that unconformably overlie older Planum Boreum units. On top, the residual ice cap forms the *Planum Boreum 4 unit* (ABb_4), which rests unconformably on underlying materials [15]. The Planum Boreum 2 unit appears to be made up of a sandy, dark layer, which is the source of veneers of material that appear to contribute to erosion of the spiral troughs and related undulations [16].

South polar stratigraphy: In contrast to the north polar region, the south polar region exposes a geologic record that extends into the Noachian Period [17]. Here, the oldest rocks form the *Noachis Terra unit* and consist of impact breccia and melt, volcanic materials, and eolian and other sediment of the southern cratered highlands. Many impact craters within the highland terrain have undergone degradation and removal, and some unusual remnants, perhaps modified by volcanism, form the rounded massifs of the *Sisyphi Montes unit* [18]. Also, outpourings of likely volcanic material dur-

ing the Late Noachian through Early Hesperian formed the *Aonia Terra*, *Malea Planum*, and *Terra Cimmeria units*.

Throughout the Hesperian, the nearly circum-polar deposits of the Dorsa Argentea province were emplaced, forming a complex sequence consisting of lobate plains and superposed sinuous ridges, high-standing rugged terrain, and depressions. These unusual characteristics have led to various interpretations [see 2 and references therein]. We divide the Dorsa Argentea province into eight units that differ markedly from those mapped by [1]. The province includes: (1) a thick basal sequence of layered deposits exposed within the pits of Cavi Angusti and Sisyphi Cavi, (2) a high-standing rugged member that includes pitted cones and ridges, (3) five units of plains materials, and (4) a thick, fine-grained friable planar deposit that caps mesas and plateaus of Cavi Angusti. We suggest that the deposits and structures are best explained collectively by cryovolcanic eruptions and discharges of volatile-rich, fluidized slurries formed by the mixing of subsurface volatiles with fine-grained, unconsolidated crustal material and perhaps cryoclastic ash. This activity may have arisen from instabilities in Hesperian aquifers and triggering events caused by seismic shaking, fracturing, intrusions, and loading by polar deposition [2].

Some of the impact craters surrounding Planum Australe, including Richardson crater, are partly infilled by layered mound deposits capped in some cases by ripples that may be frozen dunes. In Richardson, the dunes appear to be buried by the Planum Australe 1 unit. These combined deposits form the *Richardson unit* (AAr).

The *Planum Australe 1 unit* (AAa_1) forms the majority of Planum Australe, the south polar plateau, reaching a maximum thickness of ~3 km within the plateau's thickest region, Australe Mensa. The unit is exposed along plateau margins and within canyons, and its basal layer sequences are perhaps Early Amazonian in age. A regional unconformity identified in the chasmata of Promethei Lingula and the curvilinear canyons of Australe Scopuli divides the Planum Australe 1 unit into the lower and upper members. The erosion associated with the unconformity was primarily wind and sublimation driven, and occurred after approximately one-third of the Planum Australe 1 unit stratigraphy was emplaced. The unconformity's orientation and outcrop expression indicates the chasmata formed by down-cutting of Planum Australe 1 unit surface depressions formed where the unit overlies uneven substrate [19] and marks the initiation of curvilinear canyon formation within Australe Scopuli [20]. The lowest 500 m of the Australe Mensa stratigraphy includes many local unconformities. In higher sequences, several layers that can be traced throughout most of Australe Mensa show unconformities that are up to 50 km long; they are seen at multiple exposure locations and indicate that regional erosive events punctuated emplacement of the relatively younger sequences of this region. The oldest regional unconformity in Australe Mensa occurs where this section of the plateau reaches 1 km thickness and thus may occur at the same stratigraphic position as the upper/lower member contact seen in other plateau regions; current mapping efforts will determine if such a correlation can be made.

The *Planum Australe 2 unit* (AAa_2) unconformably buries eroded Planum Australe 1 surfaces. The unit was emplaced after the canyons had largely reached their current form and after the plateau margins underwent extensive removal from Argentea, Promethei, and Parva Plana. The unit is <300 m thick and is comprised of layers that are slightly thicker than those of the Planum Australe 1 unit.

The *Planum Australe 3 unit* (AAa_3) crops out mostly in a series of narrow, shallow (<~200 m) curvilinear Australe Mensa canyons between 270°E and 30°E and on the floors of canyons that cut the southernmost sections of Australe Scopuli [21]. The unit is ~300 m thick and is comprised of 6-7 uniformly thick, conformable layers; individual layers have undergone differential erosion, resulting in an outcrop profile of cliffs and terraces. The characteristic low-to-intermediate albedo of the individual layers suggests they are relatively dust rich. The unit unconformably overlies the Planum Australe 1 and 2 units.

The *Planum Australe 4 unit* (AAa_4) delineates the residual ice cap, the bright, <~10 m-thick veneer centered between 225°E through 45°E and poleward of ~82°S. The upper member consists of the high-albedo CO_2-dominated sections [22] of the residual ice cap and constitutes the majority of the deposit's areal extent. The lower member is a thin basal layer consisting of water ice [23-24] that forms the moderate-albedo margins of the residual ice cap. The unit unconformably overlies the Planum Australe 1 through 3 units.

Synthesis of polar geology: Polar deposits include atmospheric volatile and dust precipitates and aeolian dunes and sheets made up of basaltic fines that have undergone some moderate cementation and weathering and extensive aeolian reworking. Our mapping studies generally indicate that the availability of dust, sand, and volatiles controlled by climate conditions and geologic activity and the variable circum-polar wind patterns controlled by topography and weather conditions have resulted in a complex history of accumulation and erosion at Planum Boreum and Planum Australe. Both climate-related cycles operating at differing time scales as well as unique geologic and climatic events have driven these processes. However, we find no compelling evidence for glacial-like deformation and for basal melt-water discharge of polar deposits. First-order comparison of the polar stratigraphies indicates a plausible scenario for synchronous phases of deposition and erosion (Figure 1).

References: [1] Tanaka K.L. and Scott D.H. (1987) *USGS Map I-1802-C*. [2] Tanaka K.L. and Kolb E.J. (2001) *Icarus 154*, 3-21. [3] Tanaka K.L. et al. (2005) *USGS Map SIM-2888.* [4] Langevin Y. et al. (2005) *Science 307*, 1584-1586. [5] Tanaka K.L. (2006) *4th Mars Polar Sci. Conf.* Abs. #8079. [6] Tanaka K.L. et al. (2006) *LPSC XXXVII*, Abs. #2344. [7] Tanaka K.L. et al. (in press) Icarus. [8] Skinner J.A., Jr. (2006) *LPSC XXXVII*, Abs. #1476. [9] Wyatt M.B. et al. (2004) *Geology 32*, 645-648. [10] Byrne S. and Murray B.C. (2002) *JGR 107*, 5044. [11] Mustard J.F. et al. (2001) *Nature 412*, 411. [12] Fortezzo C. and Tanaka K.L. (2006) *4th Mars Polar Sci. Conf.* Abs. #8079. [13] Milkovich S.M. and Head J.W. (2005) *JGR 110*, doi:10.1029/2004JE002349. [14] Tanaka K.L. (2005) *Nature 437*, 991. [15] Skinner J.A., Jr. et al. (2006) *4th Mars Polar Sci. Conf.* Abs. #8083. [16] Rodriguez J.A.P. et al. (2006) *LPSC XXXVII*, Abs. #1437. [17] Kolb E.J. and Tanaka K.L. (in review) *USGS SIM map.* [18] Rodriguez J.A.P. and Tanaka K.L. (2006) *4th Mars Polar Sci. Conf.* Abs. #8066. [19] Kolb E.J. and Tanaka K.L. (2006) *Mars* 2, 1-9. [20] Kolb E.J. and Tanaka K.L. (2006) *4th Mars Polar Sci. Conf.* Abs. #8085. [21] Kolb E.J. and Tanaka K.L. (2006) *LPSC XXXVII*, Abs. #2408. [22] Bibring et al. (2006) Nature 428, 627. [23] Byrne, S., and Ingersoll, A.P. (2003) Science 299, 1051. [24] Titus, T.N., Keiffer, H.H., and Christensen, P.R. (2003) Science 299, 1048.

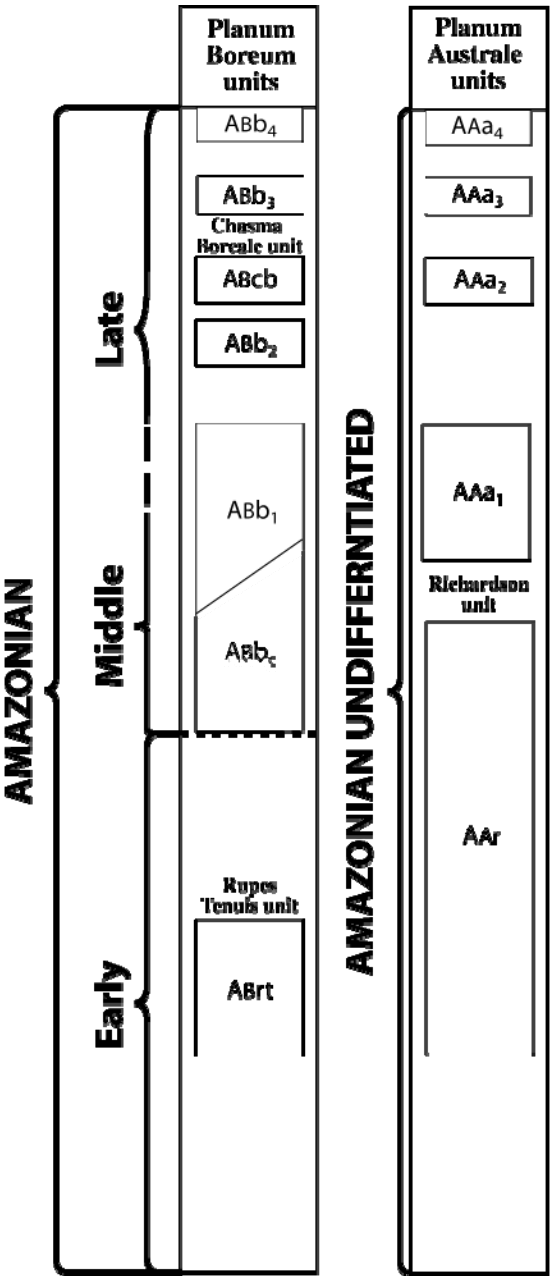

Figure 1. *Possible correlation of units making up Planum Boreum and Planum Australe. The relative ages of Planum Boreum units are approximately constrained by stratigraphic position and a few crater densities [7], whereas Planum Australe units are mainly constrained by stratigraphic relations thus far. Therefore, the vertical position of the Planum Australe unit boxes are aligned with Planum Boreum units based on the proposed correlations in [7] for illustrative purposes, but their correct positions are uncertain. See text for unit names associated with the symbols.*

GEOLOGIC MAPPING OF THE MEDUSAE FOSSAE FORMATION ON MARS (MC-8 SE AND MC-23 NW) AND THE NORTHERN LOWLANDS OF VENUS (V-16 AND V-15). J. R. Zimbelman, CEPS/NASM, Smithsonian Institution, Washington, D.C. 20013-7012 (zimbelmanj@si.edu).

Introduction: This report summarizes the status of a mapping project supported by NASA grant NNX07AP42G, funding for which became available on July 18, focusing on the mapping of the Medusae Fossae Formation (MFF) on Mars. The report also briefly discusses the status of maps of Venus and Ascraeus Mons, begun under previous NASA grants but which are still in progress.

MC-8 SE: Mapping in the eastern portion of MFF was initiated at 1:500K scale using the best available Viking images, then mapping commenced at 1:4M scale to provide a broader context. THEMIS daytime IR coverage was used for mapping at 1:2M scale, which we concluded was the best scale for portraying the MFF geology at both local and regional perspectives [1]. A 1:2M scale map for the MC-8 SE quadrangle (0° to 15°N lat., 202.5° to 225°E long.) (Fig. 1) was presented at the 2007

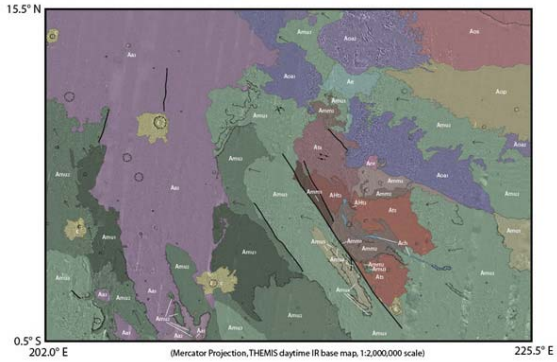

Figure 1. 2007 version of the MC-8 SE geologic map. The area shown includes a 0.5° margin beyond the actual quadrangle boundaries.

Mappers meeting, and only slight revisions have been made to the unit boundaries and structural features of that map. The map should be submitted for technical review during the fall of 2008.

As a result of the mapping, we have identified six subunits to the upper member of MFF and three subunits to the middle member of MFF, expanding on the units as designated by Scott and Tanaka [2]. Conclusive evidence for the origin of the enigmatic MFF materials remains elusive, but considerable progress has been made in using recent data sets to evaluate the numerous hypotheses of formation that have been proposed for MFF, leading to a volcanic (ignimbrite) origin as the most probable explanation [2]. Results from the MARSIS radar sounder [3] show that MFF materials are more than 2 km thick at the Gordii Dorsum escarpment (center of Fig. 1), and they appear to be superposed on relatively level northern plains materials at this location.

MC-23 NW: This quadrangle (0° to 15°S lat., 135° to 157.5°E long.) includes two large exposures of the lower member of MFF, the member displaying the largest degree of erosion of all MFF materials [4]. CTX (Fig. 2) and HiRISE (Fig. 3) data are proving to

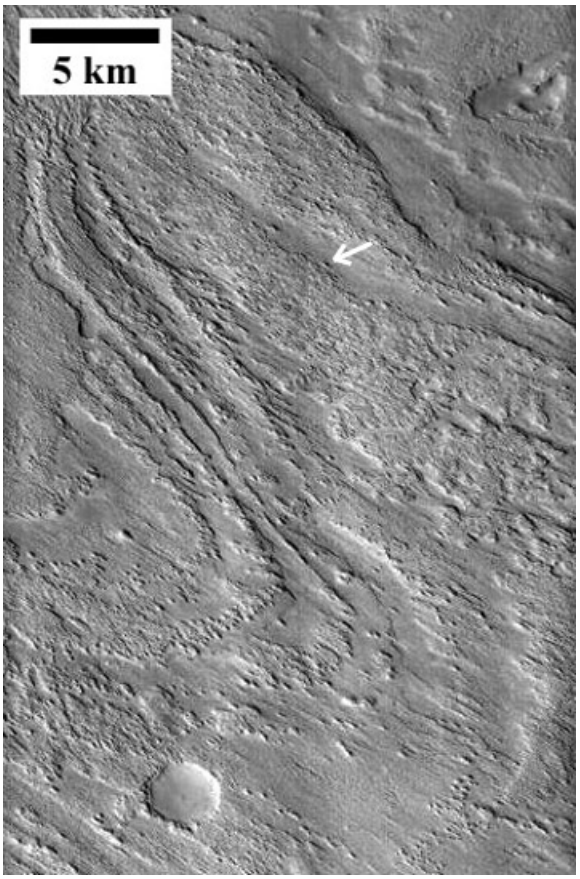

Figure 2. Portion of CTX frame PSP_003690_1756, showing arcuate layering exposed by the erosion of the lower member of MFF. Arrow indicates yardang shown in Fig. 3. 5.3 m/p, center at 5.0°S, 147.3°E, NASA/JPL/MSSS.

be particularly useful in refining the interpretations of the eroded MFF materials. For example, CTX (Fig. 2) reveals layering that could represent a plunging

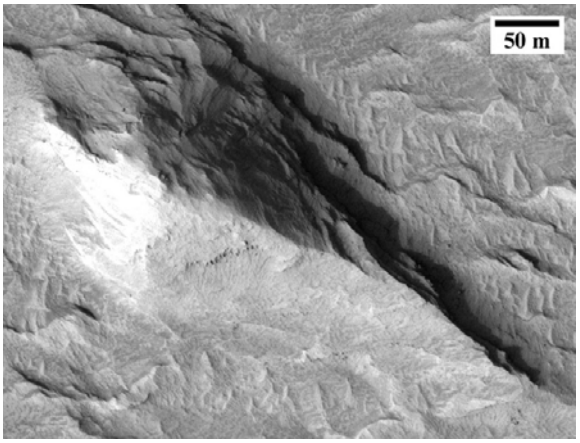

Figure 3. Portion of HiRISE frame PSP_003690_1755 showing a yardang comprised of MFF materials (see arrow in Fig. 2). Competent layers generate local cliffs within the eroded materials. 54 cm/p, center at 4.5°S, 147.3°E, NASA/JPL/U of A.

anticline, or perhaps flow unit components if emplaced as an ignimbrite [5]. HiRISE (Fig. 3) reveals competent layers in the MFF materials evidenced as prominent breaks in slope that are also the source of m-scale blocks that have collected downslope [5]. The eroded lower member of MFF has recently been recognized as displaying sinuous ridges that appear to represent inverted topography derived from the flow of sediments during the time represented by the base of the MFF deposits [6], supported in part by results obtained from the on-going mapping of MC-23 NW. We are concentrating on the mapping of MC-23 NW before starting work on MC-16 NW in order to obtain initial descriptions and interpretations of the lower member of the MFF materials, to complement the unit identifications for the middle and upper members of MFF obtained from mapping of MC-8 SE.

V-16 and V-15: Geologic mapping of both quadrangles on Venus was completed several years ago, but difficulties in matching unit lines generated on a photographic print base map to current digital base maps has delayed the review process [7]. We have been able to reposition all unit and structure lines (by hand) on the V-16 map to match the digital base, and are now proceeding to make unit polygons from the new line work. The V-16 map and text has been reviewed and thoroughly revised, but it is now waiting on having the map registered to the digital base map before proceeding further. We are hoping to have the V-16 map digital files to the USGS by the end of 2008. The V-15 line work will also need to be transferred to a digital base map, so once the V-16 map is in an acceptable state, we hope that the V-15 map can be submitted for review during 2009.

Ascraeus Mons: W. Brent Garry (post-doc at CEPS) is actively working on generating a new geologic map of the Ascraeus Mons volcano on Mars. He presented our preliminary work at the 2007 Mappers meeting [8]. However, he is very busy with a variety of other research projects at present, and we do not anticipate having a completed map ready for review until 2009 at the earliest. This map is being done in Arc-GIS, utilizing the wide variety of data sets now available for Mars. The map will be the completion of geologic mapping of the three individual Tharsis Montes volcanoes, all at 1:1M scale, that was initiated in the 1990s.

References: [1] Zimbelman, J.R. (2007) Planetary Geology Mappers Meeting Abstracts, ZIMBELMANa2007PGM.pdf. [2] Mandt, K.E., et al. (in review) JGR, 2008JE003076. [3] Watters, T.R., et al. (2007) Science, 318 (Nov. 16), 1125-1128. [4] Greeley, R., and Guest, J. (1987) USGS Map I-1802-B, 1:15,000,000 scale. [5] Zimbelman, J.R. (2008) Joint Assembly Abstract P34A-05. [6] Burr, D.M., et al. (in review) Icarus. [7] Zimbelman, J.R. (2007) Planetary Geology Mappers Meeting Abstracts, ZIMBELMANb2007PGM.pdf.[8] Gary, W.B., and Zimbelman, J.R. (2007) Planetary Geology Mappers Meeting Abstracts, GARRY2007PGM.pdf.

GEOLOGIC MAPPING OF THE ZAL, HI'IAKA, AND SHAMSHU REGIONS OF IO. M. K. Bunte, D. A. Williams, and R. Greeley. School of Earth and Space Exploration, Arizona State University, Box 871404, Tempe, Arizona 85287, (Melissa.Bunte@asu.edu).

Introduction: We have produced regional geologic maps of the Zal, Hi'iaka, and Shamshu regions of Io's antijovian hemisphere based on *Galileo* mission data. Here we discuss the geologic features, summarize the map units and structures that are present, discuss the nature of volcanic activity, and give an analysis of the volcanic, tectonic, and gradational processes that affect the regions in order to better understand Io's geologic evolution.

Zal Region: The Zal region (25-45˚N, 65-85˚W) consists of Zal Patera (120 km wide x 197 km long), two major mountains (north and south Zal Montes) which border Zal Patera to the west and south [1], and an unnamed patera ("Patera A") west of south Zal Montes. The Zal region includes at least two hotspots detected by *Galileo*: one along the western scarp of the Zal Patera volcano and one at the "Patera A" volcano. The floor of Zal Patera has been partly resurfaced by dark lava flows since *Voyager* imaging; portions of the patera floor appear unchanged during the *Galileo* mission. Mountains exhibit stages of degradation. The western bounding scarp of Zal Patera appears to be a fissure source vent for multiple silicate lava flows. The Zal Montes and Patera complex appears to be an example of volcano-tectonic interactions [1, 2]. Several of the flow units emanate from the fissure at the western scarp [2].

Hi'iaka Region: The Hi'iaka region (~12˚S-5˚N, 75-87˚W) consists of Hi'iaka Patera, a large (60 km wide x 95 km long) patera, north and south Hi'iaka Montes which border Hi'iaka Patera to the west and south and are L-shaped mirror-images of each other, west Hi'iaka Montes, a small isolated peak, and an unnamed patera ("Patera B") located south of north Hi'iaka Montes. The region includes one hotspot at Hi'iaka Patera. The floor of the patera exhibits flow deposits of differing ages. The eastern scarp of Hi'iaka Patera may be a fissure source vent for the patera floor materials. The Hi'iaka Montes and Patera complex appears to be an example of volcano-tectonic interactions [1, 2].

Shamshu Region: The Shamshu region (~15˚S-5˚S, 55-77˚W) consists of Shamshu Patera, three mountain units (west, north, and south Shamshu Mons), and a small unnamed patera ("Patera C") southwest of Shamshu Mons.

Map Units: Material units and structural features in regions are consistent with SSI-and *Voyager*-based maps of other regions [3, 4, 5, 6, 7, 8]. We have identified 19 units derived from five types of materials: plains, mountains, patera floors, flows, and diffuse deposits. *Plains* are thought to consist of silicate crust mantled by dark silicate and bright sulfurous explosive and effusive deposits [9, 10]. The plains are formed by combinations of over-lapping effusive flows, mass wasting of flow materials, SO_2 sapping scarps and pits, deposits from volcanic plumes containing SO_2 and sulfur frosts, and pyroclastic flows [11, 12, 13]. Based on color, we subdivide the plains into yellow (sulfur-dominated), white (SO_2-dominated), and red-brown (radiation-altered) subunits. *Mountain* materials are often visible only in low-sun images where shadows highlight scarps, ridges, grooves, and mountain peaks [2, 13, 14]. We characterize three types of mountain materials: lineated (containing well-defined ridges and grooves, interpreted to be tectonically-uplifted crustal blocks), mottled (containing lobes and hills, interpreted to be materials displaced by mass movement that is likely the result of SO_2 sapping [2, 12]), and undivided (mountain material that is characterized by aspects of both the mottled and lineated units, but is dominated by neither). Plateaus can exhibit characteristics of any type of mountain materials. *Patera floor materials* are compositionally similar to flow materials but are emplaced within the bounding scarps of paterae. We characterize two subunits: bright and dark (sulfuric and silicate lavas coated by sulfurous deposits; e.g., [3, 4, 15]). *Flow* materials are typified by their generally linear morphology (lengths >> widths) and sharp contacts [3, 4, 5, 6]. Like patera floors, lava flow materials are characterized using morphology, color and albedo as undivided, bright (sulfur-dominated), or dark (silicate-dominated and associated with active hotspots [15, 16, 17]). Albedo variations in the dark flows are thought to indicate surface exposure: the freshest flows are generally darkest. Color tint of flows is due to mantling by diffuse material. Flows with intermediate albedos and ill-defined contacts make up undivided flow materials. *Diffuse deposits* thinly mantle underlying topography and typically occur near active volcanoes. Colors are interpreted to be indicative of the dominant chemical constituent: sulfur, sulfur dioxide, silicate, either short-chain sulfur and/or sulfur chlorides, and products of silicate-sulfur alteration, respectively [18, 19]. Dark, white, bright, and red diffuse deposits are present.

Structural Features: These regions contain a variety of structural features, including scarps, ridges, grooves, pits, graben, and lineaments. Scarps delineate

both mountains and plains. Most grooves, lineaments, and ridges are found in the mountain units. The plains contain several scarps and depressions indicative of tectonic activity. None of these features are found within the flow fields. No positive relief volcanic constructs such as domes, cones, or shields are resolvable; however, flow morphologies suggest the presence of a shield in the Zal region. As in all previous Io images, no impact craters were detected, supporting the contention that the surface of Io is perhaps only a few million to a few tens of millions of years old [20].

Discussion: Our mapping provides insight into the geologic processes that are active in these regions of Io. Each region exhibits various forms of volcanic activity, including hotspots, Promethean style flows, fissure vents, and pyroclastic and diffuse deposits. Both silicate and sulfur-rich lava flows are present; individual flows appear to be of different ages, i.e., in different stages of alteration inferred from their differing albedo and color. The paterae appear to be active compound flow fields but not flooding lava lakes. The detection of a plume by LORRI on *New Horizons* [21, 22] confirms that Zal is currently active, producing small-scale Pele-type plumes.

Strike-slip faulting and subsequent rifting likely separated the mountain units, opening vents for lava flow and creating pull-apart basins that became the paterae. The formation of the paterae may be related to the locations of the mountain units in that the crust at the location of the paterae is more susceptible to foundering due to the weakness near the scarps. We show possible reconstructions of the original mountain configurations and possible sequences for the progression of events that formed the current complex appearances.

The mountain units appear to be tectonically related by rifting, although they each exhibit different degradation features suggestive of SO_2 sapping and mass wasting. Morphologies and cross-cutting relationships of several flows suggest that mountain structures were uplifted and modified. We speculate that degradational effects are progressive and that the level of degradation of each of the mountain and plateau units is influenced greatly by the proximity to active vents [12]. Lineated mountain material is the least degraded of the mountain units. Degradation causes the destruction of the lineated texture; perhaps this destruction is aided by mantling deposits infilling the grooves. Further degradation by mass wasting or by SO_2 sapping creates depressions, debris aprons, or lobes [12]. Mottled materials are still more degraded and may degrade into layered plains.

The bounding scarps of Zal, Hi'iaka, and Shamshu Paterae are aligned with the scarps of their mountain counterparts. A similar alignment between "Patera B" and Hi'iaka Montes also exists. These alignments suggest a tectonic control for the formation of the paterae. Multiple episodes of deposition likely occurred to cover the patera floors.

A trend in the progression of volcanic activity has become apparent due to the mapping results. Areal extent of flows is measurable and can be used to infer volume and viscosity of material. The oldest flows (plains), as indicated by superposition, cover large areas. The youngest flows (dark flows) cover smaller areas. Large areal extent indicates high volume and/or low viscosity whereas small areal extent indicates low volume and/or high viscosity. This difference in areal extent indicates that, as time passed, flows may have progressed from high to low volume and from low to high viscosity. A reduction in areal extent may also indicate a decrease in volume flow rate. As indicated by areal extent, the volume decrease between patera floor and flow materials may be directly related to the tectonic activity of the region. As the faulting and rifting process began, high volumes of material were erupted from the fissure vent that was created. As the rifting process continued, lower volumes of lavas were erupted from the fissure.

Acknowledgements: This work was supported by NASA through the Outer Planets Research Program and the Planetary Geology and Geophysics Program.

References: [1] Radebaugh, J. et al., (2001) *JGR*, 106, 33,005; [2] Turtle, E.P. et al., (2001) *JGR*, 106, 33175; [3] Williams, D.A. et al., (2002) *JGR*, 107, 5068; [4] Williams, D.A. et al., (2004) *Icarus* 169, 80; [5] Williams, D.A. et al., (2005) *Icarus* 177, 69; [6] Williams, D.A. et al., (2007) *Icarus* 186, 204; [7] Wilhelms, D.E., (1972) *Astrogeology* 55; [8] Wilhelms, D.E., (1990) In: Greeley & Batson (Eds.), *Planetary Mapping*, Cambridge University Press, pp. 208; [9] Bart, G.D. et al., (2004) *Icarus* 169, 111; [10] Keszthelyi, L.P. et al., (2004) *Icarus* 169, 271; [11] McEwen, A.S. et al., (2000) In: Zimbelmann & Gregg (Eds.), *Environmental Effects on Volcanic Eruptions: From Deep Oceans to Deep Space*, Kluwer Academic/Plenum Publishers, pp. 179; [12] Moore, H.J. et al., (2001) *JGR*, 106, 33,223; [13] Schenk, P.M. et al., (2001) *JGR*, 106, 33201; [14] Jaeger, W.L. et al., (2003) *JGR*, 108 (E8), 5093; [15] Lopes, R.M.C. et al., (2001) *JGR*, 106, 33053; [16] Lopes, R.M.C. et al., (2004) *Icarus* 169, 140; [17] McEwen, A.S. et al., (1997) *GRL*, 24, 2443; [18] Spencer, J.R. et al., (2000) *Science* 288, 1208; [19] Kieffer, S.W. et al., (2000) *Science* 288, 1204; [20] Johnson, T.V. et al., (1979) *Nature*, 280, 746; [21] Spencer, J.R. et al., (2007a) *Science*, 318, 240; [22] Spencer, J.R. et al., (2007b) *Workshop on Ices, Oceans, and Fire: Satellites of the Outer Solar System*, Abstract #1357.

GLOBAL GEOLOGIC MAP OF EUROPA. T. Doggett[1], P. Figueredo[1,*], R. Greeley[1], T. Hare[2], E. Kolb[1], K. Mullins[2], D. Senske[3], K. Tanaka[2] and S. Weiser[1], [1]School of Earth and Space Exploration, Arizona State University, Tempe, AZ, [2]U.S. Geological Survey, Flagstaff, AZ, [3]Jet Propulsion Laboratory, California Institute of Technology, Pasadena, CA, (*currently at the ExxonMobil Research Company, Houston, TX).

Introduction: Europa, with its indications of a sub-ice ocean, is of keen interest to astrobiology and planetary geology. Knowledge of the global distribution and timing of Europan geologic units is a key step for the synthesis of data from the *Galileo* mission, and for the planning of future missions to the satellite.

The first geologic map of Europa [1] was produced at a hemisphere scale with low resolution *Voyager* data. Following the acquisition of higher resolution data by the *Galileo* mission, researchers have identified surface units and determined sequences of events in relatively small areas of Europa through geologic mapping [2-6] using images at various resolutions acquired by *Galileo*'s Solid State Imaging (SSI) camera [7]. These works [2-6] provided a local to sub-regional perspective and employed different criteria for the determination and naming of units. Unified guidelines for the identification, mapping and naming of Europan geologic units were put forth by [8] and employed in regional-to-hemispheric scale mapping [9,10] which is now being expanded into a global geologic map.

Methodology: A global photomosaic [11] of *Galileo* and *Voyager* data was used as a basemap for mapping in ArcGIS, following suggested methodology of allo-stratigraphy for planetary mapping [12]. Due caution was exercised given that the mosaic has a resolution varying from 12.6 to 0.23 km per pixel, as well as variations in illumination and viewing geometry, to avoid making distinctions between units that are artifacts of these variations. In areas of high resolution coverage, contacts were marked as definite, and left as queried in areas of low resolution coverage. The cut-off between these two mapping regimes is a resolution of 1.7km/pixel.

Material Units: The following units have been defined in global mapping (Figure 1), and are listed in stratigraphic order from oldest to youngest:

Ridged Plains Material (unit p_1). Forms globally extensive plains that appear smooth at regional or global resolution, but are intensely ridged at higher resolution. Characterized by cross-cutting ridges and troughs at multiple scales, with various geometries including arcuate, sinuous and anastomosing. It is disrupted in some localities by pits and domes and is sparsely cratered.

Argadnel Regio Unit (p_2). In Argadnel Regio the ridged plains unit is disrupted by wide cycloid lineaments and "wedges" to a degree that warrants a definition as a separate, younger plains unit.

Dark Plains Material (unit p_3). Has three occurrences: at the north pole, and in two equatorial regions centered on the sub-Jovian and anti-Jovian points respectively. It embays surrounding plains (p_1, p_2) units, but is cross-cut by numerous lineaments continuing from adjacent units. At low resolution, the inter-ridge areas are filled with dark material; a high resolution image at the north pole (E25POLE01) shows the inter-ridge areas to be chaos-like. Whether the ridges cross-cut a previously formed chaos region, or simply resisted break-up into chaos, is unclear.

Lineaments. Distinct from the densely spaced ridges in p_1 are the widely spaced lineaments that consistently cross-cut younger plains units (p_1, p_2 and p_3). These lineaments appear to represent a middle period of the geologic time represented by Europa's current surface, with some lineaments being overprinted by younger chaos and plains units, and all but two craters (the exceptions being Tyre and Callanish, which have some superimposed lineaments).

Disrupted Plains Material (unit p_4). Forms a hummocky terrain which is cross-cut by narrow lineaments, mostly troughs. It has a sharp contact with surrounding plains units (p_1 and p_3), which it embays, and a sharp contact with the chaos unit that in turn embays it. Triple bands coming from surrounding plains become obscured within the unit, transitioning to narrow troughs or fading altogether.

Lenticulated Plains Material (unit p_l). Forms regions where a plains unit (p_1 or p_2) acts as a matrix upon which lenticuale have been emplaced. No craters are observed within the lenticulated plains, consistent with a young age, or simply too little areal coverage. It is either younger or contemporaneous with p_3, p_4 and chaos units. It is cross-cut by most, but not all, lineaments. They can either be younger or contemporary to more continuous chaos units, and were called micro-chaos in some regional mapping [3].

Chaos Material (unit ch). Disrupted terrain which forms dark albedo features in global or regional resolution, having sharp embaying contacts with brighter, smoother plains units. In low resolution can also have transitional areas of dark albedo spots in a light albedo matrix, but this could also be equivalent to what has been mapped as lenticulated plains in high resolution. At higher resolution the chaos is seen to be hummocky plains, with plates of younger plains units in a matrix

of dark, knobby material. This unit has several separated occurrences globally, with different appearances, but nothing that could not be explained by differences in photometry and resolution within the base mosaic. Chaos is younger than all surrounding material units, with some cross-cutting lineaments. A sub-type is elevated or knobby chaos that is younger than other chaos units [9, 10].

References: [1] Lucchitta and Soderblom, in *The Satellites of Jupiter*: 521, 1982; [2] Senske et al., *LPSC* XXIX, #1743, 1998; [3] Prockter et al., *JGR., 104*: 16531-16540, 1999; [4] Kadel et al., *JGR*, 105, 22657-22669, 2000; [5] Figueredo et al., *JGR*, 107, 10.1029/2001JE001591, 2002; [6] Kattenhorn, *Icarus*, 157, 490-506, 2002; [7] Belton et al., *Space Science Reviews*, 60, 413-455, 1992; [8] Greeley et al., *JGR*, 105, 22559, 2000; [9] Figueredo and Greeley, *JGR*, 22629-22646, 2000; [10] Figueredo and Greeley, *Icarus*, 167, 287-312, 2004; [11] USGS, I-2757, 2003; [12] Skinner and Tanaka, *LPSC XXXIV*, #2100, 2003.

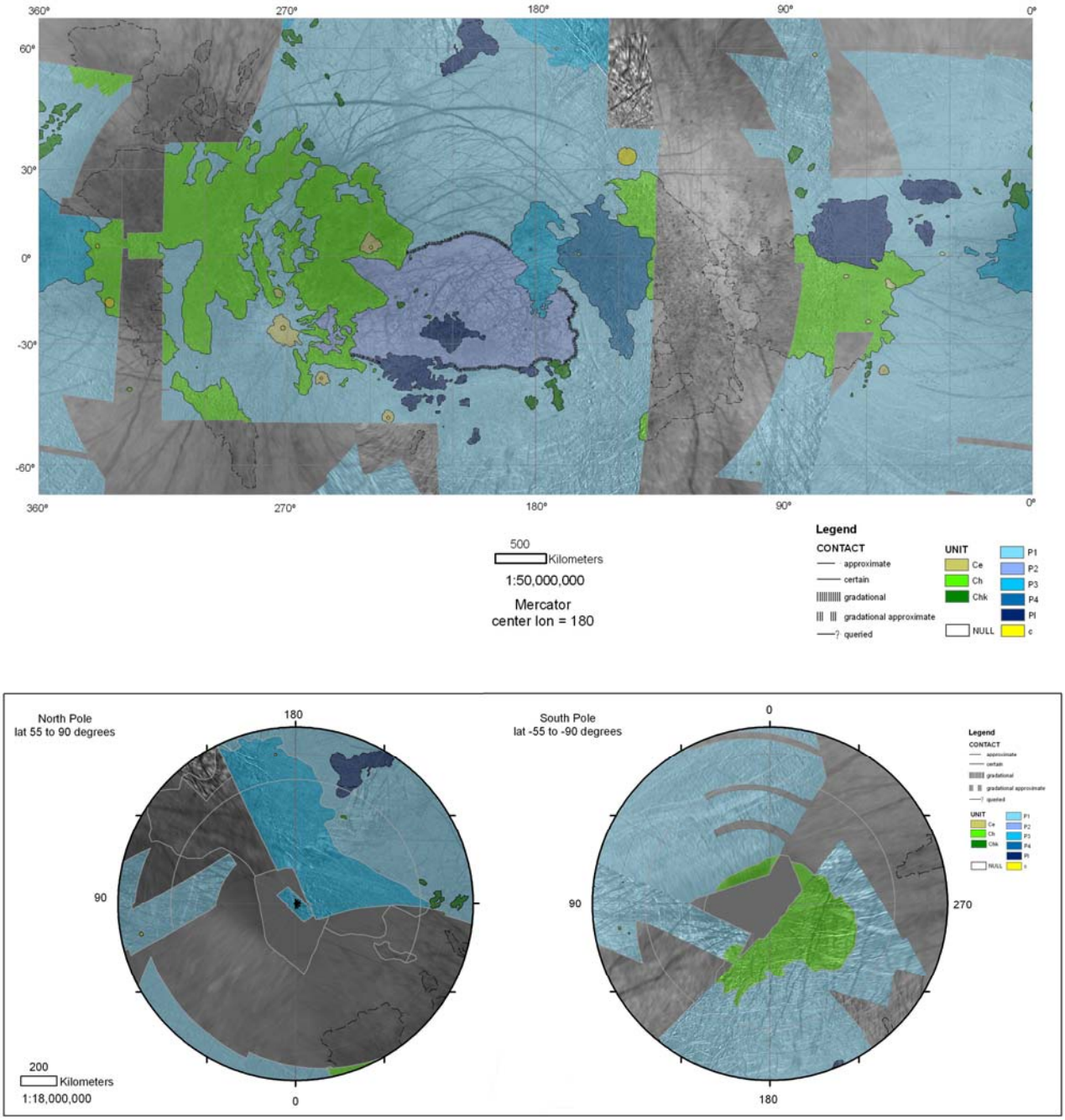

Figure 1: Global geologic map of Europa.

MATERIAL UNITS, STRUCTURES/LANDFORMS, AND STRATIGRAPHY FOR THE GLOBAL GEOLOGIC MAP OF GANYMEDE (1:15M). G. Wesley Patterson[1], James W. Head[2], Geoffrey C. Collins[3], Robert T. Pappalardo[4], Louise M. Prockter[1], and Baerbel K. Lucchitta[5], [1]Applied Physics Laboratory, Laurel, MD 20723, (Wes.Patterson@jhuapl.edu), [2]Brown University, Providence, RI, 02912, [3]Wheaton College, Norton, MA, 02766, [4]Jet Propulsion Laboratory, Pasadena, CA, 91109, [5]USGS, Flagstaff, AZ, 86001.

Introduction: In the coming year we will complete a global geological map of Ganymede that represents the most recent understanding of the satellite on the basis of Galileo mission results. This contribution builds on important previous accomplishments in the study of Ganymede utilizing Voyager data [e.g., 1-5] and incorporates the many new discoveries that were brought about by examination of Galileo data [e.g., 6-10]. Material units have been defined, structural landforms have been identified, and an approximate stratigraphy has been determined utilizing a global mosaic of the surface with a nominal resolution of 1 km/pixel assembled by the USGS. This mosaic incorporates the best available Voyager and Galileo regional coverage and high resolution imagery (100-200 m/pixel) of characteristic features and terrain types obtained by the Galileo spacecraft. This map has given us a more complete understanding of: 1) the major geological processes operating on Ganymede, 2) the characteristics of the geological units making up its surface, 3) the stratigraphic relationships of geological units and structures, and 4) the geological history inferred from these relationships. A summary of these efforts is provided here.

Material units: We recognize four fundamental geologic materials on Ganymede; dark, light, reticulate (**r**), and impact material [11,12]. Type localities for each unit have been identified. On the basis of our mapping, dark material on Ganymede has been subdivided into three units; cratered (**dc**), lineated (**dl**), and undivided (**d**), while light material has been subdivided into four units; grooved (**lg**), subdued (**ls**), irregular (**li**), and undivided (**l**). Impact material encompasses palimpsest, crater, and basin materials. Palimpsest material is further subdivided into four units; three of these are distinguished on the basis of their stratigraphic relationship with light material units ($\mathbf{p_1}$, $\mathbf{p_2}$ and **pu**) and the fourth is an interior plains unit (**pi**). Five crater units – fresh ($\mathbf{c_3}$), partially degraded ($\mathbf{c_2}$), degraded ($\mathbf{c_1}$), unclassified (**cu**), and ejecta (**ce**)- comprise the crater materials, and two units – rugged (**br**) and smooth (**bs**) - comprise the basin material.

Structures and Landforms: Several important structures and landforms on Ganymede have been identified and mapped (Fig. 1). These include; furrows, domes, grooves, secondary craters, depressions, and crater rays. Furrows are typically organized into vast multi-ringed systems and are the oldest recognizable structures on the surface, predating essentially all craters larger than 10 km in diameter [13]. Individual furrows (Fig. 1a) are characterized by linear to curvilinear troughs bounded by raised rims, which are generally bright. They are represented on the global map as lines drawn on dark material units. They extend from tens to hundreds of kilometers in length and are typically ~6 to 20 km wide, with generally flat or u-shaped floors and sharp raised rims [1,7]. Domes on Ganymede are features associated exclusively with the interiors of craters having diameters between ~60 km and ~175 km (Fig. 1b). They are typically circular in map view and occur within central pits. In cross-section they are steep-sided with flat-topped to concave profiles that can reach heights of up to ~1.5 km above surrounding materials [14]. Grooves (Fig. 1c) represent subparallel ridges and troughs observed within many light material units and their formation is attributed to extensional tectonism [1,6]. Secondary craters (Fig. 1d) are represented by fields of uniform small pits oriented radially to subradially and surrounding large fresh craters, partly degraded craters, palimpsests, and basin materials. Depressions (Fig. 1e) have been interpreted to represent caldera-like source vents for icy volcanism, with ~30 having been recognized from image data of Ganymede [10,15]. Finally, crater rays (Fig. 1f) have been mapped and represent the distinguishing characteristic between fresh and partly degraded craters.

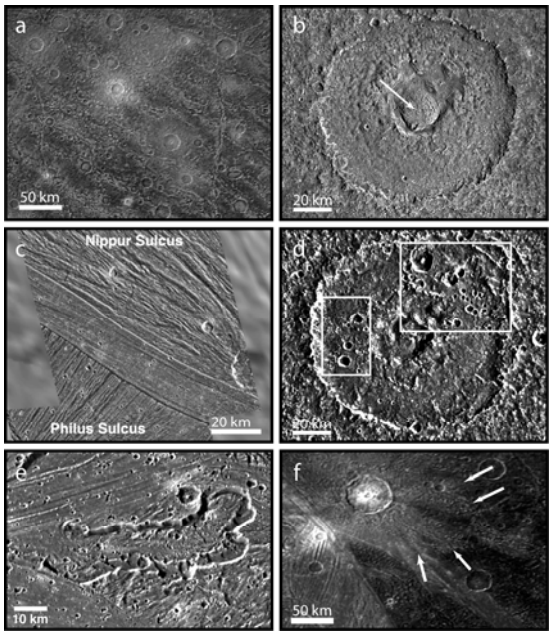

Fig. 1. Examples of structures and landforms represented on the global geologic map of Ganymede, including; (a) furrows,

(b) domes, (c) grooves, (d) secondary craters, (e) depressions, and (f) crater rays.

Stratigraphy: As part of our global mapping effort, we have identified ~4000 craters >10km in diameter across the surface of Ganymede. This dataset has enabled us to calculate crater densities (on a global-scale) for each of the material units we have defined (Table 1). It has also provided a valuable link to previous regional estimates of crater densities calculated for various material types utilizing counting areas 10 to 100 times smaller [e.g., 1,16].

Table 1.

	10 km[a]	20 km	30 km	Area (x 10^6 km^2)
Light				
grooved	39±2 (44±3)[b]	14±1 (14±2)	8±1	9.29 (5.71)
irregular	30±4 (20±5)	13±3 (5±2)	6±2	1.94 (0.992)
subdued	42±2 (39±3)	18±1 (15±2)	9±1	8.24 (4.90)
Dark				
cratered	85±2 (97±2)	32±1 (34±1)	15±1	21.9 (16.3)
lineated	67±8 (69±8)	19±4 (20±4)	8±3	1.06 (1.01)
Reticulate				
reticulate	39±12 (39±12)	18±8 (18±8)	4±4	0.28 (0.28)
Impact				
Palimpsest	61±7	23±4		1.37
Basin	19±5	11±4		0.80

[a] Number of craters ≥ the quoted diameter, normalized to 10^6 km^2.

[b] Numbers in parenthesis indicate values calculated from image data at resolutions ≤ 1.5 km/pixel.

These data confirm that dark cratered material is the oldest material on Ganymede and that light materials formed substantially later. Dark lineated material and reticulate terrain have crater densities on the higher end of light material units, suggesting they mark a transition into the formation of light materials. Palimpsests are older then light materials, dark lineated material, and reticulate terrain, but younger then dark cratered terrain. Finally, Gilgamesh basin appears to be younger then light materials.

Beyond crater statistics, the mapping of groove orientations within polygons of light material and the cross-cutting relationships of those polygons with respect to each other have given us insight into the time sequence and driving mechanism for their formation [17,18]. To determine a time-sequence of formation for light material, ~2000 light material polygons were run through a sorting algorithm [19,20]. The results suggested that four episodes (Fig. 2) of light material formation could describe the observed distribution of the orientations of grooves within polygons of light material. Using this distribution, and the fact that light material appears to form predominantly by extension [1,6,21], it was suggested that a strain history for light material formation could be determined [18]. This history was then compared to various driving mechanisms proposed to have led to the formation of light material and it was determined that stresses due to internal differentiation provided the best fit to the data.

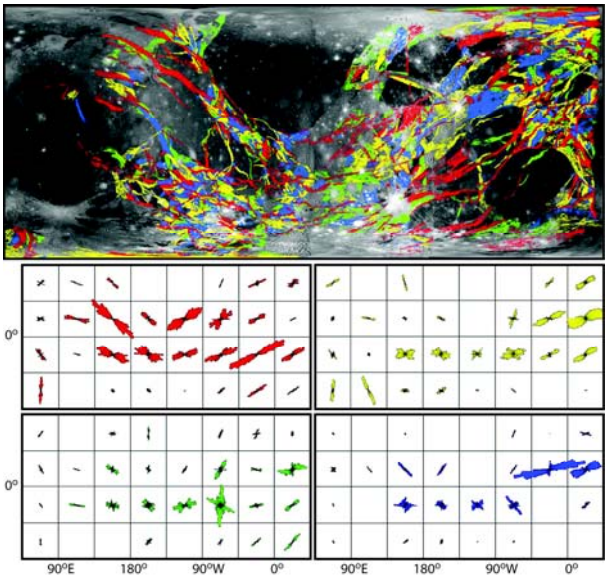

Fig. 2. Global image mosaic of Ganymede with 4 episodes of light material formation superposed (red, yellow, green, and blue). Variability of the orientations with latitude and longitude of groove sets within each episode are shown.

Summary: In compiling the first global geologic map of Ganymede, we have been able to integrate valuable insights garnered from the Galileo mission into extensive work done mapping quadrangles of the satellite's surface based on Voyager data [e.g., 3-5]. New map units have been described and some previously determined ones have been combined, important structures and landforms have been recognized and classified, and a global stratigraphy has been determined. Finally, based on these mapping efforts, a driving mechanism for the formation of light material has been proposed.

References: [1] Shoemaker et al., in The Satellites of Jupiter, 435-520, 1982; [2] McKinnon and Parmentier, in Satellites, 718-763, 1986; [3] J.E. Guest et al., USGS Map I-1934, 1988; [4] D.E. Wilhelms, USGS Map I-2242, 1997; [5] B.K. Lucchitta et al., USGS Map I-2289, 1992; [6] Pappalardo et al., Icarus, 135, 276-302, 1998; [7] Prockter et al., Icarus 135, 317-344, 1998; [8] Prockter et al., JGR 105, 22,519-22,540, 2000; [9] Oberst et al., Icarus 140, 283-293, 1999; [10] Schenk et al., Nature 410, 57-60, 2001; [11] Patterson et al., LPSC XXXVIII #1098, 2007; [12] Patterson et al., USGS Open-File Report 2007-1233, 2007; [13] Passey and Shoemaker, in The Satellites of Jupiter, 379-434, 1982; [14] Schenk et al., in Jupiter, 427-456, 2004; [15] Lucchitta, Icarus, 44, 481-501, 1980; [16] Murchie et al., Icarus 81, 271-297, 1989; [17] Collins, LPSC XXXVIII #1999, 2007; [18] Collins, LPSC XXXIX #2254, 2008; [19] Crawford and Pappalardo, Astrobiology, 2004; [20] Martin et al., LPSC XXXVII, 2006; [21] Collins et al., Icarus, 135, 345-359, 1998.

GLOBAL GEOLOGIC MAPPING OF IO: PRELIMINARY RESULTS. D.A. Williams[1], L.P. Keszthelyi[2], D.A. Crown[3], P.E. Geissler[2], P.M. Schenk[4], Jessica Yff[2], W.L. Jaeger[2], J.A. Rathbun[5]. [1]School of Earth & Space Exploration, Arizona State University, Tempe, Arizona 85287 (David.Williams@asu.edu); [2]Astrogeology Team, U.S. Geological Survey, Flagstaff, Arizona; [3]Planetary Science Institute, Tucson, Arizona; [4]Lunar and Planetary Institute, Houston, Texas; [5]Department of Physics, University of Redlands, Redlands, California.

Introduction: We are preparing a new global geologic map of Jupiter's volcanic moon, Io. Here we report initial results of our mapping: a preliminary distribution of material units in terms of areas (Table 1) and a visual representation (Figure 1). We also discuss some of the problems in Io geology we hope to address with the mapping.

Previous Work: During Year 1 of this project, we developed techniques for global mapping using a low-resolution *Galileo* regional mosaic [1]. During Year 2 (February 2006) we received our mapping base, a series of 1 km/pixel mosaics, produced by the USGS, from the combined *Galileo-Voyager* image data sets [2]. Global mapping has been done using ArcGIS™ software on the USGS mosaics. We have also begun production of an Io database [3] that will include most Io data sets to address the surface changes due to Io's active volcanism.

Results: Io's surface is dominated by plains material, thought to consist of Io's silicate crust covered by pyroclastic deposits and lava flows of silicate and sulfur-bearing composition. Many plains areas contain flow fields that cannot be mapped separately due to a lack of resolution or modification by alteration processes. Discrete lava flows and flow fields are the next most abundant unit, with bright (sulfur?) flows in greater abundance than dark (silicate?) flows. The source of most of Io's heat flow, the paterae, are the least abundant unit in terms of areal extent.

Future Work: Our immediate focus is to complete a draft map by end of July 2008. Upon completion of the draft map for peer review, we will use the new map to investigate several specific questions about the geologic evolution of Io that previously could not be well addressed, including: a) comparison of the areas vs. the heights of Ionian mountains to assess their stability and evolution; b) correlation and comparison of *Galileo* Near-Infrared Mapping Spectrometer (NIMS) and Photopolarimeter-Radiometer (PPR) hot spot locations with the mapped locations of dark vs. bright lava flows and patera floors to assess any variations in the types of sources for Io's active volcanism; and c) creation of a global inventory of the areal coverage of dark and bright lava flows to assess the relative importance of sulfur vs. silicate volcanism in resurfacing Io, and to assess whether there are regional concentrations of either style of volcanism that may have implications on interior processes.

References: [1] Williams, D.A. et al. (2007), *Icarus*, *186*, 204-217. [2] Becker, T. and P. Geissler (2005), *LPS XXXVI*, Abstract #1862. [3] Rathbun, J.A. and S.E. Barrett (2007), *LPS XXXVIII*, Abstract #2123.

Figure 1 (next page). Preliminary global map of Io, in which the entire surface has been characterized into material units and structures. Diffuse deposits are also shown. The completed map is to be submitted to the USGS by end of July 2008.

Table 1. Preliminary distribution of geologic units as percentage of Io.

Material Unit	Area (km^2)	Area (%)	Material Unit	Area (km^2)	Area (%)
Red-brown plains	1.41E7	33.4	Bright patera floors	1.84E5	0.4
Bright (yellow) plains	7.68E6	18.4	Dark patera floors	1.93E5	0.5
White plains	3.75E6	8.9	Undivided patera floors	6.75E5	1.6
Layered plains	1.84E6	4.4	**Total Patera Floors**	1.05E6	**2.5**
Region of poor resolution (Likely R-b plains)	7.20E5	1.7			
			Bright lava flows	1.80E6	4.3
Total Plains	2.81E7	**66.6**	Dark lava flows	1.23E6	2.9
			Undivided lava flows	8.70E6	20.6
Lineated mountains	6.40E5	1.5	**Total Lava Flows**	1.17E7	**27.8**
Mottled mountains	8.05E4	0.2			
Undivided mountains	5.54E5	1.3	Bright (yellow) diffuse dep.	8.76E5	2.1
Tholi (domes)	5.25E4	0.1	White diffuse deposits	2.90E6	6.9
Total Mountains	1.33E6	**3.1**	Red diffuse deposits	3.61E6	8.6
			Dark diffuse deposits	2.68E5	0.6
			Green diffuse deposits	4.09E3	0.01

Note: Diffuse deposits are superposed on all other materials, and cover 18.2% of Io's surface.

Global Geologic Map of Io

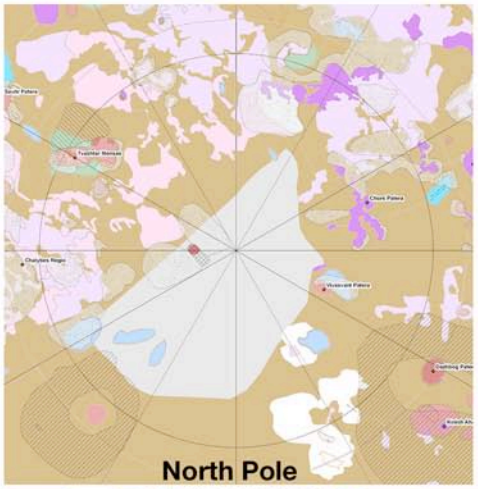

Legend

- Yellow bright plains material
- White bright plains material
- Red-brown plains material
- Layered plains material
- Bright flow material
- Dark flow material
- Undivided flow material
- Volcanic vent
- Hotspot
- Bright patera floor material
- Dark patera floor material
- Undivided patera floor material
- Lineated mountain material
- Mottled mountain material
- Undivided mountain material
- Tholus material
- Cone or shield
- Bright diffuse material
- White diffuse material
- Red diffuse material
- Dark diffuse material
- Poor resolution
- Lineament
- Ridge
- Depression
- Scarp